

USE OF TISSUE TRANSGLUTAMINASE (VARIANT 2)-TRANSDUCED
MESENCHYMAL STEM CELLS IN CARTILAGE TISSUE ENGINEERING

by

Ayşe Ceren Çalıkođlu Koyuncu

Submitted to Graduate School of Natural and Applied Sciences
in Partial Fulfillment of the Requirements
for the Degree of Doctor of Philosophy in
Biotechnology

Yeditepe University

2018

USE OF TISSUE TRANSGLUTAMINASE (VARIANT 2)-TRANSDUCED
MESENCHYMAL STEM CELLS IN CARTILAGE TISSUE ENGINEERING

APPROVED BY:

Prof. Dr. Gamze Torun Köse
(Thesis Supervisor)

Prof. Dr. Dilek Telci

Assoc. Prof. Dr. Elif Damla Arısan

Assist. Prof. Dr. Deniz Yücel

Assist. Prof. Dr. Hüseyin Çimen

DATE OF APPROVAL:/..../2018



*Dedicated to my beloved baby girl
who gave me the best feelings in life*

ACKNOWLEDGEMENTS

First of all, I would like to present my sincere gratitude to my mentor Prof. Dr. Gamze Torun Köse who constantly guided and supported me with her excellent knowledge and experiences during this study, as well as in my whole graduate and post-graduate life. It has always been an honor for me working with her.

It is a great pleasure to thank to my co-advisor Prof. Dr. Dilek Telci for guiding me with her immense knowledge throughout this study.

I also would like to appreciate to precious jury members for their contributions and excellent suggestions in this work.

I would like to appreciate to Prof. Dr. Fikretin Şahin who provided me the opportunity to complete my post-graduate studies at this department.

I am thankful to Hande Duru for her help in scanning electron microscopy studies. I also would like to thank Binnur Kıratlı and Dilek Öztürk for their help in confocal microscopy.

I am grateful to my lab partner Ayşe Hande Nayman for her brilliant knowledge and for her help during this study. I also would like to thank dear YUTEG members Görke Gürel Peközer, İrem Ayşe Kanneçi Altınışık, Görkem Özdemirli, Özge Acar, Ayşegül Atasoy Zeybek, Ezgi İrem Bektaş, Nergis Abay for being such kind and supportive friends.

Last but not least, I appreciate to my lovely family for supporting me patiently during this work, and for their faith and endless love throughout my entire life. I wish to present special gratitude to my best friend, my husband, Cihat, for encouraging me all the time during my studies in patience, and emotionally supporting me when I was in desperation, which greatly helped me finish this study.

ABSTRACT

USE OF TISSUE TRANSGLUTAMINASE (VARIANT 2)-TRANSDUCED MESENCHYMAL STEM CELLS IN CARTILAGE TISSUE ENGINEERING

Articular cartilage defects are increasing among the individuals because of the side-effects of the developing technology, such as obesity that causes serious joint degeneration. Since cartilage is incapable of self-healing upon severe degeneration due to the lack of blood vessels, cartilage tissue engineering is gaining importance in the treatment of cartilage defects. This study was designed to improve cartilage tissue regeneration by expressing tissue transglutaminase variant 2 (TGM2_v2) in mesenchymal stem cells (MSC) derived from bone marrow of rats (rBMSCs). For this purpose, MSCs transduced with TGM2_v2 were grown and differentiated on three-dimensional poly(butylene succinate) (PBSu) and poly-L-lactide (PLLA) blend scaffolds. The constructs were characterized by scanning electron microscopy and MTS assay for the topographical analysis and cell viability, respectively. Chondrogenic differentiation analyses were performed throughout 3 weeks. Alcian Blue staining and immunofluorescence assay were carried out to observe the chondrogenic matrix deposition, while real-time PCR was performed to examine the expression levels of cartilage specific genes. It was demonstrated that the transduced cells could not only successfully express the short form TG2 (TG2-S), but also deposited the protein onto the scaffolds. In addition, they could spontaneously produce cartilage specific proteins without any chondrogenic induction, as shown by Alcian Blue staining and collagen type 2 and aggrecan immunofluorescence. Similarly, real-time PCR results suggested that TGM2_v2 expression provided the cells the ability of chondrogenic differentiation without addition of any differentiation factors. In conclusion, the TGM2_v2 gene transfer to MSCs could be taken into consideration in the future cartilage tissue engineering applications using PBSu:PLLA scaffolds.

ÖZET

DOKU TRANSGLUTAMİNAZ (VARYANT 2) İLE TRANSDÜKLENMİŞ MEZENKİMAL KÖK HÜCRELERİN KIKIRDAK DOKU MÜHENDİSLİĞİNDE KULLANILMASI

Gelişmekte olan teknolojinin yan etkilerinden doğan obezite gibi hastalıklar yüzünden oluşan ciddi eklem kıkırdağı hasarları her geçen gün bireyler arasında artış göstermektedir. Kıkırdak dokusu, kan damarları ihtiva etmemesinden dolayı, kendi kendini yenileyememekte ve bu sebeple doku hasarlarının tedavisinde kıkırdak doku mühendisliğinin önemi gittikçe artmaktadır. Bu çalışmada, doku-transglutaminaz (varyant 2) ile transdüklenmiş sıçan kemik iliği kaynaklı mezenkimal kök hücreleri (sKİMKH) kullanılarak kıkırdak doku yenilenmesi amaçlanmıştır. Bunun için hücreler doku-transglutaminaz-varyant 2 (TGM2_v2) geni ile transdükledikten sonra, poli(bütülen süksinat) (PBSu) ve poli-L-laktit (PLLA) karışımı iskeleler üzerinde büyütülüp, farklılaştırılmıştır. Oluşan yapılar taramalı elektron mikroskobu ve MTS analizi ile sırasıyla topografik ve hücre canlılığı bakımından karakterize edilmiş ve ardından üç hafta boyunca kondrojenik farklılaşma testlerine tabi tutulmuşlardır. Kondrojenik matriks depolanmasını gözlemek için Alsiyan mavisi boyaması ve immünboyama; kıkırdağa özgü genlerin ifadesini incelemek içinse eş zamanlı-polimeraz zincir reaksiyonu yapılmıştır. Sonuç olarak, transdüklenmiş hücrelerin TGM2_v2'yi hem gen hem protein düzeyinde başarılı bir şekilde ifade ettikleri ve iskeleler üzerinde depolayabildikleri gözlenmiştir. Bu hücreler aynı zamanda kıkırdağa özgü proteinleri, herhangi bir kondrojenik induksiyon olmadan kendiliğinden üretebilmişlerdir. Benzer bir şekilde, eş zamanlı-polimeraz zincir reaksiyonu sonucunda TGM2_v2 transdüksiyonunun hücrelere kendiliğinden kıkırdağa farklılaşma potansiyeli sağladığı görülmüştür. Özetle, TGM2_v2 ile transdüklenmiş sKİMKHler ve PBSu:PLLA ile oluşturulmuş olan bu yapı, gelecekte yapılacak olan kıkırdak doku mühendisliği çalışmalarında kullanmak üzere göz önünde bulundurulmalıdır.

TABLE OF CONTENTS

ACKNOWLEDGEMENTS	iv
ABSTRACT.....	v
ÖZET	vi
LIST OF FIGURES	xi
LIST OF TABLES	xvi
LIST OF SYMBOLS/ABBREVIATIONS.....	xvii
1. INTRODUCTION.....	1
1.1. CARTILAGE	1
1.1.1. Articular Cartilage	2
1.1.2. Articular Cartilage Defects	10
1.1.3. Treatments for Articular Cartilage Defects	11
1.2. CARTILAGE TISSUE ENGINEERING	13
1.2.1. Cell Sources	13
1.2.2. Scaffolds	15
1.2.3. Stimulating Factors	18
1.3. TISSUE TRANSGLUTAMINASE (TRANSGLUTAMINASE-2)	21
1.3.1. Transglutaminase-2 in ECM Regulation and Cartilage Tissue	25
1.3.2. Transglutaminase-2 Isoforms	26
1.4. AIM OF THE STUDY	29
2. MATERIALS	30
2.1. PRODUCTION OF LENTIVIRAL PLASMIDS AND LENTIVIRUSES	30
2.2. ISOLATION OF MSCS FROM RAT BONE MARROW	31
2.3. GROWTH OF RBMSCS	31
2.4. TRANSDUCTION OF RBMSCS.....	32
2.5. ISOLATION AND GROWTH OF RAT KNEE CHONDROCYTES	32
2.6. TGM2_V2 GENE EXPRESSION ANALYSIS	33
2.7. TG2-S PROTEIN ANALYSIS	33
2.8. FLOW CYTOMETRY.....	34

2.9.	CELL PROLIFERATION ASSAY	34
2.10.	PREPARATION AND CHARACTERIZATION OF SCAFFOLDS	34
2.11.	DIFFERENTIAL GENE EXPRESSION ANALYSIS.....	35
2.12.	IMMUNOFLUORESCENCE ASSAYS	35
2.13.	ALIZARIN RED STAINING.....	36
2.14.	ALCIAN BLUE STAINING	36
2.15.	MECHANICAL ANALYSIS	37
3.	METHODOLOGY	38
3.1.	PRODUCTION OF LENTIVIRAL PLASMIDS AND LENTIVIRUSES	38
3.1.1.	Bacterial Streaking.....	40
3.1.2.	Mini-inoculation	41
3.1.3.	Inoculation and Plasmid Isolation.....	41
3.1.4.	Transfection of Human Embryonic Kidney-293T Cells.....	44
3.2.	ISOLATION AND GROWTH OF CELLS	45
3.2.1.	Isolation and Growth of rBMSCs	45
3.2.2.	Characterization of rBMSCs by Flow Cytometry	45
3.2.3.	Isolation and Growth of Rat Knee Chondrocytes	46
3.3.	GENE TRANSFER TO RBMSCS	46
3.3.1.	Construction of Blasticidin Kill Curve	46
3.3.2.	Construction of Protamine Sulfate Kill Curve.....	47
3.3.3.	Transduction of rBMSCs	47
3.3.4.	Selection of the Transduced Cells	48
3.4.	ANALYSES OF TRANSDUCTION EFFICIENCY AND CHARACTERIZATION OF TRANSDUCED CELLS	48
3.4.1.	Fluorescence Microscopy	48
3.4.2.	Flow Cytometry	48
3.4.3.	Total RNA Isolation.....	49
3.4.4.	Real-Time PCR.....	49
3.4.5.	Protein Extraction	50
3.4.6.	Western Blotting	51
3.4.7.	Cell Proliferation Assay.....	51
3.5.	PREPARATION AND CHARACTERIZATION OF SCAFFOLDS	52

3.5.1.	Preparation of PBSu Scaffolds	52
3.5.2.	Preparation of PBSu:PLLA Scaffolds	52
3.5.3.	Cell Seeding onto the Scaffolds.....	52
3.5.4.	Fluorescence Microscopy	53
3.5.5.	Scanning Electron Microscopy (SEM).....	53
3.5.6.	Cell Proliferation Assay.....	53
3.5.7.	Gene Expression Analyses.....	53
3.5.8.	Immunofluorescence Assays	54
3.5.9.	Alizarin Red Staining.....	55
3.5.10.	Alcian Blue Staining	56
3.5.11.	Mechanical Analysis	56
3.6.	STATISTICAL ANALYSES.....	56
4.	RESULTS AND DISCUSSION.....	57
4.1.	VERIFICATION OF TGM2_V2 SEQUENCE IN PLASMID	57
4.2.	GROWTH OF RBMSCS AND RAT KNEE CHONDROCYTES	63
4.3.	TRANSFECTION AND TRANSDUCTION STUDIES.....	64
4.3.1.	Determination of Transfection Efficiency by Fluorescence Microscopy	64
4.3.2.	Determination of Transduction Efficiency by Fluorescence Microscopy	65
4.3.3.	Flow Cytometry Analysis For the Verification of Transduction Efficiency	67
4.4.	CHARACTERIZATION OF TRANSDUCED CELLS	70
4.4.1.	TGM2_v2 Gene Expression Analysis for the Verification of Transduction Efficiency	70
4.4.2.	Western Blotting for the Observation of TG2-S Protein Expression	73
4.4.3.	Cell Viability Assay to Examine Cell Proliferation.....	74
4.5.	CHARACTERIZATION OF THE SCAFFOLDS.....	76
4.5.1.	Fluorescence Microscopy of the Cell-Seeded PBSu Scaffolds to Observe Cell Attachment and Morphology.....	77
4.5.2.	SEM of the Scaffolds for Topographical Analysis.....	82
4.5.3.	Cell Viability on Scaffolds to Observe Cell Proliferation	85
4.6.	EXPRESSION OF CARTILAGE-SPECIFIC GENES	88
4.7.	IMMUNOCHEMISTRY OF THE CELL-SEEDED SCAFFOLDS	93
4.7.1.	TG2 Deposition Into the Scaffolds	93

4.7.2. Immunochemistry of ECM and Nuclei.....	96
4.8. ALCIAN BLUE STAINING FOR CHONDROGENIC DIFFERENTIATION	108
4.8.1. Deposition of sGAG by the Cells on TCP.....	108
4.8.2. Deposition of sGAG by the Cells on PBSu:PLLA Scaffolds.....	114
4.9. ALIZARIN RED STAINING FOR OSTEOGENIC DIFFERENTIATION.....	116
4.10. MECHANICAL ANALYSIS OF THE CELL-SCAFFOLD CONSTRUCTS ..	118
5. CONCLUSION	119
6. FUTURE PROSPECTS.....	120
REFERENCES	121
APPENDIX A.....	138
APPENDIX B	139
APPENDIX C	140
APPENDIX D.....	141
APPENDIX E	142
APPENDIX F	143

LIST OF FIGURES

Figure 1.1. Arthroscopical image of human knee.....	3
Figure 1.2. Cross section of the long bone and its osteochondral tissue structure	4
Figure 1.3. Schematic overview of chondrogenesis	5
Figure 1.4. The schematic representation of the chondrocyte and its ECM.....	7
Figure 1.5. Structure of aggrecan.....	8
Figure 1.6. Schematic representation of a thin collagen fibril in cartilage	10
Figure 1.7. Classification of cartilage defects.....	11
Figure 1.8. Diagram of the ACI and MACI techniques	13
Figure 1.9. Transamidation reaction mechanism of transglutaminases.....	22
Figure 1.10. Summary of the reactions that are catalyzed by TG2	24
Figure 1.11. Schematic representation of TG2 transcript isoforms	27
Figure 1.12. Functional domains of full length TG2 and TG2-S transcripts.....	28
Figure 3.1. Plasmid maps of psPAX2, pMD2.G, pHTGM2_v2, and pEGFP	38
Figure 3.2. Sequencing primer binding sites on the hTGM2_v2 plasmid vector.....	43
Figure 4.1. Sequence chromatogram of hTGM2_v2 gene inside the vector	59

Figure 4.2. BLAST results of the original and the plasmid vector sequences of TGM2_v2	61
Figure 4.3. NIH BLAST results of segment 1 and segment 2	63
Figure 4.4. Bright field images of passage zero rBMSCs and passage zero rat knee chondrocytes.....	64
Figure 4.5. Fluorescence microscopy of HEK-293T cells after 24 hours and 48 hours of transfection with pEGFP plasmid vector	65
Figure 4.6. rBMSCs after 24 hours of transduction with lentiviral particles encoding EGFP	66
Figure 4.7. rBMSCs after 4 days of transduction with lentiviral particles encoding EGFP.	66
Figure 4.8. rBMSCs after 7 days of transduction with lentiviral particles encoding EGFP.	67
Figure 4.9. Flow cytometry analyses of rBMSCs transduced with lentiviral particles encoding EGFP.....	68
Figure 4.10. Flow cytometry results showing the stemness of rBMSCs after TGM2_v2 transduction.....	69
Figure 4.11. Relative expression of hTGM2_v2 in transduced P5 rBMSCs.....	72
Figure 4.12. Agarose gel electrophoresis of real-time PCR products	73
Figure 4.13. Western blot with TG2 antibody and β -actin antibody	74

Figure 4.14. Comparison of cell viabilities of transduced cells after 1, 7, and 14 days of incubation in growth media	75
Figure 4.15. Effect of chondrogenic differentiation medium on the viabilities of transduced and non-transduced rBMSCs after 1, 7, and 14 days of incubation	76
Figure 4.16. Fluorescence microscopy of rBMSCs transduced with lentiviruses encoding EGFP on 2% PBSu scaffolds 35 days after cell-seeding.....	78
Figure 4.17. Fluorescence microscopy of EGFP-transduced rBMSCs on 4% PBSu scaffolds 35 days after cell-seeding	79
Figure 4.18. Fluorescence microscopy of rBMSCs transduced with lentiviruses encoding EGFP on 6% PBSu scaffolds 35 days after cell-seeding.....	80
Figure 4.19. Fluorescence microscopy of rBMSCs transduced with lentiviruses encoding EGFP on 8% PBSu scaffolds 35 days after cell-seeding.....	81
Figure 4.20. SEM of 1%, 2%, 4%, 6%, 8%, 10% PBSu scaffolds.....	83
Figure 4.21. Scanning electron micrographs of 4% and 6% PBSu:PLLA scaffolds.....	84
Figure 4.22. Scanning electron micrographs of cell-seeded PBSu:PLLA (6%) scaffolds at day 1, day 14, and day 21.	85
Figure 4.23. Viability of transduced and non-transduced cells on 6% PBSu:PLLA scaffolds after 1, 7, and 14 days of incubation in growth media.....	86
Figure 4.24. Cell viabilities on 6% PBSu:PLLA scaffolds at day 1, 14, and 21	88
Figure 4.25. Relative expressions of Sox9, Col2a1, Agc, Col1a1, Col10a1 with respect to 18SrRNA housekeeping gene	92

Figure 4.26. Confocal microscope images of transduced rBMSCs, chondrocytes, and non-transduced rBMSCs on 6% PBSu:PLLA scaffolds on day 1, day 14, and day 21 showing TG2 deposition	94
Figure 4.27. Confocal microscope images of transduced rBMSCs, chondrocytes, and non-transduced rBMSCs on 6% PBSu:PLLA scaffolds on day 14 and day 21 showing TG2 deposition.....	95
Figure 4.28. Immunofluorescence images of transduced and non-transduced rBMSCs on day 14	96
Figure 4.29. Immunofluorescence images of non-transduced and transduced rBMSCs on day 21	97
Figure 4.30. Immunofluorescence images of transduced and non-transduced rBMSCs on day 21-collagen type X staining	99
Figure 4.31. Confocal microscopy of the cell-seeded scaffolds at day 1	101
Figure 4.32. Confocal microscopy of the cell-seeded scaffolds at day 14	102
Figure 4.33. Confocal microscopy of the cell-seeded scaffolds at day 21	103
Figure 4.34. Confocal microscopy of the cell-seeded scaffolds at day 1 for collagen I....	105
Figure 4.35. Confocal microscopy of the cell-seeded scaffolds at day 14 for collagen I..	106
Figure 4.36. Confocal microscopy of the cell-seeded scaffolds at day 21 for collagen I..	107
Figure 4.37. Alcian Blue staining results of transduced rBMSCs, non-transduced rBMSCs, and chondrocytes after 4 days of incubation in normal growth medium.....	109

Figure 4.38. Alcian Blue staining results of transduced rBMSCs, non-transduced rBMSCs, and chondrocytes after 4 days of incubation in chondrogenic differentiation medium.....	110
Figure 4.39. Alcian Blue staining results of transduced rBMSCs, chondrocytes, and non-transduced rBMSCs after 10 days of incubation in normal growth medium	112
Figure 4.40. Alcian Blue staining results of transduced rBMSCs, chondrocytes, and non-transduced rBMSCs after 10 days of incubation in chondrogenic differentiation medium	113
Figure 4.41. Alcian Blue staining of cell-seeded 6% PBSu:PLLA scaffolds on day 1, 14, and 21	115
Figure 4.41. Alizarin Red staining of transduced and non-transduced rBMSCs on day 14 of incubation taken by bright field microscope.....	117

LIST OF TABLES

Table 1.1. The family of transglutaminases.....	23
Table 1.2. Classification of TG2 isoforms.....	27
Table 3.1. Properties of the sequencing primers for TGM2_v2 gene in pHGM2 plasmid.	42
Table 3.2. Nomenclature of the experimental groups.....	47
Table 3.3. Real-time PCR parameters	50
Table 3.4. Rattus Norvegicus primers for Col2a1, Col1a1, Agc, Sox9, Col10A1, 18SrRNA, and their properties	54
Table 4.1. Summary of flow cytometry results showing rBMSCs transduced with lentiviral particles encoding EGFP	68
Table 4.2. Positivity of mesenchymal stem cell markers of transduced rBMSCs.....	70
Table 4.3. Grading of the attachment of transduced cells on PBSu scaffolds at day 35 according to Figures 4.16 to 4.19	82
Table 4.4. Compressive moduli of the cell-seeded PBSu:PLLA (6%) scaffolds	118

LIST OF SYMBOLS/ABBREVIATIONS

18SrRNA	18 Svedberg unit ribosomal RNA
3-D/3D	Three dimensional
ACI	Autologous Chondrocyte Implantation
Agc	Aggrecan
BMP	Bone morphogenetic protein
BSA	Bovine serum albumin
cDNA	Complementary deoxyribonucleic acid
CH	Chondrocyte
Col	Collagen
Col1a1	Collagen type I, alpha 1 chain
Col2a1	Collagen type II, alpha 1 chain
Col10a1	Collagen type X, alpha 1 chain
CS	Chondroitin sulfate
DCM	Dichloromethane
DMEM	Dulbecco's Modified Eagle Medium
DNA	Deoxyribonucleic acid
dNTP	Deoxyribonucleotide triphosphate
DPBS	Dulbecco's Phosphate Buffered Saline
ECM	Extracellular matrix
EDTA	Ethylenediaminetetraacetic acid
EGFP	Enhanced green fluorescent protein
EMT	Epithelial-to-mesenchymal transition
FBS	Fetal bovine serum
FDA	Food and Drug Administration
FGF	Fibroblast growth factor
FN	Fibronectin
GAG	Glycosaminoglycan
GAPDH	Glyceraldehyde 3-phosphate dehydrogenase
HA	Hyaluronic acid
HBSS	Hank's Balanced Salt Solution

HPLC	High-performance liquid chromatography
HS	Heparan sulfate
IGF	Insulin-like growth factor
iPSC	Induced pluripotent stem cell
KS	Keratan sulfate
MACI	Matrix-Assisted Autologous Chondrocyte Implantation
MMP	Matrix metalloprotease
MOI	Multiplicity of infection
MSC	Mesenchymal stem cell
MTS	3-(4,5-dimethylthiazol-2-yl)-5-(3-carboxymethoxyphenyl)-2-(4-sulfophenyl)-2H-tetrazolium, inner salt
OA	Osteoarthritis
OC	Only cells
ORF	Open reading frame
PBSu	Poly (butylene succinate)
PCL	Poly (ϵ -caprolactone)
PCR	Polymerase chain reaction
PDLA	Poly (D-lactide)
PEG	Poly (ethylene glycol/oxide)
Pen/Strep	Penicillin/Streptomycin solution
PGA	Polyglycolide (PGA)
PHBV	Poly (3-hydroxybutyric acid-co-3-hydroxyvaleric acid)
PLA	Poly(lactide)
PLCL	Poly (L-lactide-co- ϵ -caprolactone)
PLGA	Poly (D,L-lactide-co-glycolide)
PLLA	Poly (L-lactide)
PPF	Poly (propylene fumarate)
PS	Protamine sulfate
PU	Polyurethane
PVA	Poly (vinyl alcohol)
rBMSCs	Rat bone marrow derived mesenchymal stem cells
rHuBMP-2	Human bone morphogenetic protein-2
RNA	Ribonucleic acid

RT	Room temperature
RT-PCR	Reverse Transcription-PCR
SDSC	Synovium-derived stem cells
SEM	Scanning electron microscope
sGAG	Sulphated GAG
Sox9	SRY (sex determining region Y)-box 9
TGF- β	Transforming growth factor- β
TGM2	Transglutaminase-2 or Tissue transglutaminase (gene)
TGM2_v2	Transglutaminase-2/Tissue transglutaminase_variant 2 (gene)
TG2	Transglutaminase-2 or Tissue transglutaminase (protein)
TG2-S	Transglutaminase-2/Tissue transglutaminase-short form (protein)
TLC	Thin layer chromatography
tTG	Tissue transglutaminase (gene and/or protein)
WWB	Wavy-wall bioreactor

1. INTRODUCTION

As our world becomes more technological and modern, cartilage defects at weight-bearing joints are increasing among the individuals, causing severe pain to the patients. Obesity, heavy sports, alcohol consumption and aging may result in the development of degenerative joint diseases [1]. As cartilage tissue has an inadequate ability to repair/regenerate spontaneously, most of the patients suffer from pain and disability. There are various medical and surgical treatment methods for the articular cartilage defects; however, none of these methods bring the tissue functions back. As an alternative to the common treatments of articular cartilage defects, cartilage tissue engineering plays an important part in new tissue formation. The technique utilizes a suitable scaffold for the cells to attach and generate a cartilage tissue by the stimulation of additional biological factors [2]. Scaffold must have appropriate mechanical properties so that the cells can adhere to and deposit a cartilaginous matrix. By combining the scaffolds with proper cells and stimulants, the most encouraging goal of tissue engineering would be to regenerate the damaged cartilage. Additionally, gene therapy can be applied in this technique in order to boost the chondrogenic capabilities of cells. This study was aimed to improve cartilage tissue regeneration by using transglutaminase 2 (variant 2)-transduced mesenchymal stem cells. To achieve this goal, transduced cells were grown and differentiated on three-dimensional poly(butylene succinate) (PBSu) and poly(L-lactide) (PLLA) blend scaffolds, and then these constructs were examined in terms of cartilage tissue regeneration.

1.1. CARTILAGE

Cartilage is a type of flexible and tough connective tissue that is present in various parts of our body such as nose, ear, knees, hips, spine, ribs and Eustachian tubes. The tissue supplies structural support and protection for the surface of bones, acting as a shock absorber especially at the joints [3]. Cartilage is composed of chondrocytes and the extracellular matrix (ECM) that these cells produce, which are called as “chondrons” [4], and does not have any interaction with circulatory, lymphatic, and nervous system. However, it provides its nutrients via diffusion from the synovial fluid that surrounds the tissue [5]. In addition,

the tissue is very hypoxic, indicating that it has a limited rate of cellular growth and tissue regeneration upon damages [3].

There are three types of cartilage, which are classified according to the ECM components in the tissue: Fibrocartilage, elastic cartilage, and hyaline cartilage. Fibrocartilage is found in intervertebral disks, meniscus, and temporomandibular joint. It mainly contains collagen type I, and proteoglycan aggrecan. The less water content of fibrocartilage makes the tissue tougher than the other two types. Consisting mainly of elastin fibers in addition to collagens and proteoglycans, elastic cartilage is the most elastic one among the three types of cartilage, which is found in epiglottis, ear, and Eustachian tube [6]. Being rich in type II collagen and aggrecan, the most abundant type of cartilage is hyaline cartilage, which is generally located as a cover on the surfaces of articulating joints, trachea, larynx, and bronchi [7]. Due to its load bearing feature, articular cartilage is easily damaged, therefore is an attractive research topic for the scientists in the field of tissue engineering.

1.1.1. Articular Cartilage

Articular cartilage is a specialized type of hyaline cartilage which is present in articulating parts of human body, providing mechanical support for the bones that are present at the diarthroidal joints. It prevents erosion and damaging of the subchondral bones by functioning like a cushion. Although the tissue lacks blood or lymph vessels, it uptakes nutrients and water from the synovial fluid that also contains essential cytokines and growth factors [5]. The tissue macroscopically has white, smooth, bright, and tough appearance (Figure 1.1), in addition to its extreme mechanical properties [8]. In adults, cartilage can withstand a pressure of up to 6-8 times body weight, and can experience an average of 5,000 loading cycles in daily routine [9]. This amount of pressure is necessary for a normal hyaline cartilage to maintain its functions and to obtain nutrition and water from the synovial fluid during joint loading [3].

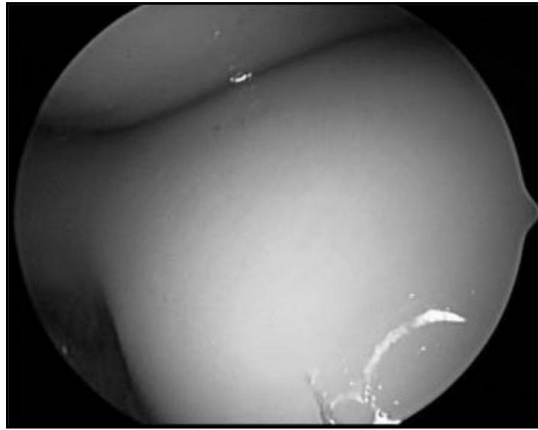


Figure 1.1. Arthroscopical image of human knee [10]

Cartilage is approximately 4 mm in thickness, and can be divided into 4 distinct zones in terms of their cellular and molecular contents: superficial, middle, deep, and calcified zone (Figure 1.2). Being the thinnest one, the superficial zone is composed of two sub-layers. The first layer covers the surface of joints, and is mainly composed of collagen fibers and little amount of polysaccharides with no cells in it. Under that sheet, the second layer which contains collagens, large amount of water, and flattened chondrocytes, is present [7]. Collagen fibrils and chondrocytes in this layer are aligned parallel to the surface of joint and these cells are responsible for production and deposition of ECM molecules upon micro-lesions [11]. Accordingly, this zone is mainly responsible for the mechanical strength of the tissue.

The middle (or transitional) zone is the thickest one, representing the 40-60 per cent of the tissue [12], and is made up of round chondrocytes that are enclosed by randomly arranged collagen fibrils. Endoplasmic reticulum (ER) and Golgi apparatus are prominent in the chondrocytes in this zone; therefore, these cells are highly active in ECM synthesis. The amounts of collagen fibers and water are very low in this zone, but it has the highest level of proteoglycan content [13] [14].

The deep zone has the lowest cell amount, and fewer amounts of proteoglycans than the upper zones; although the aggrecan content is very large. Collagen fibers in this zone are oriented perpendicularly to the subchondral bone. Similarly, chondrocytes can be observed as vertically clustered columns of large spherical cells, which again gives the tissue high compressive strength [1] [12].

Being an interface between the cartilage and its subchondral bone, the calcified zone is partly mineralized. It is positioned closest to the subchondral bone, with collagen fibers crossing through the deep zone. It has very low amount of cells compared to the other zones. These chondrocytes are smaller, and have almost no secretory functions since they are surrounded by a calcified ECM. As a result, the cells are almost metabolically inactive, and the zone is open to shear stress [13] [15].

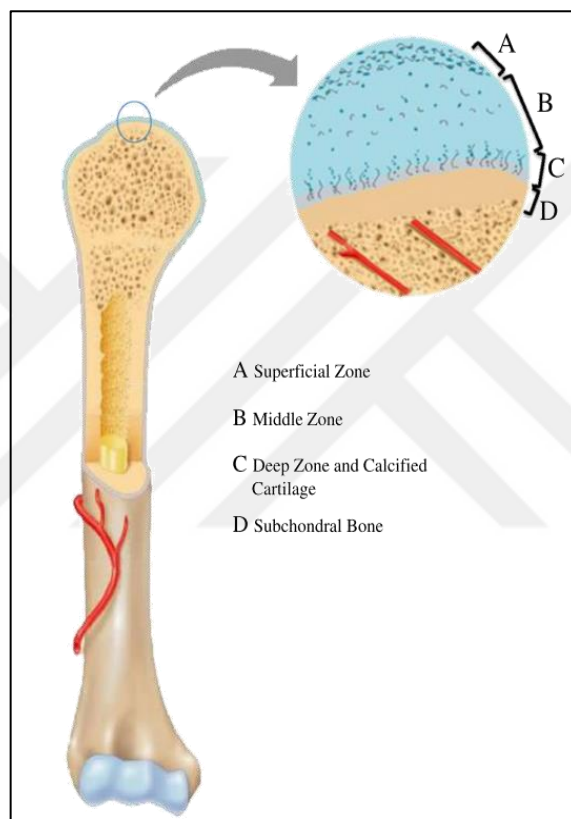


Figure 1.2. Cross section of the long bone and its osteochondral tissue structure showing the zonal architecture of cartilage and the subchondral bone [1]

1.1.1.1. Chondrocytes

Cartilage cells are called as chondrocytes, and they represent less than 10 per cent of the articular (hyaline) cartilage tissue in adults; the rest is ECM. In order for the tissue to maintain its mechanical properties, the chondrocytes play an essential role by secreting and replacing the degraded ECM molecules of the tissue [16] [17]. For this reason, mitochondria, ER and Golgi are prominently found in these cells under the microscope, in addition to lipid and glycogen stocks [13] [18]. Chondrocytes in articular cartilage also secrete large amounts of lysozyme (10 times more than other connective tissue cells) to counteract microorganisms since the tissue does not contain immune cells [11]. Besides, chondrocytes are post-mitotic cells; in other words, they do not divide and have very low apoptotic activity. Depending on the surrounding signals, chondrocytes produce matrix components, organize and maintain the integrity of cartilage ECM [19].

Normally in mature individuals, chondrocytes can be originated from MSCs in the bone marrow. In the course of embryogenesis, cartilage formation starts in the mesenchyme by MSCs condensation, which subsequently differentiate into pre-chondrocytes and start to secrete cartilaginous ECM. The stages that these cells go through are shown in Figure 1.3. At the end of this process, they develop into round-shaped mature chondrocytes, which are no longer able to proliferate, and become embedded in ECM. Endochondral ossification begins after this stage, in which the mature chondrocytes become hypertrophic, secreting calcified ECM proteins [13] [19].

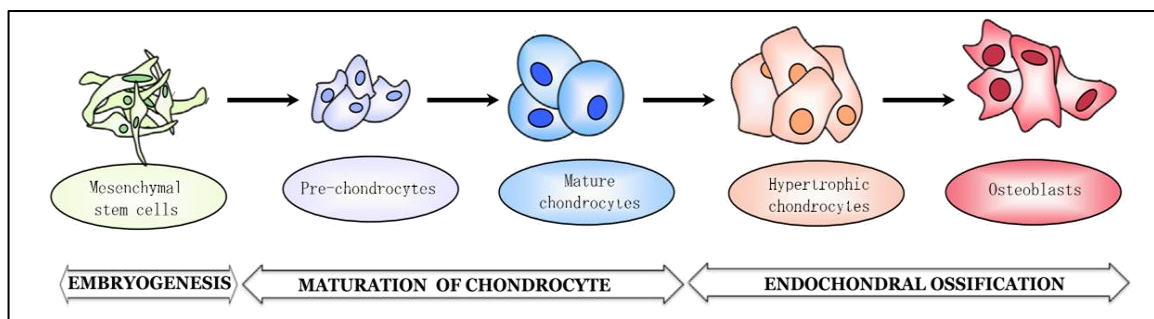


Figure 1.3. Schematic overview of chondrogenesis (Modified from Demoor *et al.* [19])

1.1.1.2. Extracellular Matrix

The ECM of articular cartilage mainly contains water, collagens, proteoglycans (PGs), glycosaminoglycans (GAGs), and proteins of non-collagenous origin (Figure 1.4). The collagen in native tissue has a tight and long triple-stranded helical structure composed of three intertwined alpha-collagen polypeptide chains, $[\alpha 1(\text{II})]_3$ [20]. In the ECM of cartilage tissue, collagen type II molecules have a major role in the caging of molecules, creating tensile strength. The non-collagenous proteins are involved in the stabilization of cartilage ECM and aid in the assembly of chondrocyte and matrix interactions [7]. The proteoglycans in the ECM (95 per cent polysaccharide and 5 per cent protein) hold large amounts of water due to the carbohydrate molecules and negative charges in their structure. As a result, the tissue can hold large amounts of water (65–80 per cent), and the rest 20-40 per cent is the dry weight constituted by collagens (60 per cent) PGs (5–10 per cent), and other proteins (20-25 per cent) [19].

Composed of polysaccharide chains, GAGs are negatively charged hydrophilic molecules of cartilage matrix, which can attract sodium ions that results in water uptake and formation of hydrogel-like structures, enabling the articular cartilage tissue to withstand compressive forces up to 100 atm [21]. GAGs such as chondroitin sulphate (CS), heparan sulphate (HS), and keratan sulphate (KS) can bind growth factors and cytokines through proteoglycans during tissue growth and repair [22].

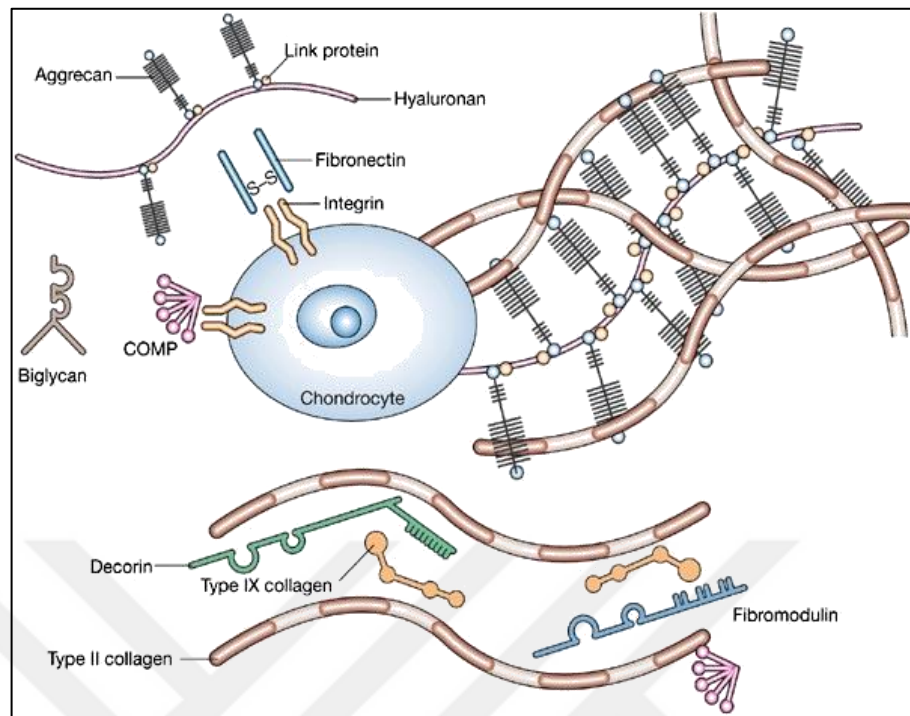


Figure 1.4. The schematic representation of the chondrocyte and its ECM [23]

The most common type of PG in hyaline cartilage is aggrecan which belongs to the family of aggregating proteoglycans (aggrecan), having molecular weight of 205 kDa, and 87 per cent CS and 6 per cent KS side chains (Figure 1.5 a). Aggrecan is a large proteoglycan containing three globular domains (G1, G2, G3) having KS and CS attachment sites [24]. It is mainly responsible for preventing collagen type II network from proteolytic degradation by coating the collagens. In addition, it provides high osmotic pressure to support the cartilage tissue as it can hold large amounts of water in this network [25]. The aggrecan is maintained within the ECM by forming large aggregates with hyaluronan (>200 MDa) Figure 1.5 b) through noncovalent binding, which occurs through their N-terminal via two hyaluronan-binding link proteins that stabilize the aggregate of approximately 100 aggrecan monomers bound on a single hyaluronan chain. This type of complex can occupy a volume of $2 \times 10^{-12} \text{ cm}^3$, equal to the size of a bacterium [20]. In the absence or degradation of aggrecan molecules, the collagen network is not reinforced well and hence the tissue is open to damages [26].

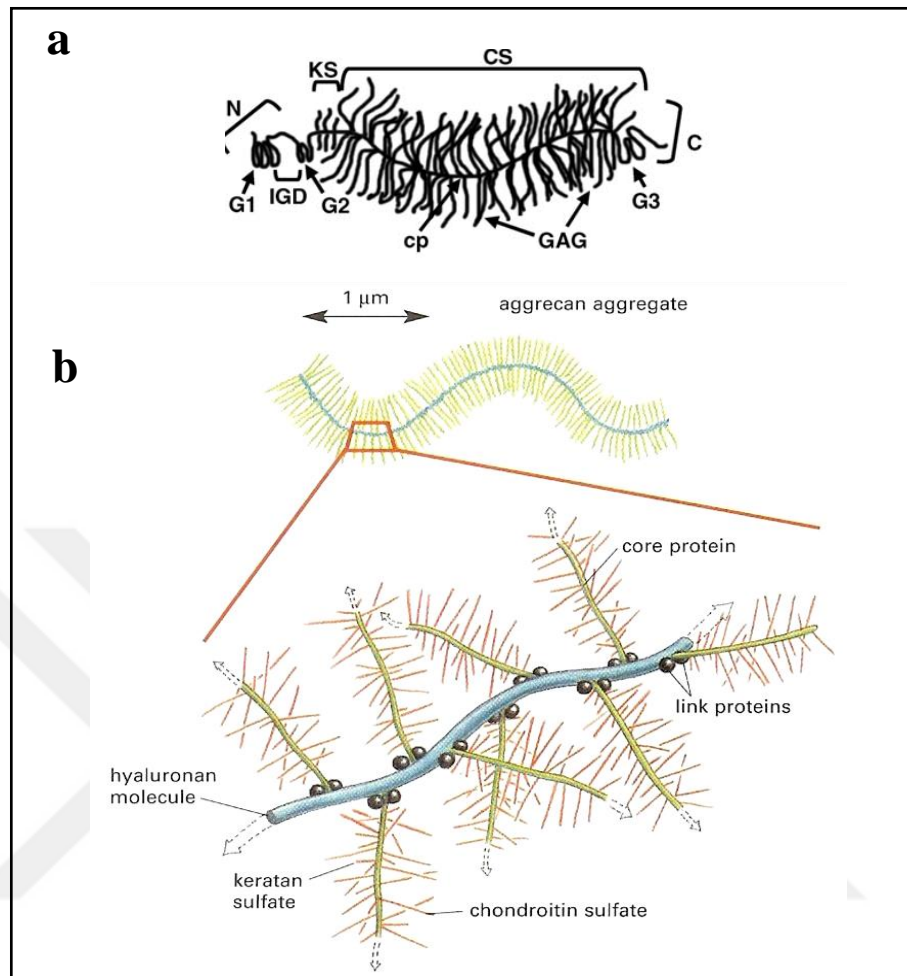


Figure 1.5. (a) . Structure of aggrecan: N: amino-terminal, G1, G2, G3: globular domains, IGD: interglobular domain between G1 and G2, cp: core protein, KS: keratan sulfate region, CS: chondroitin sulfate brush region, GAG: glycosaminoglycan chains, C: carboxyl-terminal [25]. (b) Schematic presentation of aggrecan aggregate [20].

Collagen network functions like a cage, physically locking other macromolecules inside to strengthen the tissue against tension forces (stretching). An individual collagen fiber primarily consists of three collagen polypeptide chains, each called as an alpha chain, which are tied up around one another, resulting in a long and tight triple-stranded helix [20]. Among the collagens, the type II isoform is the most abundant ones in hyaline cartilage, representing approximately 80 per cent of the total collagen amount, providing resistance against tension and shearing forces [7]. Having a molecular weight of 425 kDa, collagen type II glycoprotein has a triple helical fibrillar structure with 67 nm periodicity. Collagen type II fiber is composed of three $[\alpha 1(\text{II})]_3$ chains, and is one of the most important chondrogenic marker

(specific to chondrocytes) together with aggrecan. Due to the carbohydrate molecules in its structure, collagen type II can easily interact with water in contrast to other collagen molecules [27]. ECM homeostasis depends essentially on collagen type II framework; therefore, disruption of that network leads to reduction in mechanical strength, which brings about degenerative joint diseases [19]. Collagen type II is responsible for chondrocyte adhesion and differentiation after being produced by chondrocytes and secretion via exocytosis to ECM [20]. During the biosynthesis of collagen type II, some modifications such as hydroxylation are made to proline and lysine aminoacid residues, which are unique to collagen. It results in the formation of hydroxyproline and hydroxylysine residues, facilitating the glycosylation and hence making collagen type II the most proper constituent of cartilage (80-90 per cent of the total collagen content) [28]. The quantity and organization of collagen network in ECM vary among individuals with respect to the anatomical status and age of the person, as well as the genetic factors [29].

In addition to collagen type II, types VI, IX, X and XI are present in articular cartilage as well. Having a short collagenous central domain, collagen type VI is a glycoprotein with 5 nm fiber diameter, and 100 nm periodicity [7], which is present in the pericellular region of chondrocytes in native cartilage ECM [21]. Together with collagen type II, types IX and XI create fibre threads that form into a meshed structure, providing the entrapment of molecules inside and tensile strength to the tissue [13]. As a member of collagen subfamily, FACIT (Fibril Associated Collagens with Interrupted Triplehelices), collagen type IX is located on the outer sides of collagen fibers, allocating the fibers to create networks with proteoglycans, stabilizing the meshed structure. Collagen types IX and XI represent a few percent of the collagen amount of the tissue, conditional on the source and age of cartilage. Collagen type X is expressed by hypertrophic chondrocytes, therefore it is located in the calcified zone of articular cartilage, interfacing the bone [28]. Collagen fibrils are classified into two: thin (16-nm diameter) (Figure 1.6) and thick (~40-nm diameter). The thin collagen fibrils are mostly made up of collagen type XI having 545 kDa of molecular weight [7] [27], resulting in a crosslinked macromolecule of collagen types XI/IX/II.

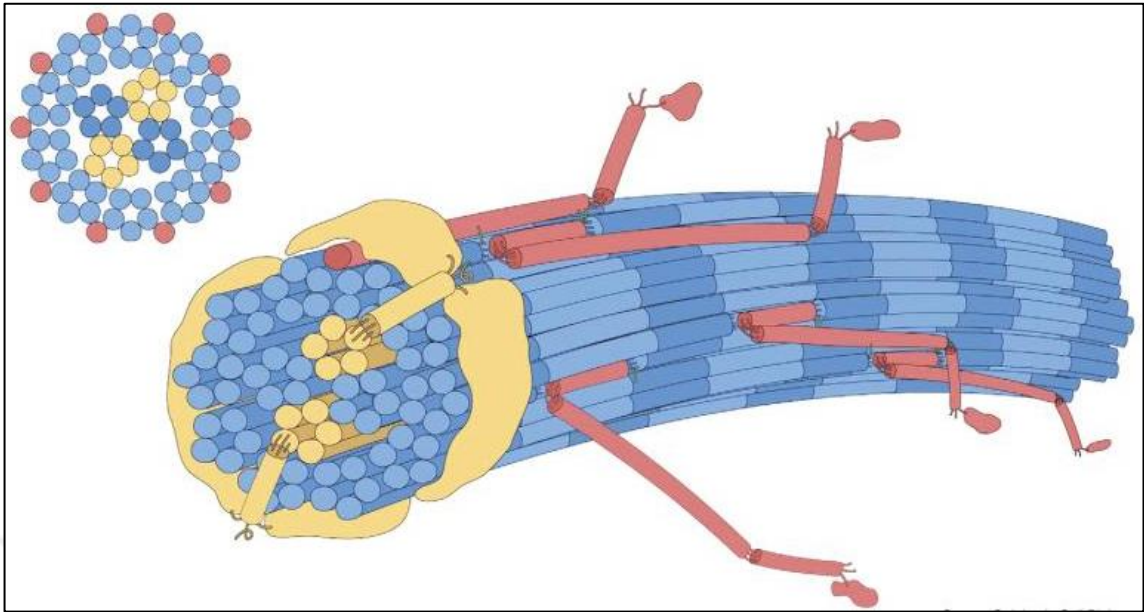


Figure 1.6. Schematic representation of a thin collagen fibril in cartilage (Blue: collagen type II; yellow: collagen type XI; red: collagen type IX) [27]

There is a very delicate balance between the anabolism and catabolism of ECM molecules inside the tissue in pathophysiological conditions. This balance is mainly regulated by the chondrocytes which synthesize not only the ECM molecules, but also the enzymes involved in degradation of ECM, such as matrix metalloprotease (MMP), aggrecanase, and hyaluronidase. The balance between anabolism and catabolism maintains the chondrogenic phenotype, giving the tissue its visco-elastic properties and resistance to shear and compressive forces. Cytokines and growth factors in the synovial fluid contribute to this balance, as well [19]. When this balance is disrupted, the degradation of ECM molecules result in the dedifferentiation of chondrocytes, and hence cartilage degeneration occurs.

1.1.2. Articular Cartilage Defects

In spite of being highly resistive to mechanical forces, articular cartilage has extremely low capability of repairing upon degeneration or destruction. Impacts, shocks, and harsh loading can damage articular cartilage, as well as aging, obesity, and genetic factors that cause malfunction in the joint. These damages will lead to swelling of the joint and dysfunction, resulting in pain and degeneration, which in turn decreases the quality of life of the patient

[30] [31]. Articular cartilage diseases can be categorized as inflammatory (e.g. rheumatoid arthritis), metabolic (e.g. chondrocalcinosis, gout), traumatic (e.g. chondral lesions), and degenerative (e.g. osteoarthritis) [19]. Traumatic and degenerative cartilage diseases do not spontaneously heal, and are the most severe ones that require surgical treatments.

Cartilage defects can be classified into different grades (Grade 1 to Grade 4) with respect to the factors like size and depth (Figure 1.7): In Grade 1 lesions, cartilage is swollen and generally softened. A lesion is called a partial thickness chondral defect, in other words Grade 2; when the diameter of the lesion is less than 1.5 cm. Grade 3 defects, also called full thickness chondral defects denote the lesions with a diameter larger than 1.5 cm. Partial thickness and full thickness defects can be distinguished such that the former one involves only the articular cartilage whereas the latter one goes down to the subchondral bone [11]. Finally, a lesion is called as Grade 4 or as an osteochondral defect when all of the cartilage tissue in the lesion is eroded and the subchondral bone is exposed [1] [32].

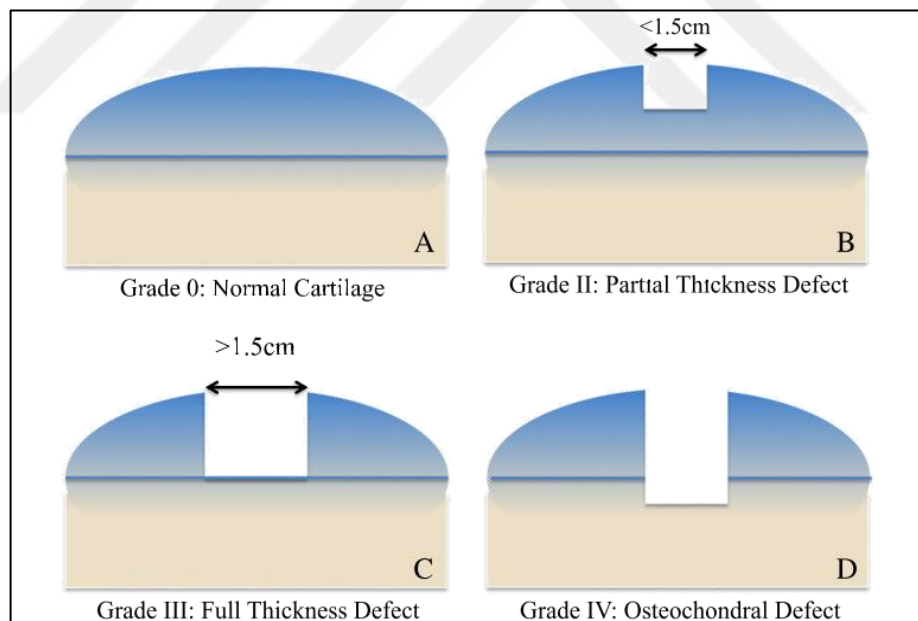


Figure 1.7. Cartilage defects classification from Grade 0 to IV [1]

1.1.3. Treatments for Articular Cartilage Defects

Various treatments have been developed to restore the function of a diseased or damaged cartilage, because the tissue is almost unable to repair itself after a serious injury. Cartilage

repair strategies mostly include surgery and can be generalized as palliative, reparative, and restorative treatment methods, and tissue engineering as an alternative technique [1]. The common principle of these therapies is to relieve the pain while preventing the onset of degenerative joint diseases like osteoarthritis. Choosing the accurate one among these treatments depends on determination of the class of defect and its healing potential, and the effects of the treatment [30]. For instance, while small defects less than 2 mm in diameter (usually Grade 1) can be treated non-surgically using medicines that reduce pain and inflammation, some Grade 2 and Grade 3 defects require surgical treatments [7].

Palliative treatment methods, which are minimally invasive, include arthroscopic debridement, chondroplasty, and abrasion arthroplasty [1]. In arthroscopic debridement, damaged cartilage is removed but not replaced [33]. Chondroplasty involves the use of LASER beams or radiofrequency based probes to smoothen the damaged edges of cartilage. Yet, chondrocyte death can be a risk due to the generation of high temperature during the operation. In abrasion arthroplasty, a rough surface is created in the damaged area in order to form fibrocartilage, though the subchondral bone is not accessed directly. These methods can be utilized in the treatment of partial thickness defects [1].

Being a little more invasive than palliative methods, reparative treatment methods involve microfracture and mosaicplasty. Microfracture (subchondral drilling) involves the stimulation of subchondral bone after drilling so that the MSCs in the bone marrow are stimulated to migrate to the damaged area and form fibrocartilage [34]. In mosaicplasty, osteochondral grafts, either autografts or allografts, which are taken from a donor site, are implanted onto the defected areas. However, some problems may occur with allografts, such as immune reaction, disease transmission, and slower remodeling compared to autografts. Similarly, autografts are associated with donor-site morbidity, and require the patient to suffer from multiple surgeries [35].

Autologous chondrocyte implantation (ACI) and matrix-assisted autologous chondrocyte implantation (MACI) are the actual restorative treatment techniques (Figure 1.8). ACI is the transplantation of healthy chondrocytes from undamaged cartilage to the defected area on the same patient, which is suitable for the revival of defected areas larger than 2 cm² [36]. Nevertheless, there are limiting factors in ACI, such as donor site morbidity and scar tissue formation [37]. Besides, ACI cannot be applied to lesions larger than 4 cm² in size and to severe osteoarthritic lesions due to the difficulties in donor site availability [38]. MACI is a

slightly advanced method of ACI in which autologous chondrocytes are combined with a biodegradable scaffold and then implanted onto the defect site [39]. MACI is also counted as a tissue engineering approach, and Hyalograft® C is a commercially available MACI construct [1].

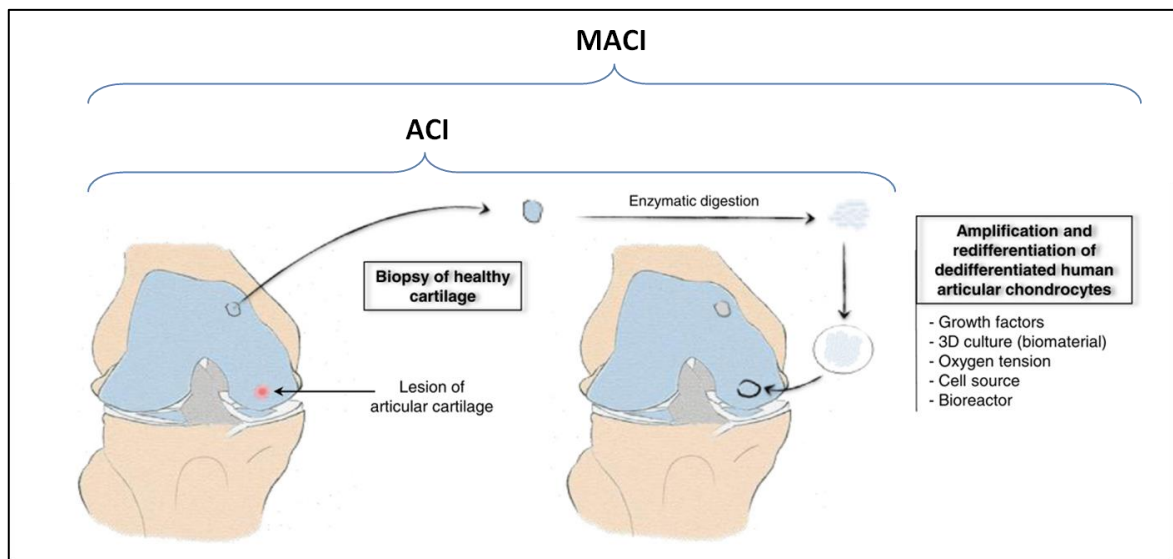


Figure 1.8. Diagram of the ACI and MACI techniques (Modified from Demoor *et al.* [19])

1.2. CARTILAGE TISSUE ENGINEERING

Tissue engineering is a promising alternative to the current treatments of cartilage defects. This technique is aimed at restoring the functions of the degenerated cartilage tissue by combining cells and scaffolds along with proper biological stimulation. The scaffold should be a mechanically stable and biocompatible cell carrier, while the cells should be capable of chondrogenic differentiation when combined with proper stimulants that can be delivered as external proteins or through gene transfer [2].

1.2.1. Cell Sources

The ideal cell source for cartilage tissue engineering is still under investigation. Various cells, from stem cells to more differentiated cells (primary cells or cell lines) are being utilized for this purpose [40] [41] [42] [43]. To our date, studies are mainly exploring the

use of autogenic, allogenic, or xenogenic (animal source) chondrocytes to repair cartilage defects [19]. Chondrocytes are much less multipotent than stem cells; therefore, it is less likely for these cells to differentiate into irrelevant cell types upon administration [44], however, the use of chondrocytes can be disadvantageous to some level due to the low amount of chondrocytes found in the body [45].

Allogenic and xenogenic chondrocytes have the risk of disease transmission and immune rejection when they are used in cartilage regeneration. Autologous chondrocyte isolation can provoke donor site morbidity. Besides, chondrocyte isolation is a very difficult process and chondrocytes can easily lose their chondrogenic phenotype during *in vitro* culture and expansion; in other words, they stop expression of specific markers (collagen type II and aggrecan), converting into bipolar-shaped fibroblastic cells rather than round-shaped chondrocytes, and begin proliferation [16][46]. These dedifferentiated chondrocytes can be induced to redifferentiate by culturing them in three dimensional (3D) scaffolds, or in an environment that includes chondrogenic differentiation factors, e.g. transforming growth factor (TGF)- β [47].

The most alternatively used promising cell types for cartilage regeneration are the MSCs, which can be obtained from the bone marrow, adipose tissue, muscle, synovial membranes, umbilical cord, dental tissues, and cartilage itself [48]. These MSCs, originating from the mesenchyme during development, are pluripotent stem cells that can differentiate into various connective tissue cell types such as bone, cartilage, tendon, and muscle [48]. However, the potential of proliferation and chondrogenic differentiation of MSCs cannot be easily ranked among the origins. Moreover, cell characteristics differ from individual to individual in different cell culture conditions [49] [50].

Induced pluripotent stem (iPS) cells can be considered as another cell source for the cartilage tissue engineering. For instance, fibroblasts can be induced towards chondrogenic lineage when incubated in proper cell culture conditions, through transdifferentiation process [51]. French *et al.* [41] showed that, human dermal fibroblasts produce GAGs and type II collagen when they are cultured in the presence of IGF-1. In another study, dermal fibroblasts obtained from mice were able to regenerate hyaline cartilage after being induced with c-myc, klf-4, and Sox9 transcription factors [52]. These iPS cells do not pose a risk of teratoma formation like embryonic stem cells (ESCs), as they are reprogrammed and differentiated at the same time [19]. Although ESCs seem attractive as a cell source for their unique

properties, there are serious problems in selection and purification of ESCs, as well as ethical issues. Furthermore, ESCs must go through an aggregation stage of embryoid bodies (EBs) before chondrogenic differentiation [48].

In recent years, co-cultures have been investigated for engineering cartilage tissue *in vitro* and *in vivo*, given that co-cultures permit communication between two cell types through molecular signals that promote differentiation and/or redifferentiation of the cells [19]. Some examples of co-culture experiments include dedifferentiated chondrocytes and healthy chondrocytes [53], chondrocytes and osteoblasts [54], chondrocytes and ESCs [42], chondrocytes and MSCs [55], chondrocytes and iPSCs [43].

1.2.2. Scaffolds

In tissue engineering, scaffolds serve as carriers for cells and biological stimulators, as well as influencing the cellular functions. Designing a proper 3D scaffold is the critical point of engineering because the scaffold morphology directly affects the efficiency of tissue regeneration. Specifically, chemical and topographical properties of the scaffolds influence cell-surface interactions [56]. Scaffolding materials are called as biomaterials which should be biocompatible so as to prevent or minimize the potential immune reactions. Biodegradability and bioresorbability are the other important features that should be controlled for accurate cell attachment, proliferation, and migration [57]. Moreover, reproducibility and proper porosity of the scaffold must be considered carefully since the pores should allow the nutrients, water and oxygen delivery to the cells, as well as providing removal of waste materials, similar to the native tissue.

The ideal scaffold should adhere and integrate with the surrounding native cartilage when implanted, and should be compatible with the tissue for mechanical and structural support, preventing tissue deformation and shrinkage [48]. Polymers are generally chosen as the major scaffold biomaterial because of their desirable mechanical properties and flexibility in designing [58].

Scaffolds can be designed to have different forms such as hydrogels, sponges, and macro/micro/nanomeses. In designing a scaffold, the critical point is to achieve a balance with respect to biodegradation. Slow degradation may slow down cartilaginous ECM

production by the cells, whereas fast degradation might be a risk for structure and shape of the construct. Furthermore, the cell seeding method and cell density inside the scaffold must be chosen delicately in order to ensure proper cell-cell and cell-scaffold interactions [19] [48].

1.2.2.1. Natural Biomaterials

Natural biomaterials are polymers which can be derived from proteins, polysaccharides, and microorganisms. Collagen, gelatin, and silk are examples of protein-origin natural biomaterials, whereas chitosan, alginate, hyaluronic acid (HA), cellulose, starch, agarose, and dextrose are some of the polysaccharide-based biomaterials. Polyhydroxyalkanoates (PHAs), poly-hydroxybutyrates (PHBs) are natural polymers that are produced by microorganisms, which also resemble the properties of the native tissue [59].

Natural polymers have many advantages including high biocompatibility, controlled cellular degradability, and biological recognition, however, their mechanical properties may show inconsistency, and batch-to-batch variations can be observed [60]. Especially, natural biomaterials that are designed as hydrogel scaffolds can have poor biomechanical properties, reducing the resistance of the materials against shear and compression forces. Besides, premature resorption may lead to reduction in the shape and size of the construct [19].

Collagen and hyaluronic acid (HA) are the most widely used natural biomaterials that are plentifully found in the connective tissues of mammalians. As a derivative of chitosan, chitin can be extracted from marine organisms and insects. Cellulose is one of the most accessible natural material from almost all organisms, including bacteria and plants [61].

PHAs, PHBs, and Poly (3-hydroxybutyric acid-co-3-hydroxyvaleric acid) (PHBV) are natural polymers that are of bacterial origin and non-toxic, in other words, the products of degradation neither cause accumulation nor increase the acidity in the implant site. Torun Köse *et al.* [62] demonstrated that a hyaline-like cartilage tissue can be obtained when articular chondrocytes are grown on PHBV scaffolds.

Because of their biocompatibility and biodegradability, as well as their unique mechanical structure, silk fibroin scaffolds have been used in skeletal tissue engineering for decades. Three dimensional silk fibroin scaffolds obtained from cocoons of silkworms supported the maintenance of human articular chondrocytes' chondrogenic morphology. They also promoted the deposition of cartilage-specific ECM by MSCs that were seeded on the scaffolds [47].

1.2.2.2. Synthetic Biomaterials

The most widely used synthetic polymers in cartilage tissue engineering are generally the derivatives of poly(α -hydroxyacids) which are namely poly(lactic acid) (PLA), poly(glycolic acid) (PGA), and poly(lactic-co-glycolic acid) PLGA. Poly(ϵ -caprolactone) (PCL), poly(propylene fumarate) (PPF), poly(urethane) (PUR), poly(1,4-butylene succinate) (PBSu), poly(ethylene glycol) (PEG), and polyphosphazene are the other types of synthetic polymers [59].

Synthetic polymers can be designed to have more controllable and precise mechanical properties, in contrast to natural materials [60]. Large-scale production with controlled degradation rate, porosity, and strength is possible with these polymers. Reproducibility and ease of manipulation by changing the polymeric structure and ingredients or processing methods are the main advantages of synthetic materials [63]. Besides, the properties of synthetic scaffolds can be adjusted according to the requirements of application, by altering the functional groups in the backbone or side chain, architecture of polymer (e.g. linear, branched, etc.), and polymeric combinations like polymer blends or copolymers [64]. On the other hand, synthetic polymers have some disadvantages as well as natural polymers. Some of their degradation products may cause an increase in inflammatory response, acidity at the site of implant, and reduction in clearance rates of degradation products [65], which may cause difficulties in control of degradation; hence cell adhesion, signaling, and matrix remodeling in turn [48].

Since the 90s, the most commonly used synthetic biomaterials are PLA, PGA, and PLGA, which are approved by United States Food and Drug Administration (FDA), due to their high biocompatibility and proper biodegradability [66] [67]. In one study, a cartilage tissue with similar properties to native one was generated when chondrocytes were grown on PGA

scaffolds for 20 weeks [68]. Similarly, nanofibrous poly(L-lactide) (PLLA) scaffolds were able to enhance a cartilage-like tissue formation [69]. Being more ductile than PLLA, PBSu, which has been used recently in cartilage and bone tissue engineering applications, is a flexible, biocompatible, bioresorbable and a biodegradable aliphatic polyester that has good mechanical properties and nontoxic degradation products [59]. Oliveira *et al.* (2011) showed that fibre mesh Chitosan/PBS scaffolds provided an enhanced cell integration for bovine articular chondrocytes hence were biocompatible [70]. Following 6 weeks of culture, histological analyses revealed that these scaffolds successfully supported the chondrogenic differentiation. Although Oliveira *et al.* (2011) used polymer extrusion method in preparation of Chitosan/PBS scaffolds, recent evidence suggested that salt leaching may be a more efficient method to prepare 3-D porous PBSu scaffolds [71] [72] [73], which was the method of choice for PBSu:PLLA scaffold preparation in this study.

Scaffold properties can be optimized according to the application by combining various biomaterials, even both natural and synthetic combinations are applicable. Examples include: Hydroxyapatite and chitosan blends for the treatment of osteochondral defects [74], poly (L-lactide-co- ϵ -caprolactone) (PLCL) to enhance chondrogenic differentiation [75], injectible *in situ* forming chitosan and HA hydrogels to support the adhesion and survival of chondrocytes, plus the chondrogenic morphology [76] [77].

1.2.3. Stimulating Factors

Stimulating factors are essential for the cells in cartilage engineering, which will induce, enhance, and accelerate the tissue regeneration. These stimulants can be in the form of biological factors, such as growth and differentiation factors, and gene therapy, or as mechanical stimulants like bioreactors [48]. During the process of engineering, each of these factors or their combinations must be carefully chosen so as to induce chondrogenic differentiation and preservation of the chondrogenic phenotype throughout cartilage regeneration.

1.2.3.1. Soluble Factors

Growth and differentiation factors are usually necessary for the initiation of specific chondrogenic pathways and maintenance of the chondrogenic phenotype. These factors used in cartilage tissue engineering, such as TGF- β , insulin-like growth factor (IGF), bone morphogenetic protein (BMP), fibroblast growth factor (FGF), and other soluble factors like HA, and chondroitin sulfate, are generally added to the culture media or soaked by scaffolds.

Among the most studied differentiation factors in cartilage tissue engineering, the TGF- β family has more than 20 members expressed in mammals [78]. TGF- β 1 initiates the synthesis of chondrogenic proteins (e.g. collagen type II) plus cell proliferation. In addition, it promotes chemotaxis and inflammatory cell activation [79], as well as stimulating chondrogenesis in both embryonic and adult MSCs by boosting proliferation of cells and synthesis of ECM molecules [80].

Being a subclass of TGF family of proteins, bone morphogenetic proteins (BMPs), especially BMP-4, -6, and -7 were suggested to induce the chondrogenic differentiation proven by the increase in the synthesis of collagen type II and proteoglycans [81]. Human BMP-2 (rHuBMP-2) was shown to induce the chondrogenic differentiation of young muscle-derived MSCs in the repair of cartilage tissue [82].

Being 70 aminoacids long molecule, insulin-like growth factor (IGF) 1 (IGF-1), was shown to be related to cartilage repair [83]. It induces chondrogenic differentiation, indicated by the increase in the expression of collagen type II and proteoglycan synthesis [79].

Fibroblast growth factor (FGF) is required during the development and repair of the tissue, in addition to the maintenance of chondrogenic phenotype of monolayer chondrocytes, increasing the chondrocyte proliferation which results in additional ECM deposition and fast repair [78].

1.2.3.2. Mechanical Stimulation

Since cartilage requires mechanical forces not only during development, but also for tissue maintenance, mechanical signals such as compression, tension, shear, can be introduced using bioreactors to enhance cartilage tissue regeneration [83]. These forces result in the

increase of the expression of cartilage specific genes (i.e. type II collagen and aggrecan) [84]. Hydrostatic pressure provides chondroprotective effects and the chondrogenic differentiation of MSCs. Direct compression stimulates and accelerates the chondrocytes and stem cells, improving tissue formation [19].

Bioreactors enhance nutrient transport by supporting the supply of nutrients and oxygen and provide a hydrodynamic environment, along with adjustment of temperature, pH, and mechanical stress in order to promote the synthesis of cartilage specific ECM within the scaffolds before implantation [3] [85]. On the contrary, high seeding density is required in bioreactor culture for the formation of a tissue [48].

Bioreactors that are currently being used for cartilage tissue engineering can be classified as: parallel-plate bioreactors, rotating wall bioreactors, concentric cylinder bioreactor, and wavy-wall bioreactor (WWB). The novel bioreactors are designed to decrease fluid shear stresses and increase axial mixing. In addition, spinner flasks and perfusion bioreactors provide better cell adhesion and distribution [48] [85]. When the direct perfusion bioreactors are used for perfusing a cell suspension directly through the pores of a 3-D scaffold, homogeneously seeded constructs can be obtained, which is essential for thick scaffolds particularly [86]. A successful study was carried out by Pei *et al.*, [87] who engineered a hyaline cartilage tissue in a rotating bioreactor system using synovium-derived stem cells (SDSCs) that are of mesenchymal origin.

1.2.3.3. Gene Therapy

Cells can be genetically-engineered to express essential biological molecules through gene transfer. Both viral (lenti-/retro-/adenoviral) and non-viral (polymers and liposomes) techniques are appropriate for gene transfer via transduction. The efficiency of transduction is quite high with viral vectors but the risk of disease transmission is high as well, but in contrast, non-viral vectors display lower transfection efficiencies and have fewer safety issues [48]. In addition to vectors, micro-RNAs to control chondrocyte genes and small interfering RNAs to silence ECM degrading enzymes can be used [19]. The first clinical gene therapy application for cartilage regeneration was done in 1996, in which a vector encoding an anti-arthritis cytokine was given to the joints of rheumatoid arthritis patients [88].

Lentiviral vectors are able to infect both dividing and non-dividing cells, different from the retroviruses which can only infect dividing cells. They can integrate into the genome of the infected cell which assures that the new generations will also contain the therapeutic gene in their genomes. In addition, lentiviral vectors are more stable than the other viral vectors [89]. Lentiviral transduction is generally performed by incubating the cells with the medium containing the viruses. However, incubation alone with the viruses results in low transduction efficiencies; therefore a cationic polymer is added in order to increase the efficiency of transduction. Polybrene (hexadimethrine bromide) is a cationic polymer that is commonly used in lentiviral and retroviral transduction. It aids the viruses in adsorbing onto the cell membrane simply by neutralizing the electrostatic repulsion between the cell surface and the viruses, although it inhibits the MSC proliferation after lentiviral transduction [90]. Therefore, another cationic polymer, Protamine Sulfate (PS), which was shown to be non-toxic and efficient [91], is preferred in lentiviral transduction of MSCs.

1.3. TISSUE TRANSGLUTAMINASE (TRANSGLUTAMINASE-2)

Transglutaminases are a family of calcium-dependent enzymes responsible for the post-translational covalent crosslinking of proteins by creating amide bonds between glutamine and lysine residues (Figure 1.9) [92]. These bonds are quite resistant to proteolytic degradation, which provide the formation of stable polymeric networks without the need of additional factors [93]. The crosslinked products are often of high molecular mass and accumulate in different tissues for different functions, such as epidermal differentiation, seminal vesicle coagulation, fibrin-clotting, and wound healing [94].

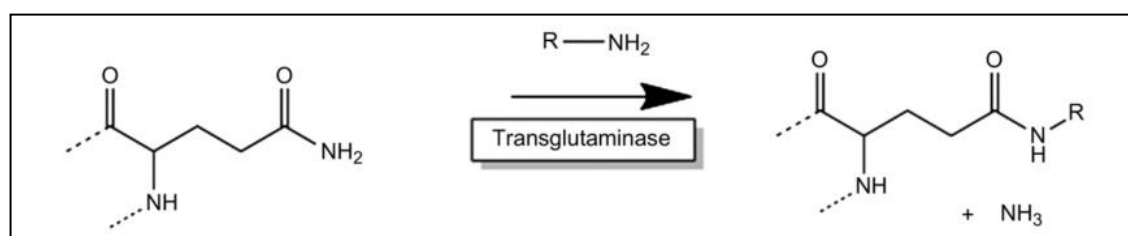


Figure 1.9. Transamidation reaction mechanism of transglutaminases [93]

There are different forms of transglutaminases with different functions, which are listed in Table 1.1. Among them, transglutaminase-2 (TG2) or tissue transglutaminase (tTG) is a 77 kDa and 686 amino acids long (in humans) GDP-GTP binding enzyme with ubiquitous tissue expression and pleiotropic functions [95]. TG2 has four domains with distinct structures: a β -sandwich domain at N-terminus, exposing fibronectin and integrin binding sites, a catalytic core domain, and two β -barrel domains at C-terminus containing GTP/GDP binding and phospholipase C (PLC) binding sites [96].

As illustrated in Figure 1.10. TG2 can be located in cytosol, nucleus, cell membrane, and extracellular matrix [97]. It is mostly found in the cytosol where it catalyzes the covalent crosslinking of proteins with an ϵ -(γ -glutamyl)-lysine (isopeptidyl) bond in a calcium dependent manner. This irreversible crosslinking is formed *in vivo*, between a glutamine residue (glutamine donor) of one protein and a lysine residue (glutamine acceptor) of another protein. TG2 also acts in transamidation by incorporating primary amines into proteins [94], which depends on Ca^{2+} binding/GTP dissociation. Binding of Ca^{2+} or GTP triggers a conformational change in the protein structure. When the enzyme is Ca^{2+} bound, it transforms into open and active form, exposing the active site cysteine residue which triggers the transamidation activity [98]. On the contrary, GTP binding suppresses the transamidation activity by reducing the affinity of the enzyme for calcium, hence driving the enzyme into close and inactive form, preventing the protein substrates from entering the active site [99]. TG2 is present in its closed conformation on the cell membrane and cytosol, functioning as deaminase, GTPase, protein kinase and protein disulphide isomerase [100] to regulate intracellular Ca^{2+} homeostasis, cell proliferation and apoptosis through GTP binding [101].

Table 1.1. The family of transglutaminases [102]

Tgase type	Synonyms	Residues and molecular mass in kDa	Gene name	Gene map locus	Function
Factor XIII A	Fibrin stabilizing factor	732 (83)	F13A1	6p24-25	Blood clotting, wound healing
Type 1 Tgase	Keratinocyte Tgase	814 (90)	TGM1	14q11.2	Cell envelope formation in the

					keratinocyte differentiation
Type 2 Tgase	Tissue Tgase	686 (80)	TGM2	20q11-12	Cell death, differentiation, adhesion, matrix stabilization
Type 3 Tgase	Epidermal Tgase	692(77)	TGM3	20q11-12	Cell envelope formation in terminal keratinocyte differentiation
Type 4 Tgase	Prostate Tgase	683(77)	TGM4	3q21-22	Reproductive function
Type 5 Tgase	Tgase X	719 (81)	TGM5	15q15.2	Epidermal differentiation
Type 6 Tgase	Tgase Y	-	TGM6	20q11 15	Not characterized
Type 7 Tgase	Tgase Z	710(80)	TGM7	15q15.2	Not characterized

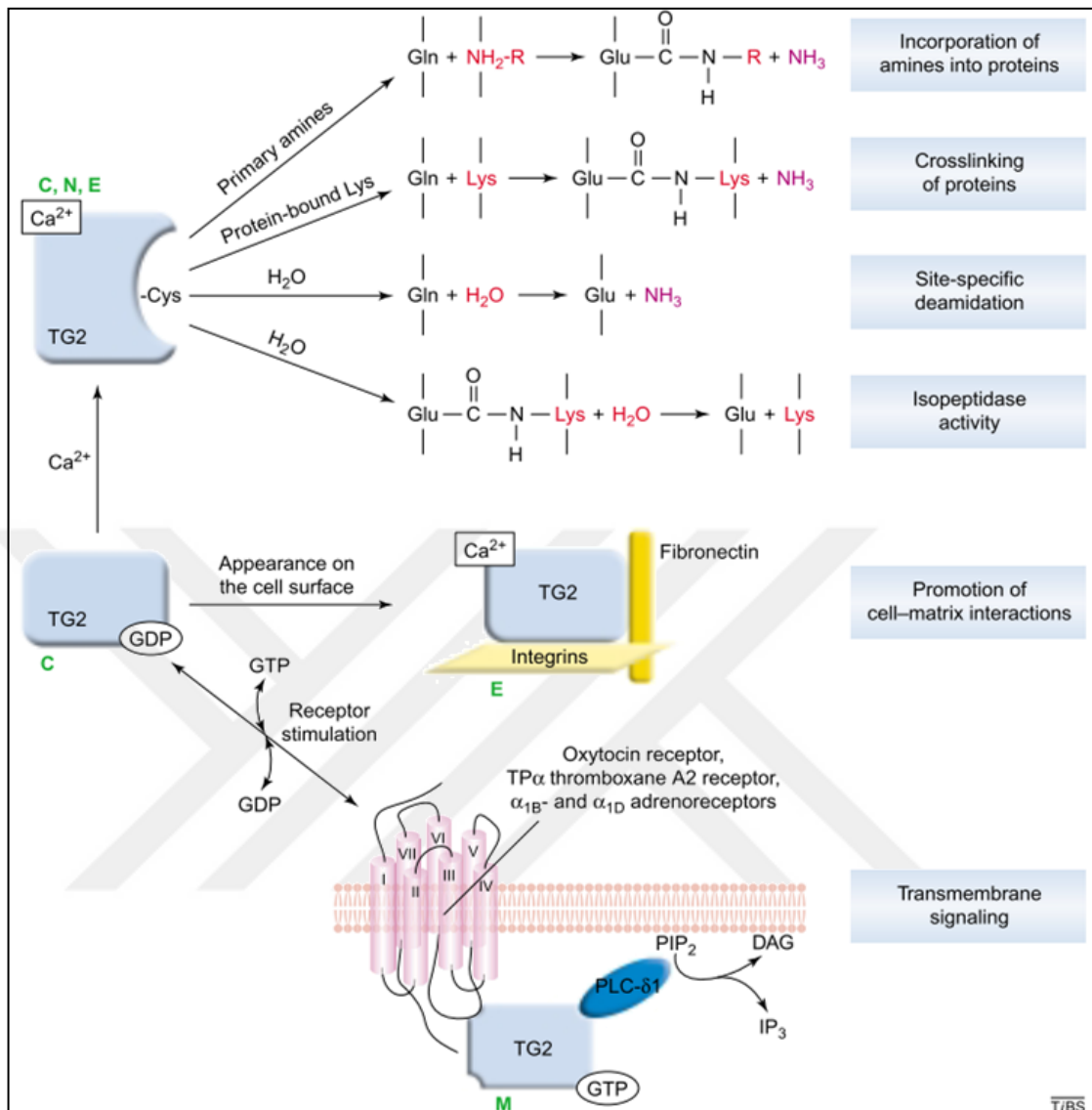


Figure 1.10. Summary of the reactions that are catalyzed by TG2, in the cytosol (C), nucleus (N), cell membrane (M) and ECM (E). All of these activities, except isopeptidase, take place in intact cells [97].

Externalized TG2 can be located both on the cell surface and on ECM where it functions as a coreceptor for fibronectin (FN) in cell adhesion associated with integrins [103]. Having a high affinity for FN, TG2 can make a complex with FN in the ECM via the 42 kDa gelatin-binding domain of FN [104], acting as a scaffold when it is bound with integrin [99]. The interaction of TG2 with integrin occurs mainly at the extracellular domains of integrin β subunits, which aids in adhesion, spreading and motility of cells independent of its crosslinking activity [97]. As a result of covalent interaction with the $\beta 1$, $\beta 3$ and $\beta 5$ integrin

subunits, TG2 in the cell surface forms stable ternary complexes with integrins and FN [104][105][106]. Interaction between integrin and TG2 can further be stabilized by the formation of disulfide bonds [107]. The TG2-FN complex induces cell adhesion by binding to the heparan sulfate chains on syndecan-4 (a cell membrane proteoglycan), which is independent of RGD-binding [108]. A study by Song *et al.* [103] suggested that genetically engineering MSCs to overexpress TG2 enhanced the MSCs attachment, spreading and migration onto a matrix, as well as the assembly of focal adhesion complexes *in vitro*.

1.3.1. Transglutaminase-2 in ECM Regulation and Cartilage Tissue

When externalized from the cells, TG2 is actively involved in ECM remodeling in different tissues by crosslinking various extracellular molecules including collagen, FN, fibrinogen, vitronectin, osteonectin, osteopontin, osteocalcin, and laminin [102]. In addition, it is involved in the covalent crosslinking of growth factors like TGF- β [109–112]. By crosslinking latent TGF β -binding protein-1 (LTBP-1), TG2 promotes the synthesis and activation of TGF- β 1 in NF- κ B-dependent manner [113]. TGF β enhances the binding of FN to the cell surface, which is mediated by α 5 β 1 integrin [104], regulating the synthesis and deposition of ECM molecules and the expression of TG2 on cell surface. This results in a positive feedback loop in which TG2 functions in the conversion of latent TGF- β 1 (~300 kDa) into active form (25 kDa) that induces TG2 expression in turn [114] [115]. TGF- β is expressed at high levels in normal cartilage tissue, inducing the synthesis of cartilage ECM molecules [116]. During chondrogenesis the expression of transcription factor Sox9, which is required for the expression of cartilage specific molecules such as collagen type II and aggrecan, is controlled by TGF- β [117]. Considering that TGF- β is an inducer of chondrocyte differentiation, TG2 must also contribute to the process as well as to the maintenance of tissue integrity, since cartilage is constantly exposed to mechanical stress [118].

In cartilage tissues, only two of the transglutaminases are expressed: TG2 and factor XIII. At the early stages of chondrocyte differentiation TG2 is not present, while its expression starts before chondrocyte hypertrophy, suggesting that TG2 stimulates the transition of chondrocytes from mature to pre-hypertrophic state of differentiation [119]. During bone development, TG2 induces osteogenic differentiation and matrix mineralization [35]. TG2

has been explored to crosslink scaffolds and chondrogenic differentiation factors onto scaffolds. In 1997, Jürgensen *et al.* [120] proposed TG2 as “biological glue” for cartilage tissue instead of the commercial fibrin glue Tissucol©. Human recombinant TG2 was reported for its use in crosslinking elastin-like polypeptide hydrogels designed for cartilage repair, in which cells maintained their chondrocytic phenotype *in vitro*, and deposited cartilage-specific ECM [121]. Crosslinking of collagen type XI by guinea pig liver TG2 on 3D nanofibrous PLLA scaffolds were reported to enhance the attachment and chondrogenic differentiation of human MSCs [122]. Similarly, TG2 was used to crosslink TGF- β 3 on electrospun nanofibrous PLLA/collagen type II scaffolds to induce human MSC differentiation towards chondrogenic lineage [110]. It was reported that crosslinking of TGF- β 3 was irreversible and induced the chondrogenic differentiation of human MSCs, which could be a solution to the cost problem of TGF- β 3 addition to the chondrogenic differentiation media. These findings suggest that TG2 can be an important factor to consider in cartilage tissue engineering applications.

1.3.2. Transglutaminase-2 Isoforms

The full length transcript of TGM2 was first identified by Gentile *et al.* in 1991 [95]. Up to date, six different alternatively spliced TG2 isoforms of different C-termini have been identified. The names of the isoforms and their properties are given in Table 1.2. Variant 1 encodes the longest isoform with 687 amino acids, while variant 2 differs in 3'UTR, resulting in a peptide of 548 amino acids long [123]. The third variant was found to be 349 amino acids long and 38 kDa, being much smaller than the other transcripts [124]. The molecular weights of isoforms 4a and 4b are similar to that of the full length transcript, but again their C-termini are shorter [125]. Predicted variants X1 and 5 are reported in the NCBI website (NC_000020.11). Figure 1.11 illustrates the comparison of transcript variants in terms of amino acid sequences.

Table 1.2. Classification of TG2 isoforms

Isoform (variant) name	Alias	Molecular weight (kDa)	Peptide length (aa)	NCBI Accession number
TGM2_v1	Isoform 1	75	687	NM_004613.2
TGM2_v2	Isoform 2, TGH, Tgase S, TG2-S	62	548	NM_198951.1
TGM2_v3	Isoform 3, TGH2	38	349	S81734.1
TGM2_v4a	tTGv1	75	674	N/A
TGM2_v4b	tTGv2	70	645	N/A
Variant X1	Isoform c	N/A	606	NC_000020.11
Variant 5	Isoform d	N/A	627	NC_000020.11

In almost all human tissues, expression level of these isoforms was found correlated but lower than that of full-length transcript. The highest expression belonged to TGM2_v1, followed by TGM2_v2, then TGM2_v4b, TGM2_v4a and TGM2_v3. Similarly, among the isoforms, the expression of TGM2_v2 had the most similar trend to that of full length transcript, whereas TGM2_v3 expression had almost no correlation [126].

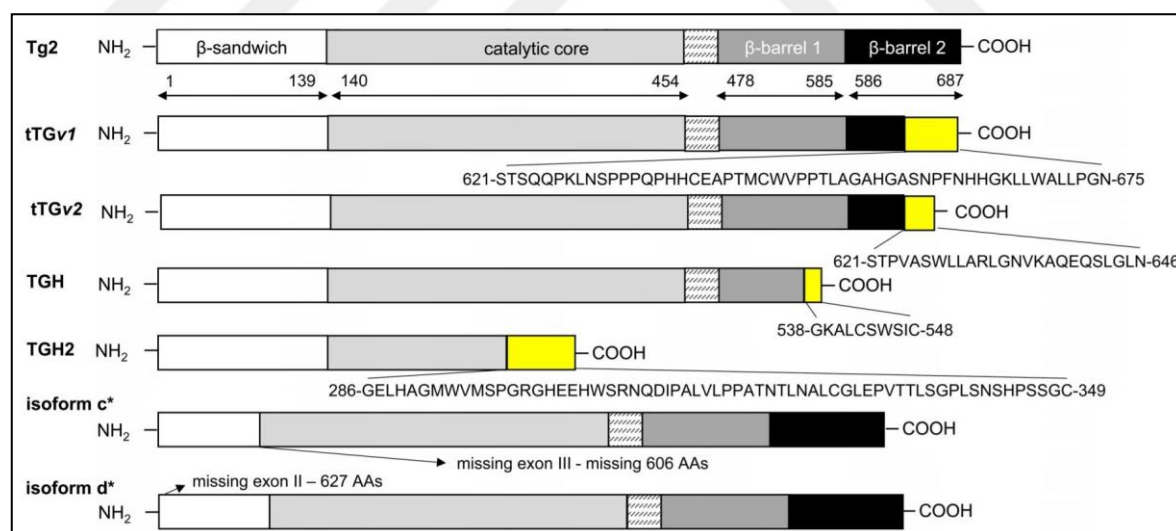


Figure 1.11. Schematic representation of TG2 transcript isoforms. Arrows show the amino acid boundaries of each domain. The white, grey, and black boxes show the shared amino acid sequences, while the yellow boxes represent the alternating C-termini (Modified from Bianchi *et al.* [127]).

The second isoform of TG2, also known as the short form, is named as TG2-S. This transcript only differs from the full length (long form) in C-terminus, which results in the loss of GTP-binding Arginine-580 residue [128], as seen in Figure 1.12, and possess lower transamidation activity (<5 per cent residual) than the long form [115]. In 2006, Antonyak *et al.*[129] showed that the short form of TG2 caused cell death in fibroblasts via induction of apoptosis, yet the mechanism underlying this induction remains unclear. It was only found that this apoptotic activity is not related to the transamidation activity of TG2-S. On the other hand, TG2-S was shown to induce differentiation of neuroblastoma cells, while the long form suppressed this process [128]. Besides, in the same study, TG2-S was presented as a candidate for its potential use for the treatment of cancers that occur due to Myc oncoprotein overexpression. GTP-binding domain of TG2 is responsible for the epithelial-to-mesenchymal transition (EMT) in mammary epithelial cells [33] and epidermal cancer stem cells [34], and GTP-binding-deficient form of TG2 was shown to reduce stem cell properties of epithelial cells without change in their differentiation ability [33]. The role of TG2-S in MSCs differentiation is still unclear. These conflicting findings make the short form of TG2 attractive for investigation in different cell types since the intracellular GTP level of a cell determines its fate towards apoptosis or differentiation [130].

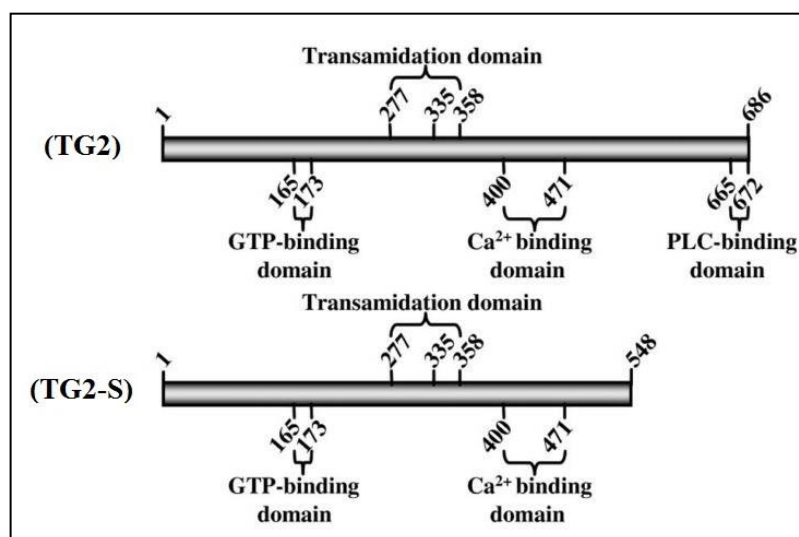


Figure 1.12. Functional domains of full length TG2 (upper) and TG2-S (lower) transcripts.

The numbers represent the positions of amino acids (Modified from Antonyak *et al.*, [129]).

1.4. AIM OF THE STUDY

In our study, cartilage tissue regeneration was aimed by using TG2-S-transduced MSCs derived from bone marrow of rats and grown on poly(butylene succinate) and poly(L-lactide) blend scaffolds. Bone marrow derived MSCs are proven to be good candidates for cartilage engineering [131], and PBSu and PLLA have many successful uses in this area [70][73][132][133]. In cartilage tissue, the ECM is the main component; if the ECM is damaged, so does the tissue. Therefore, ECM formation is one of the major factors to be considered in tissue engineering of cartilage. Due to the ECM crosslinking ability of TG2, studies have been exploring the use of TG2 for crosslinking of scaffolds as mentioned in section 1.3.2, indicating that TG2 could be examined for its use in cartilage tissue engineering. A major drawback of addition of TG2 on the scaffold could be the gradual clearance of the enzyme from the scaffold since it has a short half-life of approximately 11 h [134]. We hypothesized that genetically engineering bone marrow-derived MSCs to express TGM2_v2 gene would overcome this problem, providing better cell-ECM interactions due to enhanced cell-matrix connections, along with increase in chondrogenic differentiation capacity of MSCs due to deficiency in GTP-binding. Continuous endogenous expression of TGM2_v2 could eliminate the problem with the addition of high cost differentiation factors like TGF- β s. In addition, since the short form of TG2 has reduced crosslinking capacity in comparison to long form, the possibility of osteogenic differentiation and hypertrophy formation would be reduced.

The novelty of this study comes from the fact that TG2-S has never been studied in cartilage tissue engineering. Besides, this is the first study in which MSCs were transduced with TGM2_v2.

2. MATERIALS

2.1. PRODUCTION OF LENTIVIRAL PLASMIDS AND LENTIVIRUSES

- LB Broth, Miller (Acumedia, Neogen, USA)
- LB Agar, Miller (Acumedia, Neogen, USA)
- Ampicillin (100 mg/mL) (Sigma Aldrich, USA)
- Bacterial stock (E.coli with different plasmids: eGFP & hTGM2-variant 2) (VectorBuilder, Cyagen Biosciences, USA)
- PureLink® HiPure Plasmid DNA Purification Kit, Midiprep (Invitrogen, Thermo Fisher Scientific, USA)
- Isopropanol (Sigma Aldrich, USA)
- Ethanol (Sigma Aldrich, USA)
- Calcium chloride (CaCl₂) (Sigma Aldrich, USA)
- Sodium chloride (NaCl) (Sigma Aldrich, USA)
- Di-Sodium hydrogen phosphate (Na₂HPO₄) (Sigma Aldrich, USA)
- HEPES buffer, 1M (Sigma Aldrich, USA)
- pMD2.G plasmid (envelope) (Addgene, USA)
- psPAX2 plasmid (packaging) (Addgene, USA)
- Virion-producing Human Embryonic Kidney cell line (HEK-293T) (ATCC, USA)
- Dulbecco's Modified Eagle Medium (DMEM) high glucose + GlutaMAX™ (Gibco, Thermo Fisher Scientific, USA)
- Penicillin/Streptomycin solution (Pen/Strep) (Thermo Fisher Scientific, USA)
- Fetal Bovine Serum (FBS) (Gibco, Thermo Fisher Scientific, USA)
- Dulbecco's Phosphate Buffered Saline (DPBS) (Thermo Fisher Scientific, USA)
- Fluorescence Microscope (Axio Vert.A1, Carl Zeiss, Germany)
- Syringe filter (0.45 µm) (Merck Millipore, USA)
- High-Speed PPCO Centrifuge Tubes (Beckman Coulter, USA)
- Ultracentrifuge (Avanti® J-25, Beckman Coulter, USA)

2.2. ISOLATION OF MSCS FROM RAT BONE MARROW

- Spraque-Dawley rats (10 weeks old)
- Glass carbondioxide chamber
- DMEM high glucose + GlutaMAX™ (Gibco, Thermo Fisher Scientific, USA)
- DMEM alpha modification + GlutaMAX™ (Gibco, Thermo Fisher Scientific, USA)
- Penicillin/Streptomycin solution (Gibco, Thermo Fisher Scientific, USA)
- Surgical scissors
- Surgical forceps
- Surgical clamps
- Surgical blades
- Sterile syringes (Isolab, Germany)
- Centrifuge tubes (Thermo Fisher Scientific, USA)
- Centrifuge (Sigma, Germany)
- Carbondioxide incubator (Steri-Cycle CO₂ Incubator, Thermo Fisher Scientific, USA)
- Laminar flow hood (TELSTAR Bio-II-A, Class II Cabinet, Telstar Life Sciences, Spain)

2.3. GROWTH OF RBMSCS

- DMEM alpha modification + GlutaMAX™ (Gibco, Thermo Fisher Scientific, USA)
- Penicillin/Streptomycin solution (Thermo Fisher Scientific, USA)
- Fetal Bovine Serum (FBS) (Gibco, Thermo Fisher Scientific, USA)
- Carbondioxide incubator (Steri-Cycle CO₂ Incubator, Thermo Fisher Scientific, USA)
- Laminar flow hood (TELSTAR Bio-II-A, Class II Cabinet, Telstar Life Sciences, Spain)

2.4. TRANSDUCTION OF RBMSCS

- Rat bone marrow derived mesenchymal stem cells
- DMEM alpha modification + GlutaMAX™ (Gibco, Thermo Fisher Scientific, USA)
- Penicillin/Streptomycin solution (Thermo Fisher Scientific, USA)
- Fetal Bovine Serum (FBS) (Gibco, Thermo Fisher Scientific, USA)
- Blasticidin S HCl (Thermo Fisher Scientific, USA)
- Dulbecco's Phosphate Buffered Saline (DPBS) (Thermo Fisher Scientific, USA)
- Protamine Sulfate (Sigma Aldrich, USA)
- Fluorescence Microscope (Axio Vert.A1, Carl Zeiss, Germany)

2.5. ISOLATION AND GROWTH OF RAT KNEE CHONDROCYTES

- Spraque-Dawley rats (10 weeks old)
- Glass carbondioxide chamber
- DMEM high glucose + GlutaMAX™ (Gibco, Thermo Fisher Scientific, USA)
- DMEM alpha modification + GlutaMAX™ (Gibco, Thermo Fisher Scientific, USA)
- Penicillin/Streptomycin solution (Thermo Fisher Scientific, USA)
- Fetal Bovine Serum (FBS) (Gibco, Thermo Fisher Scientific, USA)
- Collagenase Type II (Gibco, Thermo Fisher Scientific, USA)
- DMEM F12-Ham (Gibco, Thermo Fisher Scientific, USA)
- L-glutamine (Gibco, Thermo Fisher Scientific, USA)
- Surgical scissors
- Surgical forceps
- Surgical clamps
- Surgical blades
- Sterile syringes
- Centrifuge tubes (Thermo Fisher Scientific, USA)
- Centrifuge (Sigma, Germany)
- Carbondioxide incubator (Steri-Cycle CO₂ Incubator, Thermo Scientific)

2.6. TGM2_V2 GENE EXPRESSION ANALYSIS

- Dulbecco's Phosphate Buffered Saline (DPBS) (Thermo Fisher Scientific, USA)
- GeneJET RNA Purification Kit (Thermo Fisher Scientific, USA)
- Sensiscript® RT Kit (Qiagen, Germany)
- Oligo(dT)₁₈ primer, 100 µM (Fermentas, Thermo Fisher Scientific, USA)
- RiboLock™ RNase Inhibitor, 40u/µL (Fermentas, Thermo Fisher Scientific, USA)
- Maxima SYBR Green, ROX qPCR Master Mix, 2X (Thermo Fisher Scientific, USA)
- Human TGM2, Hs_TGM2_1_SG QuantiTect Primer Assay (Qiagen, Germany)
- Rat 18SrRNA, Rn_Rnr1_1_SG QuantiTect Primer Assay (Qiagen, Germany)
- Nanodrop (Nanodrop 2000, Thermo Fisher Scientific, USA)
- CFX Touch™ Real Time PCR Detection System (Bio-Rad, USA)

2.7. TG2-S PROTEIN ANALYSIS

- RIPA Lysis Buffer System, 1X (Santa Cruz Biotechnology, USA)
- Bolt 4-12% Bis-Tris Plus (Novex, Thermo Fisher Scientific, USA)
- Bolt MES SDS Running Buffer (20X) (Novex, Thermo Fisher Scientific, USA)
- Bolt LDS Sample Buffer (4X) (Novex, Thermo Fisher Scientific, USA)
- Bolt Sample Reducing Agent (10X) (Novex, Thermo Fisher Scientific, USA)
- Tris Hydrochloride (Tris HCl) (Fisher Scientific, USA)
- Tween® 20 (AppliChem, USA)
- SeeBlue® Plus2 Prestained Standard (Novex, Thermo Fisher Scientific, USA)
- MagicMark™ XP Western Protein Standard (Novex, Thermo Fisher Scientific, USA)
- iBlot®2 PVDF Regular Stacks (Novex, Thermo Fisher Scientific, USA)
- SMART™ micro BCA Protein Assay Kit (Intron Biotech, Korea)
- Guinea pig liver TG2 (Sigma Aldrich, USA)
- Mouse monoclonal IgG1 anti TG2 (clone CUB7402), 0.2 mg/mL (Thermo Fisher Scientific, USA)

- Mouse monoclonal IgG1 anti Beta-actin (clone C4), 0.2 mg/mL (Santa Cruz Biotechnology, USA)
- Goat anti-mouse IgG-HRP, 0.4 mg/mL (Santa Cruz Biotechnology, USA)
- SuperSignal® West Pico Complete Mouse IgG Detection Kit (Thermo Fisher Scientific, USA)

2.8. FLOW CYTOMETRY

- Dulbecco's Phosphate Buffered Saline (DPBS) (Thermo Fisher Scientific, USA)
- Trypsin-EDTA (0.25%), phenol red (1X) (Thermo Fisher Scientific, USA)
- Polystyrene Round-Bottom Tubes (BD Biosciences, USA)
- FITC Mouse Anti-Rat CD90 (BD Biosciences, USA)
- FITC Hamster Anti-Rat CD29 (BD Biosciences, USA)
- PE Mouse Anti-Rat CD31 (BD Biosciences, USA)
- PE-Cy5 Mouse Anti-Rat CD45 (BD Biosciences, USA)
- FACSCalibur™ Flow Cytometry System (BD Biosciences, USA)

2.9. CELL PROLIFERATION ASSAY

- CellTiter 96® Aqueous One Solution Cell Proliferation Assay (Promega, USA)
- Elisa Plate Reader (Elx800, Bio-Tek, USA)

2.10. PREPARATION AND CHARACTERIZATION OF SCAFFOLDS

- Poly (1,4-butylene succinate) 1,6-diisocyanatohexane-extended (PBSu, Sigma Aldrich, USA)
- Poly (L-lactide-co-D, L-lactide) 70:30 (AppliChem, USA)
- Dichloromethane (DCM) (Merck, USA)
- Sodium chloride crystals (diameters of 300-500 µm) (Sigma Aldrich, USA)
- Lyophilizator (Savant Modulyo Freeze Drying Systems, Thermo Fisher Scientific, USA)

- Scanning Electron Microscope (EVO, Carl Zeiss, Germany)
- Cacodylic Acid Sodium Salt Trihydrate (AppliChem, USA)
- Glutaraldehyde Solution, Grade I, 25% (Sigma Aldrich, USA)
- Fluorescence Microscope (Axio Vert.A1, Carl Zeiss, Germany)

2.11. DIFFERENTIAL GENE EXPRESSION ANALYSIS

- Dulbecco's Phosphate Buffered Saline (DPBS), without calcium and magnesium ions (Thermo Fisher Scientific, USA)
- GeneJET RNA Purification Kit (Thermo Fisher Scientific, USA)
- iScript cDNA synthesis kit (Bio-Rad, USA)
- Maxima SYBR Green, ROX qPCR Master Mix, 2X (Thermo Fisher Scientific, USA)
- Rat 18SrRNA, Rn_Rnr1_1_SG QuantiTect Primer Assay (Qiagen, Germany)
- Primers for Col2a1, Col1a1, Agc, Sox9, Col10A1 (Macrogen, South Korea)
- Nanodrop (Nanodrop 2000, Thermo Fisher Scientific, USA)
- CFX Touch™ Real Time PCR Detection System (Bio-Rad, USA)

2.12. IMMUNOFLUORESCENCE ASSAYS

- Dulbecco's Phosphate Buffered Saline (DPBS), without calcium and magnesium ions (Thermo Fisher Scientific, USA)
- Formaldehyde (Sigma Aldrich, USA)
- Tween® 20 (AppliChem, USA)
- Fetal Bovine Serum (Thermo Fisher Scientific, USA)
- TGM2 Mouse Monoclonal Antibody (CUB 7402) (Thermo Fisher Scientific, USA)
- Monoclonal Collagen Type I, produced in mouse, clone COL-1, ascites fluid (Sigma Aldrich, USA)
- Aggrecan antibody (H-300) rabbit polyclonal IgG (Santa Cruz Biotechnology, USA)
- COL10A1 Antibody goat polyclonal IgG (Santa Cruz Biotechnology, USA)
- COL2A1 antibody (M2139) mouse monoclonal IgG2b (Santa Cruz Biotechnology, USA)

- Goat anti-Rabbit IgG (H+L) Secondary Antibody, Alexa Fluor® 647 conjugate (Rabbit IgG (H+L) Polyclonal Secondary Antibody for IF, Flow) (Thermo Fisher Scientific, USA)
- Goat anti-Mouse IgG (H+L) Secondary Antibody, Alexa Fluor® 488 conjugate (Mouse IgG (H+L) Polyclonal Secondary Antibody for IF, ICC, Flow) (Thermo Fisher Scientific, USA)
- Rabbit anti-Goat IgG (H+L) Secondary Antibody, Alexa Fluor® 568 conjugate (Goat IgG (H+L) Polyclonal Secondary Antibody for IF, Flow) (Thermo Fisher Scientific, USA)
- 4',6-Diamidino-2-phenylindole dihydrochloride powder, BioReagent, suitable for cell culture, $\geq 98\%$ (HPLC and TLC), suitable for fluorescence (Synonym: 2-(4-Amidinophenyl)-6-indolecarbamide dihydrochloride, DAPI dihydrochloride) (Sigma Aldrich, USA)
- Mounting medium (ibidi, Germany)
- Fluorescence Microscope (AXIO, Vert.A1, Carl Zeiss, Germany)
- Confocal microscope (LSM 700, Carl Zeiss, Germany)

2.13. ALIZARIN RED STAINING

- Dulbecco's Phosphate Buffered Saline (DPBS), without calcium and magnesium ions (Thermo Fisher Scientific, USA)
- Formaldehyde (Sigma Aldrich, USA)
- Tween® 20 (AppliChem, USA)
- Alizarin Red S Solution, 1X (Merck Millipore, USA)
- Distilled water

2.14. ALCIAN BLUE STAINING

- Dulbecco's Phosphate Buffered Saline (DPBS), without calcium and magnesium ions (Thermo Fisher Scientific, USA)
- Formaldehyde (Sigma Aldrich, USA)

- Tween[®] 20 (AppliChem, USA)
- Alcian Blue PAS Stain Kit (Atom Scientific, UK)
- Alcian Blue, pH 2.5 Kit (Bio-Optica, Italy)
- Distilled water

2.15. MECHANICAL ANALYSIS

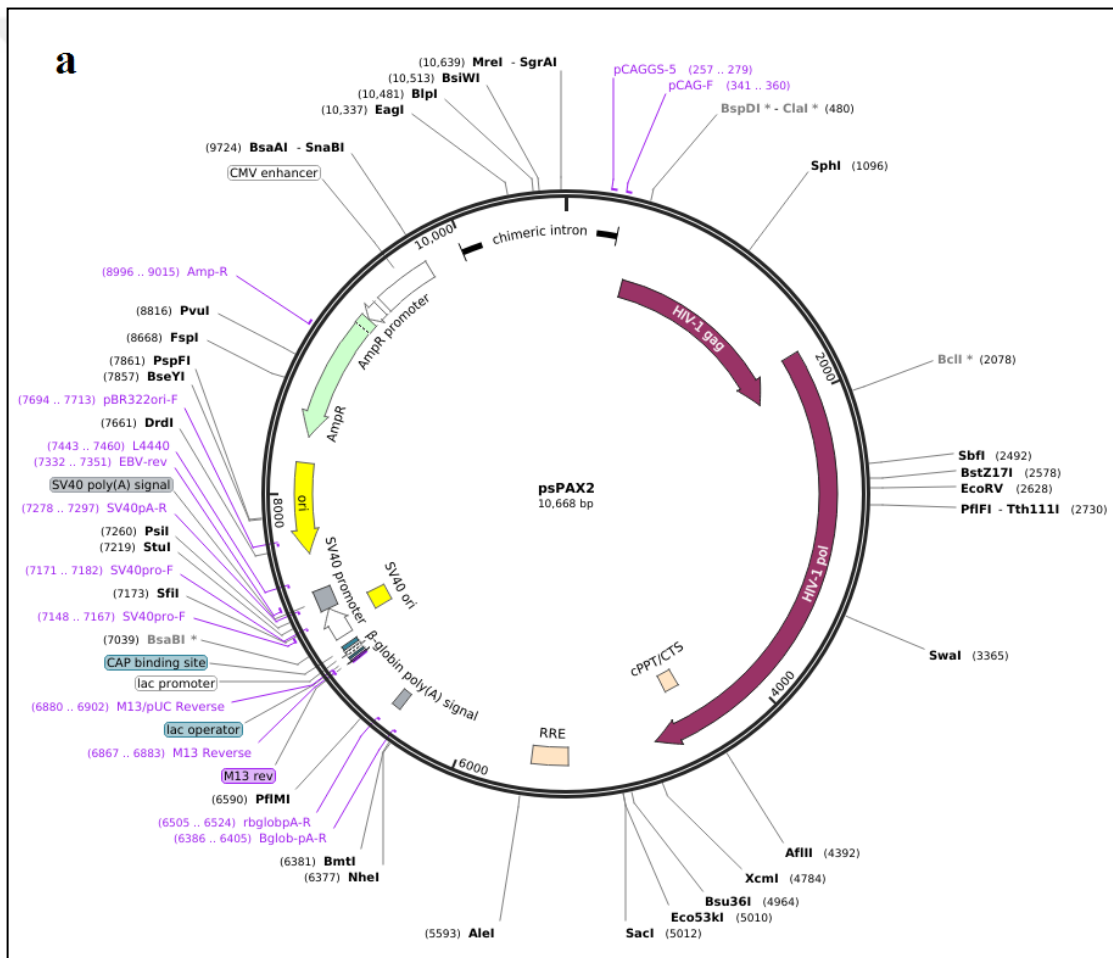
- Instron Universal Testing System (ITW, USA)
- Filter paper

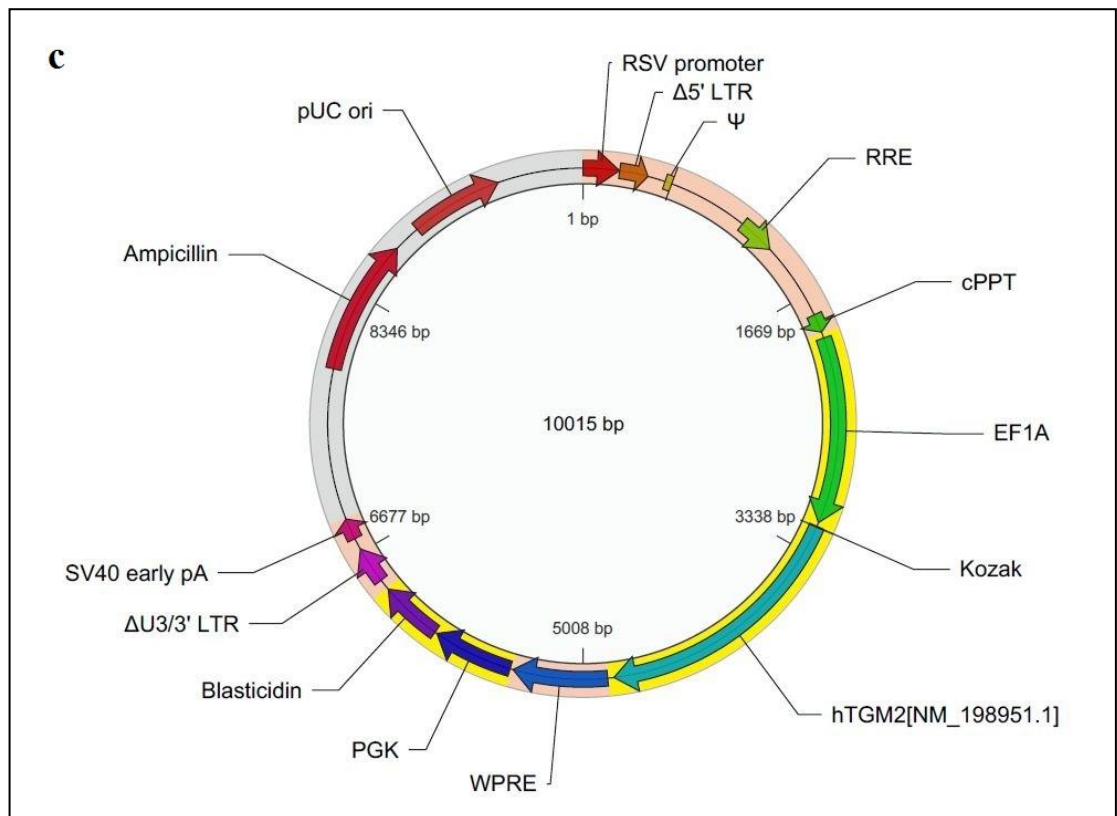
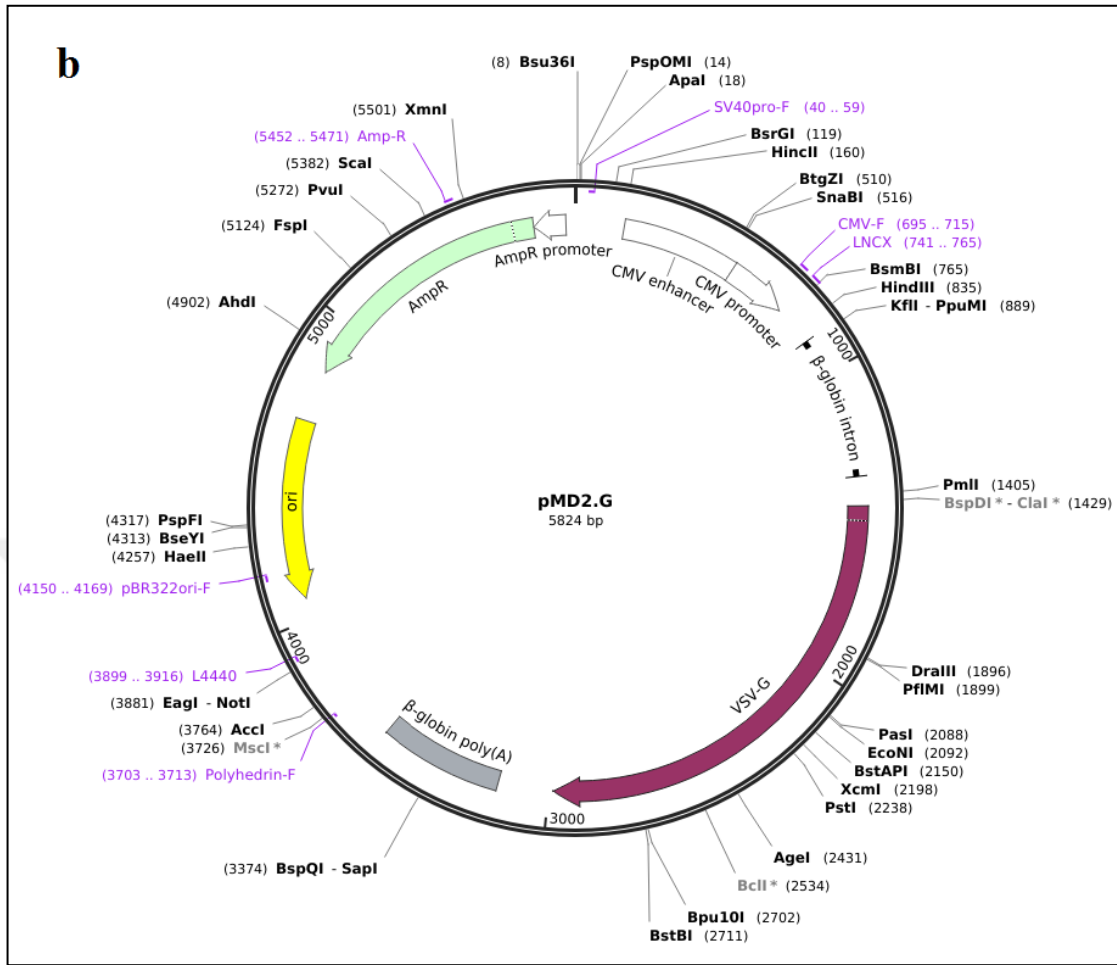


3. METHODOLOGY

3.1. PRODUCTION OF LENTIVIRAL PLASMIDS AND LENTIVIRUSES

Lentiviral human gene expression plasmids (pEGFP and pHGM2_v2) were purchased from Vector Builder (Cyagen), and packaging (psPAX2) and envelope (pMD2.G) plasmids were purchased from Addgene. The plasmid maps are shown in Figure 3.1 below.





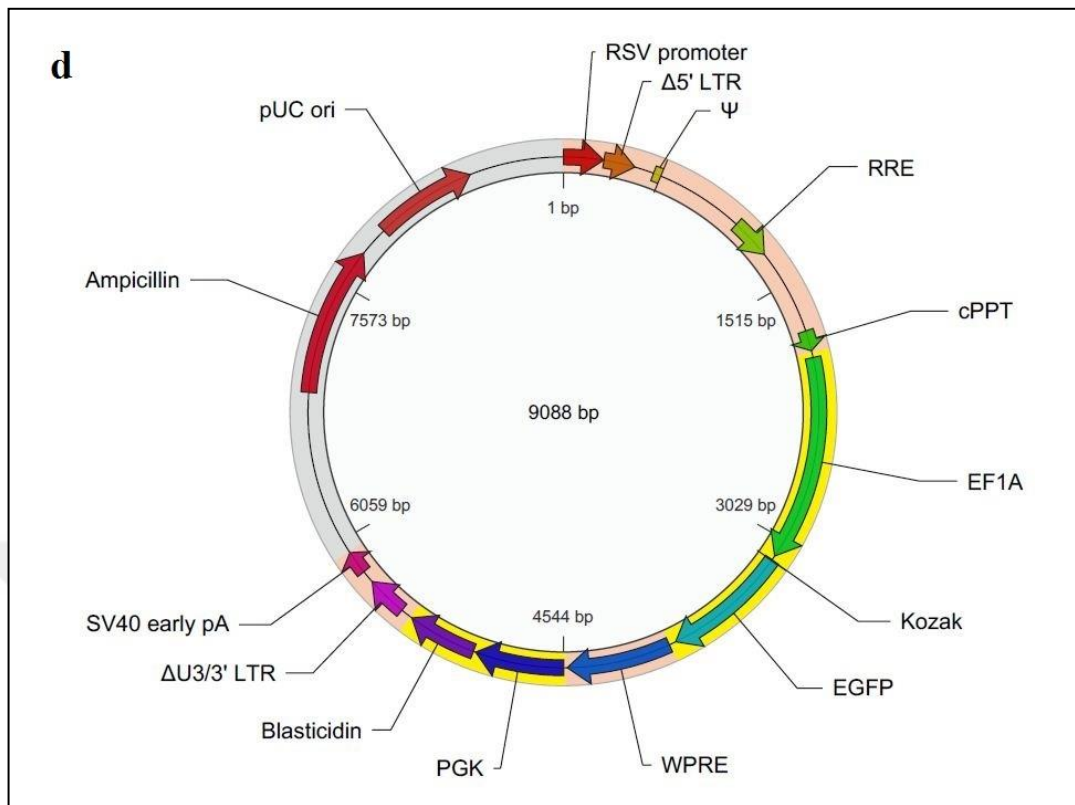


Figure 3.1. Plasmid maps of (a) psPAX2, (b) pMD2.G, (c) pHTGM2_v2, and (d) pEGFP

3.1.1. Bacterial Streaking

LB broth and LB agar were prepared by dissolving 12.5 g of broth and 3.7 g of agar in 100 mL distilled water, respectively. Both of the LBs were autoclaved at 121⁰C for 15 mins. Then, solutions were cooled down to 37⁰C and ampicillin was added in 50 μg/mL concentration. Agar was poured into Petri plates and kept at RT for solidification. Bacterial stocks that carry the plasmids were streaked onto the agar plates next to a Bunsen burner and incubated overnight at 37⁰C. Next day, the plates were placed to a cold room at 4⁰C until being used.

3.1.2. Mini-inoculation

LB broth (5 mL) was poured into 15 mL-centrifuge tubes. Single colonies were picked up from the agar plates and each of them was transferred into broth in different centrifuge tubes. The tubes were incubated at 37⁰C and 150 rpm for 6-7 hours.

3.1.3. Inoculation and Plasmid Isolation

Fresh LB broth was poured into separate Erlenmeyer flasks, each being 200 mL. Products of mini-inoculation (0.5 mL) were transferred into these flasks, which were then incubated at 37⁰C shaker (150 rpm) overnight. In the following day, the cells were sedimented by centrifuging the overnight LB culture at 4000 x g for 10 mins. Plasmids were isolated using Midiprep PureLink® HiPure Plasmid DNA Purification Kit (Invitrogen) according to the manufacturer's protocol. Briefly, the supernatants were discarded and the pellets were completely dissolved in 4 mL of R3. L7 (4 mL) was added into the tubes, and the tubes were mixed by inverting the tubes 5 times. After incubating the tubes at room temperature (RT) for 5 mins, 4 mL of N3 was added to the tubes and mixed by inverting the tube until it is homogenous. The lysate was centrifuged at 10 000 x g for 15 mins, and then the supernatants were transferred to the equilibrated columns and allowed for the solutions to drain by gravity. W8 (10 mL) was added to the columns which were subsequently placed onto sterile 15 mL centrifuge tubes. E4 (5 mL) was added to the columns. The eluted solution contained the plasmids. Isopropanol (3.5 mL) was added onto the eluate, and the solution was distributed to microcentrifuge tubes which were centrifuged at 13 000 x g for 30 mins at 4⁰C. The supernatants were discarded, and 3 mL of 70 per cent ethanol was added to the pellets. The tubes were centrifuged at 13 000 x g for 5 mins at 4⁰C. The supernatants were removed completely using a 200 µL micropipette, and the pellets were dissolved in 50 µL TE after being air-dried for 10-15 mins. The plasmid DNA concentrations were measured by using nanodrop (Nanodrop 2000, Thermo Scientific). In order to examine the purity and length of each plasmid, agarose gel electrophoresis was performed with 0.5 per cent agarose gel prepared by TBE (1X). After loading 200 ng of each plasmid DNA, the gel was run at 100V for 1 hour and visualized by ethidium bromide using transilluminator (ChemiDoc™).

The TGM2_v2 gene sequence in the phTGM2_v2 plasmid was confirmed using Sanger sequencing by Macrogen Inc (Rep. of Korea). Since the gene is very large to be sequenced at once, two sets of primers were designed so that the sequence could be amplified in two segments. The sequencing primers were given in Table 3.1 below. In addition, the primer binding sites on the plasmid were shown in Figure 3.2.

Table 3.1. Properties of the sequencing primers for TGM2_v2 gene in phTGM2 plasmid

	Primer Sequences (5'→3')		Product length (bp)
	Forward	Reverse	
Segment 1	AGCCTCAGACAGTGGTTC	CAGGCACCTCAGCACTGT	953
Segment 2	TCAAGTATGGCCAGTGCT	AGCGTATCCACATAGCGT	959

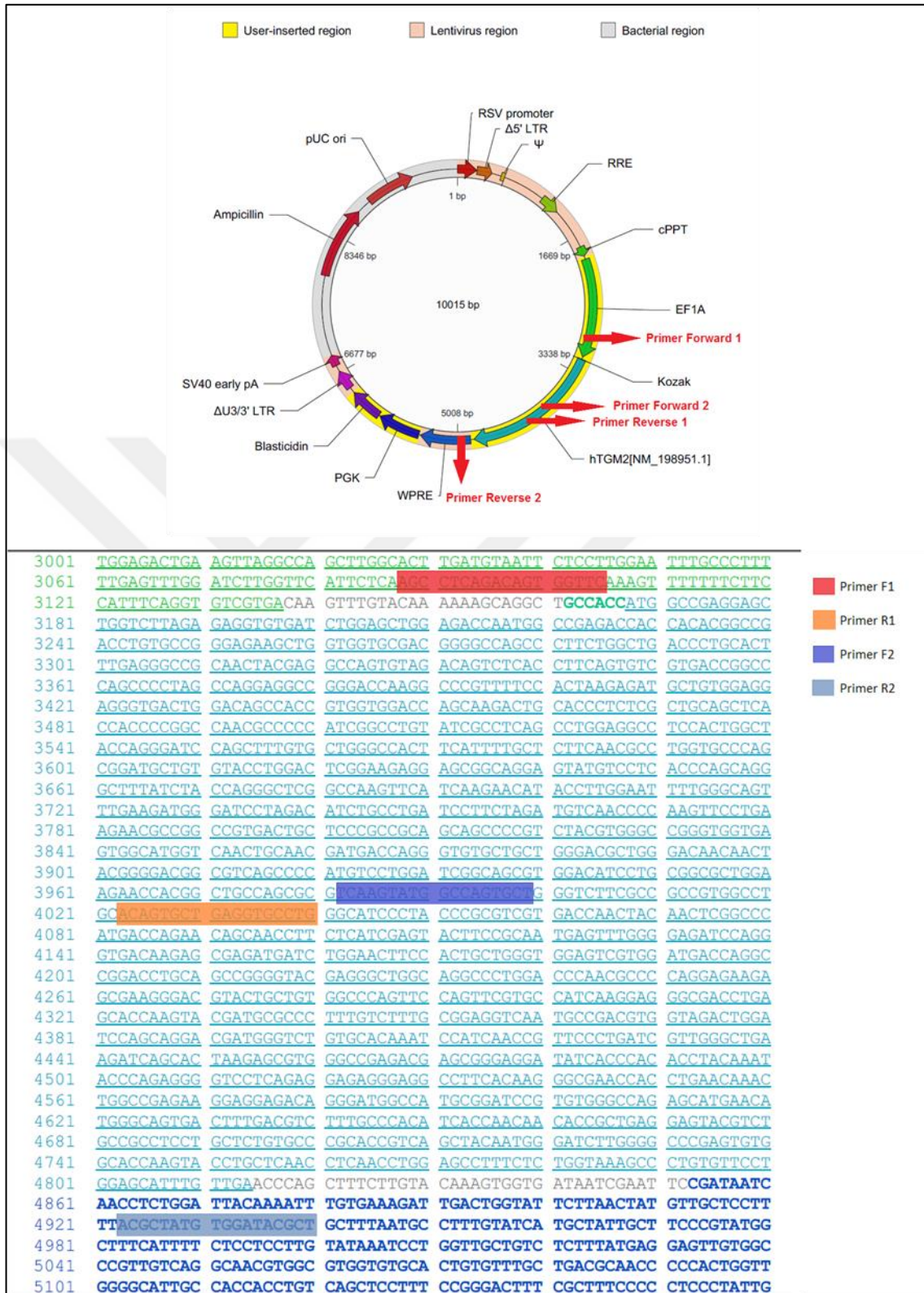


Figure 3.2. Sequencing primer binding sites on the phTGM2_v2 plasmid vector

3.1.4. Transfection of Human Embryonic Kidney-293T Cells

Human Embryonic Kidney (HEK)-293T cells were seeded on tissue culture dishes (100 mm), and cell culture media were replenished thrice a week with DMEM high glucose. When the cells reached to 70 per cent confluency, transfection was performed using the following protocol. First, HBSS buffer (2X, pH 7.05) was prepared by mixing NaCl and Na₂HPO₄ salts in HEPES buffer (1M) to make a stock solution of HBSS (2X) containing 280 mM of NaCl, 1.5 mM of Na₂HPO₄ and 50 mM of HEPES. The pH of the solution was adjusted to pH 7.05. For each plasmid, 600 µL of HBSS (2X, pH 7.05) was transferred to centrifuge tubes (15 mL) and the tubes were labeled with the plasmid names. Again, for each plasmid, 360 µL of distilled water was mixed with 240 µL of CaCl₂ (2M) in separate centrifuge tubes labeled with plasmid names. Plasmids (5 µg of psPAX2, 5 µg pMD2.G, 10 µg of pHTGM2_v2, 5 µg of pEGFP) were added onto HBSS (2X, pH 7.05) in labeled tubes. The plasmid solutions were added into the labeled tubes containing CaCl₂ solution (2M) dropwise while bubbling the solution in the tube with a 1 mL serological pipette. Latterly, all of the solutions were incubated at RT for 30 mins. Finally, the solutions were added directly into the media on the cells. For the production of lentiviral particles loaded with pHTGM2_v2, the solutions labeled with psPAX2, pMD2.G, and pHTGM2_v2 were added drop by drop in the order written. For the production of lentiviral particles loaded with pEGFP, the solutions labeled with psPAX2, pMD2.G, and pEGFP were added drop by drop in the same order. After incubating the cells overnight at 37⁰C, the media on the cells were discarded, then the cells were washed with DPBS (1X) and fresh growth medium was added. After 24 hours of transfection, the media containing the viruses loaded with pEGFP and pHTGM2_v2 were collected in separate sterile 50 mL centrifuge tubes and stored in refrigerator. After addition of 5 mL fresh culture medium onto the cells, another 24 hours-incubation was done. The media on the cells were collected again and refrigerated at the end of incubation time. During this time interval, HEK293T cells were examined under fluorescence microscope (Axio Vert.A1, Carl Zeiss, Germany) in terms of transfection efficiency (FITC filter; $\lambda_{\text{emission}}=488$ nm) both after 24 hours and 48 hours of incubation. For sterilization, high-speed PPCO centrifuge tubes were washed and incubated with 70 per cent ethanol at 4⁰C overnight. The next day, ethanol was discarded, and the centrifuge tubes were washed with sterile distilled water. Half of the media containing lentiviral particles were first filtered with 0.45 µm syringe filter into the sterile high-speed centrifuge tubes to get rid of cell debris, and then

centrifuged at 25,000 rpm (~80 000xg) for 2 hours using an ultracentrifuge (Avanti® J-25, Beckman Coulter, USA). The pellet, which contained viruses, was dissolved in 100 µL serum-free DMEM (high glucose), and stored as 10 µL aliquots at -80°C for long term usage. The remaining half of the media containing the viral particles was directly aliquoted into sterile tubes and stored at -80°C.

3.2. ISOLATION AND GROWTH OF CELLS

3.2.1. Isolation and Growth of rBMSCs

rBMSCs were isolated from 10 weeks old Sprague-Dawley rats. Briefly, after euthanizing the rats with carbon dioxide, the femurs and tibias were taken out. The femurs and tibias were washed with Dulbecco's Modified Eagle Medium (DMEM) high glucose including 10 per cent Penicillin/Streptomycin solution (Pen/Strep), and then bone marrows were transferred into centrifuge tubes with growth medium (DMEM with 10 per cent FBS, 10 per cent P/S) by using a sterile syringe. The extract was homogenized by continuous pipetting method, and then centrifuged at 500 x g for 10 minutes. The pellet was dissolved in culture medium (alpha-MEM with 10 per cent FBS and 10 per cent Pen/Strep) and incubated in CO₂ incubator at 37°C, in 5 per cent CO₂ and 90 per cent humidity. The media on the cells were replenished every other day.

3.2.2. Characterization of rBSMCs by Flow Cytometry

rBMSCs were examined for the expression of MSC surface antigens CD90 and CD29, endothelial marker CD31, and hematopoietic marker CD45. For this purpose, the cells were first trypsinized and pelleted. Each cell pellet was divided into five tubes with at least 300 000 cells in each tube. After washing one round with DPBS (1X), 1 mL of DPBS plus the antibodies were added into the tubes, leaving one tube untreated as negative control. The antibodies were incubated for 45 minutes and then the tubes were centrifuged at 300 x g for 5 mins. Again, after washing with DPBS once, the pellets were dissolved in 400 µL of DPBS, and analyzed with flow cytometer. All of the flow-cytometry analyses were carried out using FACSCalibur Flow Cytometry System (Becton Dickinson, San Jose, CA, USA).

3.2.3. Isolation and Growth of Rat Knee Chondrocytes

The same Spraque-Dawley rats from Section 3.2.1 were used for this purpose. The legs were cleared from connective tissues, and then cartilage slices were taken out from the knee joints either by scraping or cutting with surgical blades. The tissues were chopped into small pieces (1 mm) inside 6 well plates, and the tissue pieces were incubated in 2 mg/mL collagenase type II. At the end of 24 hours of incubation, the tissue pieces were collected from the plates and centrifuged at 3000 rpm for 5 mins. The pellets were washed once with DPBS (1X). After that, they were resuspended into 6 well plates with DMEM F12-Ham, supplemented with 10 per cent FBS, 1 per cent Pen/Strep, and 2 mM L-glutamine. The culture media were replenished thrice a week.

3.3. GENE TRANSFER TO RBMSCS

3.3.1. Construction of Blasticidin Kill Curve

Since the vectors contain Blasticidin resistance gene, the transduced cells could be selected with Blasticidin. Accordingly, in order to determine the optimal concentration of Blasticidin that would kill the non-transduced cells after the process, in other words to determine the Blasticidin resistance of rBMSCs, the non-transduced cells were exposed to different concentrations of Blasticidin, starting from 2 $\mu\text{g/mL}$ to 20 $\mu\text{g/mL}$. For that purpose, a stock solution of 1 mg/mL Blasticidin was prepared with sterile distilled water and then diluted to the desired concentrations with growth medium. Next, cells were seeded into 24-well plates with a density of 1000 cells/well and grown in normal growth media. After 24 hours of incubation, the media on the cells were changed with Blasticidin containing media. The media were replenished every 3 days. The growth of the cells was observed for two weeks. Another set of cells was analyzed by MTS assay after 48 and 72 hours of incubation in various concentrations of Blasticidin containing media (2 $\mu\text{g/mL}$ - 10 $\mu\text{g/mL}$). Then, a kill curve was plotted (Figure C.1).

3.3.2. Construction of Protamine Sulfate Kill Curve

In order to determine the optimal PS concentration for the transduction, different concentrations of PS stock solutions (10-100 $\mu\text{g/mL}$) were prepared. Then, cells were seeded on 24 well plates with a density of 10 000 cells/well in triplicates for each PS concentration. MTS assay was performed after 27 hours of incubation in PS (3 hrs for pre-incubation plus 24 hours for transduction), and the kill curve was constructed using the slope of the calibration curve (Figure D.1).

3.3.3. Transduction of rBMSCs

As the rBMSCs (P2) reached 70 per cent confluency, cells were treated with 50 $\mu\text{g/mL}$ protamine sulfate (PS) containing media. After 3 hours of pre-incubation in PS containing media, transduction media containing the viral particles were added directly onto the culture media.

Six different concentrations were used for TGM2_v2 transduction; in three of them viral pellet was used and in the rest of them viral medium was used. Another set of transduction was prepared for EGFP as the control for transduction efficiency. The groups were named as described in Table 3.2 below:

Table 3.2. Nomenclature of the experimental groups

Group name	Virus concentration
1X	10 μL of the pellet to make 1X concentration
1.5X	15 μL of the pellet to make 1.5X concentration
2X	20 μL of the pellet to make 2X concentration
1ML	1 mL of viral media + 1 mL of culture media (1:1 dilution)
1.5ML	1.5 mL of viral media + 0.5 mL of culture media (3:1 dilution)
2ML	2 mL of viral media (no dilution)

3.3.4. Selection of the Transduced Cells

Twenty four hours after transduction, the media on the cells were discarded carefully. The cells were washed with DPBS (1X, pH 7.4), and then fresh growth media were added. The following day, the media on the cells were replenished with 5 µg/mL Blasticidin containing media. The selection of transduced cells was performed throughout 2 weeks, changing the media every three days.

Although the non-transduced cells were eliminated from the flasks, all the processes regarding transduced-cell culturing were done in the presence of Blasticidin in the media in case there were any cellular alterations.

3.4. ANALYSES OF TRANSDUCTION EFFICIENCY AND CHARACTERIZATION OF TRANSDUCED CELLS

3.4.1. Fluorescence Microscopy

Fluorescence microscope (Axio Vert.A1, Carl Zeiss, Germany) was used to observe the viability of EGFP-transduced rBMSCs. Fluorescence images were taken after 24 hours, 4 days, and 7 days of incubation in order to examine transduction efficiency.

3.4.2. Flow Cytometry

After selection with Blasticidin, EGFP-transduced rBMSCs (P2) were analyzed with flow cytometer in order to determine the efficiency of transduction. For that purpose, the cells were detached from 6-well plate and pelleted. Approximately 500 000 cells were dissolved in 500 µL DPBS (1X) and transferred into polystyrene round-bottom tubes. The flow cytometry was performed on 1X, 2X, 1ML, and 2ML EGFP groups, while non-transduced rBMSCs were used as negative control. At the same time, the hTGM2_v2-transduced-rBMSCs were examined for the expression of mesenchymal stem cell surface antigens as described in details in Section 3.2.2.

3.4.3. Total RNA Isolation

After elimination of the non-transduced cells from the cell culture flasks, the remaining transduced cells were examined for TGM2_v2 expression. Firstly, the medium on the cells was removed and the cells were washed with DPBS (1X, pH 7.4). Subsequently, RNA isolation was carried out with GeneJET RNA Purification Kit (Thermo Fisher Scientific) according to the manufacturer's protocol. Briefly, 10 μ L β -mercaptoethanol was added onto 500 μ L of lysis buffer for approximately 5×10^6 cells, and the cells were scraped and homogenized in this solution using cell scraper. The cell homogenate (1.5 mL total) was collected into RNase-free microcentrifuge tubes. Ethanol (300 μ L) was added onto the same tube, and then the solution was transferred to the column in collection tube supplied with the kit. After centrifugation for 1 min at 13 000 x g, the column was placed into new collection tube. Wash buffer 1 was added (700 μ L) to the column and centrifugation was performed for 1 min at 13 000 x g. Discarding the flow-through, 600 μ L of Wash buffer 2 was added to the column and centrifugation was done at 13 000 x g for 1 min. An additional washing step was performed with 250 μ L of Wash buffer 2 for 2 mins at 13 000 x g. Lastly, 30 μ L of nuclease-free water was added to the center of the column and RNA was collected into an RNase-free centrifuge tube by centrifugation at 13 000 x g for 1 min. Total RNA concentrations were measured with the nanodrop. The tubes were stored at -80°C until use.

3.4.4. Real-Time PCR

First, RT-PCR was performed on total RNAs by using Sensiscript® RT Kit (Qiagen) for the first strand cDNA synthesis. Briefly, for one reaction tube 2 μ L Buffer RT (10X), 2 μ L dNTP mix (5 μ M), 2 μ L Oligo dT (10 μ M), 0.25 μ L RNase inhibitor (40 u/ μ L), and 1 μ L Sensiscript Reverse Transcriptase were mixed. For each experimental group, 28 ng of total RNA was used. RT reaction was completed by incubating the tubes first at 65°C for 3 mins, and then for 1 hour at 37°C . The cDNA amounts were measured with the nanodrop, and then real-time PCR was carried out after calculating the required volume of cDNAs for each reaction mix to contain 500 ng of cDNA. Maxima SYBR Green Master Mix was used for this purpose (Thermo Scientific). Briefly, for one reaction tube 12.5 μ L of Maxima SYBR Green/ROX qPCR Master Mix (2X) and 2.5 μ L of primer mix (10X) were mixed. After the addition of

cDNAs (500 ng), the PCR was performed according to the parameters given in Table 3.3. Human TGM2 and rat 18SrRNA primers were purchased from Qiagen as 10X stock solutions. At the end of PCR, the products were run on agarose gel electrophoresis.

Table 3.3. Real-time PCR parameters

Number of cycles	Steps	Temperature (°C)	Time
1	Initial denaturation	95	10 mins
40	Denaturation	95	15 secs
	Annealing	57	30 secs
	Extension	72	30 secs
1	Final extension	72	10 mins

3.4.5. Protein Extraction

After selection, the transduced cells were subjected to protein extraction via RIPA lysis buffer system, pH 7.4 (Santa Cruz). Briefly, culture medium was discarded and the cells were washed with DPBS (1X, pH 7.4). Prior to cell lysis, buffer solution was prepared by adding 10 μ L PMSF (200 mM in DMSO), 10 μ L sodium orthovanadate (100 mM in water), and 10 μ L protease inhibitor cocktail in DMSO per 1 mL of RIPA lysis buffer (1X, pH 7.4). Cells were scraped with this buffer (30 μ L per one well of the 6-well plate), and then collected into 1.5 mL microcentrifuge tubes. The cell lysates were sonicated for 10 seconds on ice. The total protein amount was measured using SMART™ micro BCA Protein Assay Kit (Intron Biotech) according to the manufacturer's protocol. Briefly, 100 μ L of 1:100 sample dilutions were mixed with 100 μ L of working solution, and then absorbances were measured at 562 nm after incubating the plate at 37 °C for 2 hours. Standard curve was obtained using BSA solutions ranging between 1-64 μ g/mL concentrations. The protein concentrations of the samples were calculated using to the slope of the standard curve (Figure E.1).

3.4.6. Western Blotting

For Western Blotting, i-Blot2 system was used with ready-to-use gels (Life Technologies). First of all, the proteins (~50 µg) were digested at 95°C for 5 mins. Proteins were separated in 4-12 per cent Bis-Tris Plus polyacrylamide gels. After loading into the gel, the proteins were run for a total of 1 hour. Semi-dry transfer onto PVDF membrane was performed for 7 mins at 20V. The PVDF membrane was cut into 2 parts according to the protein ladder with the aid of a surgical blade, such that TG2 (76 kDa) and β-actin (42 kDa) could be detected separately. Then, it was washed with TBS-T (0.1 per cent v/v Tween® 20) once, and immediately incubated in 5 per cent blocking solution (5 per cent w/v powdered milk in TBS-T, 1X, pH 7.5) for 1 hour on a plate shaker to prevent non-specific binding. Primary antibodies were prepared in blocking solution, making 50 ng/µL solution for anti-TG2, and 20 ng/µL for anti-β-actin. Primary antibody probing was performed overnight at 4⁰C on an orbital shaker at 27 rpm. Next day, the membranes were washed with TBS-T and secondary antibodies were blotted with a concentration of 200 ng/µL for each membrane at RT for 2 hours. After washing the membrane with TBS-T, detection reagent was added onto the membrane and incubated at RT for 5 mins. The excess reagent was drained off and the membranes were visualized with transilluminator (ChemiDoc™) (5 mins exposure).

3.4.7. Cell Proliferation Assay

In order to analyze cell viability after transduction, cells were subjected to MTS assay. For that purpose, MTS+medium mixture (1:5 v/v) was added onto the cells. After incubating them for 3 hours in an incubator, the absorbances were measured at 490 nm using Elisa Plate Reader (Elx800, Bio-Tek, USA). In order to convert the OD490 values into cell number, calibration curves were constructed for both rBMSCs and rat knee chondrocytes. For that purpose, cells were seeded on cell culture flasks with a density ranging from 10 000 to 100 000 cells per well. After 3 hours of incubation in MTS solution, the absorbance values were obtained at 490 nm, and calibration curves were plotted as OD490 vs. cell number. Figure B.1 and Figure B.2 belong to rBMSC and chondrocyte calibration curves, respectively.

3.5. PREPARATION AND CHARACTERIZATION OF SCAFFOLDS

3.5.1. Preparation of PBSu Scaffolds

PBSu pellets were dissolved in dichloromethane (DCM) to make 1 per cent, 2 per cent, 4 per cent, 6 per cent, 8 per cent, and 10 per cent solutions, individually. In order to obtain porous structures, sodium chloride crystals (300 μm –500 μm) were used. Plates were left undisturbed under the fume hood for DCM evaporation. For the following 2 days, scaffolds were dialyzed in distilled water to remove salt particles from the scaffolds. Then, they were taken out of the water, frozen at -20°C , and lyophilized. After lyophilization, the scaffolds were cut into 7 mm x 3 mm discs.

3.5.2. Preparation of PBSu:PLLA Scaffolds

PBSu and PLLA pellets were dissolved simultaneously in dichloromethane (DCM) to make 6 per cent solution (w/v) of 1:1 PBSu:PLLA blend scaffolds. The following steps were as the same as in Section 3.5.1.

3.5.3. Cell Seeding onto the Scaffolds

Previously prepared porous scaffolds were put into 48-well plates. For sterilization, 70 per cent ethanol was added onto each well, and the plates were kept at 4°C for 2 hours. Thereafter, the scaffolds were washed with DPBS (1X, pH 7.4) to remove ethanol, and then with cell culture media once prior to cell seeding. Next, the cells that were transduced with hTGM2 were detached from the culture dishes by trypsinization and counted by cell counter. Each scaffold was seeded with 50 000 cells. The plates were incubated for 5 hours in an incubator to allow cell attachment to the scaffolds. Lastly, complete growth medium (alpha-MEM) was added to each well and then the plates were placed in an incubator (Steri-Cycle CO_2 Incubator, Thermo Scientific, USA).

3.5.4. Fluorescence Microscopy

After seeding the EGFP-expressing cells onto sterile PBSu scaffolds, they were incubated for 35 days in cell culture. Then, the cell-seeded scaffolds were analyzed by fluorescence microscope (Axio Vert.A1, Carl Zeiss, Germany) in terms of cell attachment and migration.

3.5.5. Scanning Electron Microscopy (SEM)

The cell seeded scaffolds were first washed with cacodylate buffer (0.1 M, pH 7.4) for three times. Then, they were fixed in 2.5 per cent (v/v) glutaraldehyde for 1 h at RT. Following the incubation, they were washed with cacodylate buffer three times and then air dried. Lastly, they were coated with gold (5 nm in thickness) by sputter coater (Bal-tec SCD 005), and examined using SEM (Carl Zeiss, EVO) operated at an acceleration of 10.00 kV. The empty scaffolds were directly coated without fixation and washing steps, and then examined.

3.5.6. Cell Proliferation Assay

The cell-seeded scaffolds were evaluated in terms of cell attachment and proliferation by performing MTS assay. For this purpose, the samples were transferred to clean 48-well plates and washed with DPBS (1X, pH 7.4). MTS assay was performed as described in Section 3.4.7.

3.5.7. Gene Expression Analyses

3.5.7.1. Total RNA Isolation

In order to analyse the chondrogenic gene expression among the experimental groups, total RNA isolation was performed throughout 3 weeks by using GeneJET RNA Purification Kit (Thermo Fisher Scientific, USA) according to manufacturer's protocol as previously described in section 3.4.3.

3.5.7.2. Real-Time PCR

First strand cDNA synthesis and real-time PCR were carried out as described in section 3.4.4. The same PCR parameters given in Table 3.3 were used, using appropriate T_a values for each primer set as given in Table 3.4. Primers for rat Col2a1 [135], Col1a1 [135], Agc [135], Sox9 [80], and Col10a1 [135] were purchased from Macrogen, while rat 18SrRNA primers were purchased from Qiagen as 10X stock solutions. The properties of primers are given in Table 3.4.

Table 3.4. Rattus Norvegicus primers for Col2a1, Col1a1, Agc, Sox9, Col10A1, 18SrRNA, and their properties

	Primer Sequences (5'→3')		T_a values (°C)
	Forward	Reverse	
Col2a1	CACCGCTAACGTCCAGATGAC	GGAAGGCGTGAGGTCTTCTGT	59
Col1a1	CTGCCCTCGCAGGGGTTTG	GCCTGCACATGTGTGGCCGA	59
Agc	CATTCGCACGGGAGCAGCCA	TGGGGTCCGTGGGCTCACAA	60
Sox9	TGGCAGACCAGTACCCGCATCT	TCTTCTTGTGCTGCACGCGC	60
Col10A1	GGCAGCAGCACTATGACCCAA	ACAGGCCTACCCAAACGTGAGTCC	60
18SrRNA	Not supplied		60 (or 59)

3.5.8. Immunofluorescence Assays

3.5.8.1. TG2 Deposition Inside the Scaffolds

The cell-seeded scaffolds were washed with DPBS (1X) and then fixed with 3.7 per cent formaldehyde for 20 mins at RT. After incubating the samples in 1X blocking solution (3 per cent FBS and 0.1 per cent Tween® 20 in DPBS) for 10 mins at RT, primary antibody solution (TGM2 mouse monoclonal antibody 1:1000 in blocking solution) was added onto them. After 1.5 hours of incubation at RT, the antibody solution was discarded and the samples were washed with washing solution (0.1 per cent Tween 20 in DPBS) three times, each for 5 mins. Anti-mouse secondary antibody solution (4 µg/mL in blocking solution) was added onto the samples and incubated for 1 hour at RT in the dark. The antibody solutions were discarded and the samples were washed with washing solution three times, each for 5 mins. The samples were incubated in nuclei labeling solution (DAPI, 1:1000 in

blocking solution) for 15 mins at RT. Samples were washed with washing solution 3 times, mounted, and observed under the confocal microscope (LSM 700, Carl Zeiss, Germany).

3.5.8.2. Immunostaining of ECM and Nuclei

The samples were washed with DPBS (1X) and then fixed with 3.7 per cent formaldehyde for 20 mins at RT. After incubating the samples in 1X blocking solution (3 per cent FBS and 0.1 per cent Tween® 20 in DPBS) for 10 mins at RT, primary antibody solutions were added onto them. For osteogenic analyses, Col1 antibody was used. Col2a1 and Aggrecan antibodies were used for chondrogenic analyses, while Col10a1 antibody was used to observe whether the chondrogenic differentiation lead to hypertrophy or not. Col2a1, Aggrecan, and Col10a1 antibody solutions were prepared as 1:500 dilutions in blocking solution, whereas 1:2000 dilution was used for Col1 antibody. After incubating the samples overnight at 4°C, the antibody solutions were discarded and the samples were washed with washing solution (0.1 per cent Tween 20 in DPBS) three times, each for 5 mins. Secondary antibody solutions (4 µg/mL in blocking solution) were added onto the samples and incubated for 1 hour at RT in the dark. The antibody solutions were discarded and the samples were washed with washing solution three times, each for 5 mins. The samples were incubated in nuclei labeling solution (DAPI, 1:1000 in blocking solution) for 15 mins at RT. Samples were washed with washing solution 3 times, mounted, and observed under the fluorescence and confocal microscopes.

3.5.9. Alizarin Red Staining

After being incubated in osteogenic differentiation medium (Alpha-MEM GlutaMAX™ supplemented with 10 per cent FBS, 50 µg/mL L-ascorbic acid 2-phosphate sesquimagnesium salt hydrate, 100 nM dexamethasone, 10 mM B-glycerophosphate, and 1 per cent Pen Strep), the samples were fixed with 3.7 per cent formaldehyde including 0.1 per cent Tween® 20 for 30 mins, and then incubated in Alizarin Red S Solution (1X) for 30 mins at RT. After 3 rounds of washing with distilled water, the cells were examined with the inverted microscope.

3.5.10. Alcian Blue Staining

After incubation in chondrogenic differentiation medium (DMEM-high glucose GlutaMAX™ supplemented with with 1 per cent Pen/Strep, 1 per cent ITS Premix, 40 µg/mL proline, 100 µg sodium pyruvate, 50µg/mL L-ascorbic acid 2-phosphate sesquimagnesium salt hydrate, 100 nM dexamethasone, and 10 ng/mL TGF-β1), samples were fixed with 3.7 per cent formaldehyde including 0.1 per cent Tween® 20 for 30 mins. After that, the samples were stained with Alcian Blue pH 2.5 kit (Bio-Optica, Italy) according to the manufacturer's protocol. Another set of samples were stained with Alcian Blue/PAS kit (Atom Scientific, UK). Briefly, the samples were first stained with Alcian Blue for 1 hour. After 3 rounds of washing with distilled water, the samples were treated with periodic acid solution for 10 mins. Again, after washing well with distilled water, they were treated with Schiff reagent for 10 mins. Next, the samples were washed well with distilled water and treated with Haemalum Mayer for 30 seconds in order to stain nuclei. Lastly, they were washed with distilled water very well, and then observed under the inverted microscope.

3.5.11. Mechanical Analysis

The cell-seeded scaffolds were taken out of the culture and placed on filter papers in order to soak up the excess culture media. Then, they were subjected to compression test using the dynamic test system Instron (ITW, USA). The samples were compressed with a load cell of 1 kN until approximately the height of the samples were reduced to one of the third. Compressive moduli of the samples were calculated according to the recorded values.

3.6. STATISTICAL ANALYSES

MTS assay and real-time PCR were performed in triplicates. Statistical significance between the experimental groups was analyzed using one or two-way analysis of variance (ANOVA) followed by Tukey's multiple comparison test, and p values less than 0.05 were considered as statistically significant.

4. RESULTS AND DISCUSSION

In cartilage tissue, the ECM is the main component; if the ECM is damaged, so does the tissue. Therefore, ECM formation is one of the major factors to be considered in tissue engineering of cartilage. TG2 is an enzyme with ECM crosslinking and stabilizing functions [97]. In addition, it was found to stimulate epithelial to mesenchymal transition in various cells types [136][137][138][139][140]. TG2 enzyme is also called as Dr. Jekyll and Mr. Hyde due to its association with apoptosis, in addition to its functions in cell growth and differentiation [114]. There are a few studies in which TG2 was used for cartilage tissue engineering [120] [121], but none of them includes transduction of cells with TGM2_v2. Among the four isoforms of TG2, the second isoform that is known as TG2-S has the most similar expression level to that of the original full length transcript [126]. Since hypertrophy is not favored in the course of cartilage tissue engineering, the low-transamidase isoform of TG2, TG2-S, which still comprises putative syndecan-4 and FN binding site is utilized in our study. In this study, cartilage tissue regeneration was aimed by using TG2-S-transduced MSCs derived from bone marrow of rats and grown on PBSu and PLLA blend scaffolds. We wanted to utilize the mild ECM crosslinking activity of TG2-S in addition to its effects on differentiation, by genetically engineering MSCs to express TG2-S, and create a construct for cartilage tissue engineering using these transduced cells. Since TG2-S has low crosslinking capacity, the possibilities of hypertrophy formation and osteogenic differentiation could be reduced. Using TGM2_v2 gene transduction of rBMSCs to induce chondrogenic differentiation is a novel approach of our study in this area.

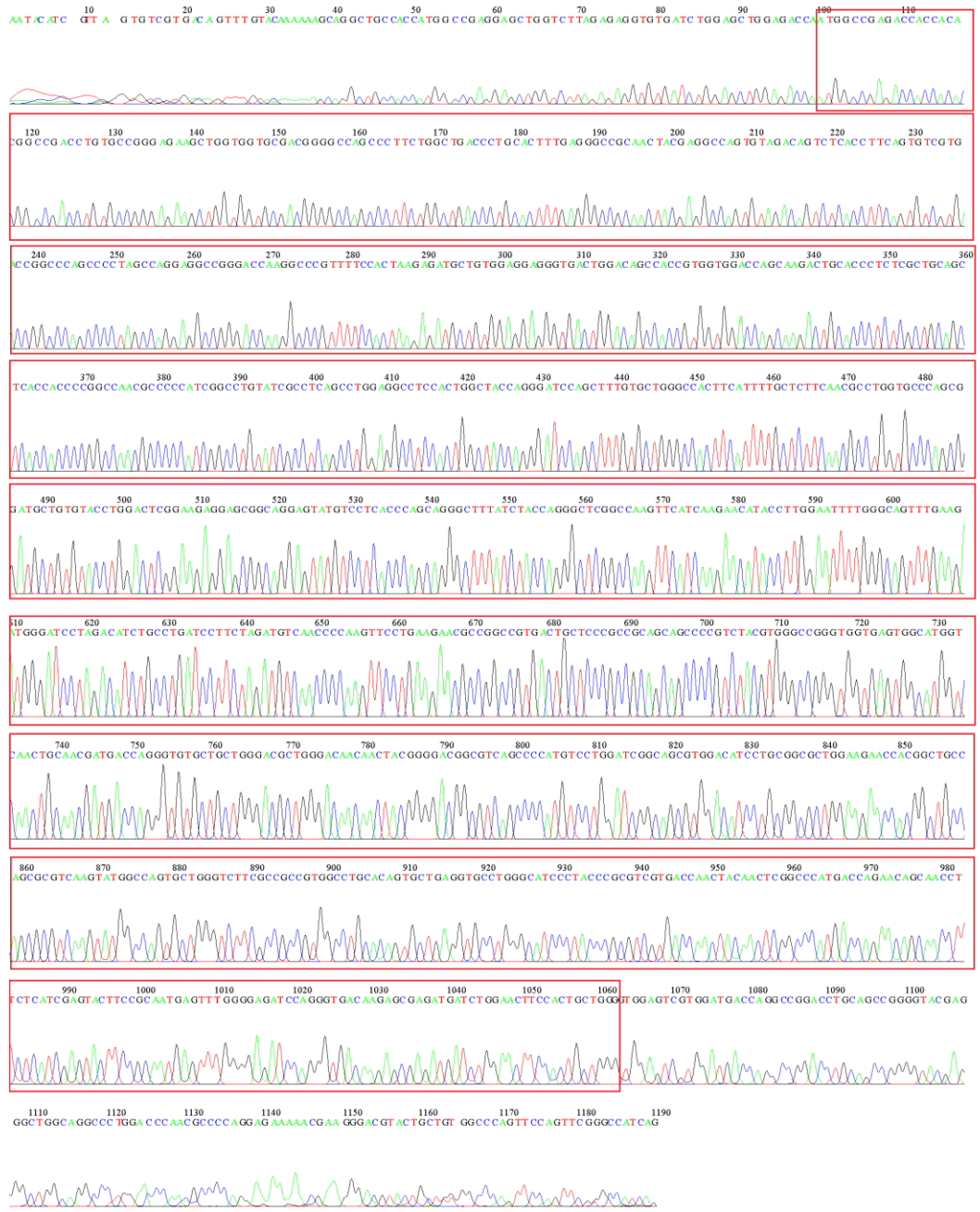
4.1. VERIFICATION OF TGM2_V2 SEQUENCE IN PLASMID

The pEGFP, phTGM2_v2, psPAX2, and pMD2.G plasmids were ran on agarose gel after plasmid isolation, in order to verify their lengths and purities. It was observed that they were purely isolated, and lengths of the plasmids were consistent with their theoretical values (Figure A.1). After that, in order to verify the sequence of human TGM2_v2 gene in our phTGM2 plasmid, sequencing was performed. The results of sequencing were obtained as two separate segments since the TGM2_v2 sequence was too long (1646 bp). The chromatogram results were shown in Figure 4.1 a and b for segment 1 and 2, respectively.

Segment 1 covers the start codon (nucleotide position: 3168-4178) and segment 2 covers the stop codon (nucleotide position: 4179-4814). The sequences that matched with the original hTGM2_v2 ORF [NM_198951.1] were marked within red boxes. No mismatches were observed within the plasmid sequence (pLV[Exp]-Bsd-EF1A>hTGM2[NM_198951.1]).



a



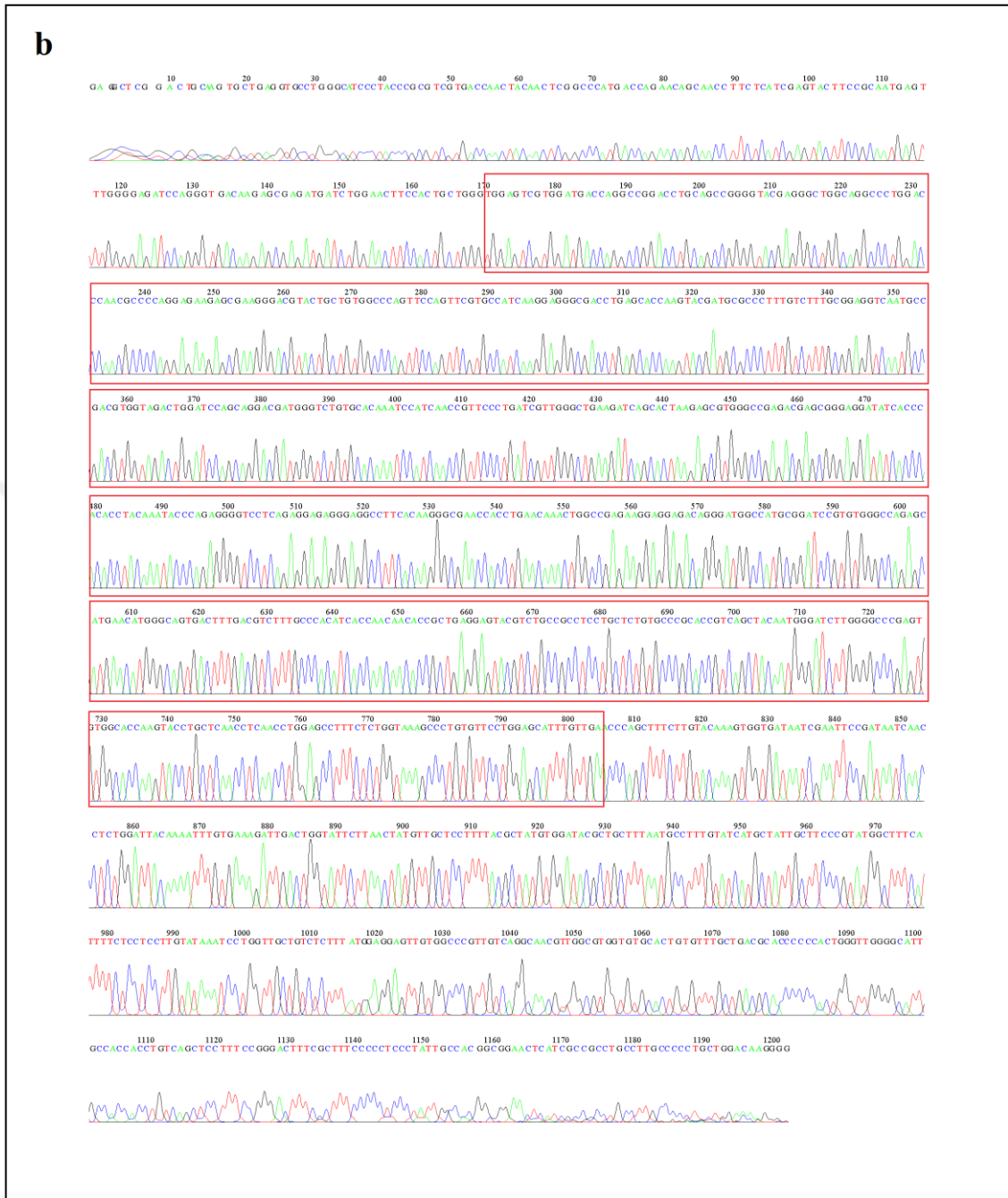


Figure 4.1. Sequence chromatogram of the (a) first and (b) second segments of hTGM2_v2 gene inside the vector. Red boxes show the properly aligned sequences with the original TGM2_v2 sequence.

The sequence results were analyzed using both Microsoft (MS) Office Word and NIH BLAST software. Microsoft Office Word analysis was shown in Figure 4.2. The matching sequences were highlighted in blue. The results indicated that TGM2_v2 gene inside the plasmid vector has the same sequence with the original gene stated in the literature [NM_198951.1], without any mismatches.

a

Homo sapiens transglutaminase 2 (TGM2), transcript variant 2, mRNA

NCBI Reference Sequence: [NM_198951.1](#)

>NM_198951.1:101-1747 Homo sapiens transglutaminase 2 (TGM2), transcript variant 2, mRNA

>170320-074_I24.DNA_Forward_1.ab1 1190

```

AATACATCGTTAGTGTCTGACAGTTTGTACAAAAAAGCAGGCTGCCACCATG
GCCGAGGAGCTGGTCTTAGAGAGGTGTGATCTGGAGCTGGAGACCAAATGGCCG
AGACCACCACACGGCCGACCTGTGCCGGGAGAGCTGGTGGTGGCAGGGGCC
AGCCCTTCTGGCTGACCTGCACITTTGAGGCGGCAACTACGAGGCCAGTGT
GACAGTCTCACCTTCAGTGTCTGACCGGCCAGCCCTAGCCAGGAGGCCGG
GACCAAGGCCCGTTTCCACTAAGAGATGCTGTGGAGGAGGTGACTGGACAG
CCACCGTGGTGGACCAGCAAGACTGCACCCCTCTCGCTGCAGCTCACCACCCG
GCCAACGCCCCCATCGGCCCTGTATCGCCTCAGCTGGAGGCCCTCCACTGG
CCAGGGATCCAGCTTTGTCTGGGCCACTTCATTTTGTCTTCAACGCCCTGGT
GCCAGCGGATGCTGTGTACTGGACTCGGAAGAGGAGCGGCAGGAGTATGTC
CTCACCACGAGGGCTTTATCTACAGGGCTCGGCCAAGTTCATCAAGAACAT
ACCTTGGAAATTTGGGCGAGTTTGAAGATGGGATCCTAGACATCTGCCCTGATCC
TTCTAGATGTCAACCCCAAGTTCCTGAAGAACCGCGCCCTGACTGCTCCCGC
CGCAGCAGCCCGCTACGTGGCCGGTGGTGGTGGTGGTGGTGGTGGTGGTGGTGG
CGATGACCAGGGTGTGGTGGTGGTGGTGGTGGTGGTGGTGGTGGTGGTGGTGGTGG
TCAGCCCATGTCTGGATCGCAGCSTGGACATCTCGCCGCTGGAGGAC
CAGGCTGCCAGCGGTCAAGTATGGCCAGTGGTGGTGGTGGTGGTGGTGGTGGTGG
CTGCACAGTGTGAGGTGGCTGGGCAATCCCTACCCCGCTGGTGGTGGTGGTGGTGG
ACTCGGCCCATGACCAGAACAGCAACTTCTCATCGAGTACTTCCGCAATGAG
TTTGGGAGATCCAGGGTGCACAGAGCGAGATGATCTGGAACTTCCAATGCTG
GGTGGAGTCTGGATGACCAGGCCGACCTGCAAGCCGGGTACGAGGGCT
CAGGCCCTGGACCAACGCCCCAGGAGAAAGCGGAGGAGGATGAGGCTGCTGG
CCAGTTCAGTTCGGCCATCAAGAGGGCGACTGAGCACCAAGTACGA
TGCGCCCTTTGTCTTTGCGGAGTCAATGCCACGCTGGTGGTGGTGGTGGTGGTGG
AGGACGATGGGTCTGTGCACAAATCCATCAACCGTTCCCTGATCGTTGGGCTG
AAGATCAGCACTAAGAGCGTGGCCGAGACGAGCGGAGGATATCACCCACAC
CTCAAAATACCCAGAGGGTCTCAGAGGAGAGGAGGCCCTTCAAGAGGGCGA
ACCACCTGAACAACTGGCCGAGAGGAGGAGACAGGGATGGCCATGGCGGATC
CGTGGGCCAGAGCATGAACATGGGCACTGACTTTGACGTCTTTGCCACAT
CACCAACAACCCGCTGAGGAGTACGCTGCGCCCTCCTGCTGTGCGCCGCA
CGTCACTACAATGGATCTTTGGGCGCCGAGTGTGGACCAAGTACTGCTC
AACCTCAACCTGGAGCCTTTCTCTGGTAAAGCCCTGTGTTCTGGAGCATTTG
TTGA

```




Figure 4.2. BLAST results of the original (left hand) and the plasmid vector (right hand) sequences of TGM2_v2, (a) first and (b) second segments. Blue highlights show the matching bases. Gray highlights belong to the plasmid sequence.

The sequence results obtained by NIH BLAST software were displayed in Figure 4.3. They were in accordance with the DNA sequencing results, confirming that the TGM2_v2 sequence inside the plasmid was 100 per cent identical to the original TGM2_v2 sequence. These results collectively showed that the TGM2_v2 sequence inside the phTGM2 plasmid perfectly matched with the original NCBI sequence, without any mismatches.



Figure 4.3. NIH BLAST results of (a) segment 1 and (b) segment 2

4.2. GROWTH OF RBMSCS AND RAT KNEE CHONDROCYTES

The rBMSCs and rat chondrocytes used in this study were isolated from 10 weeks old Sprague-Dawley rats. It was observed that the rBMSCs were growing slower than the chondrocytes, as can be detected from Figure 4.4. In addition, the chondrocytes were smaller than the rBMSCs, and had more rounded shape which is a basic indicator of chondrocytic phenotype.

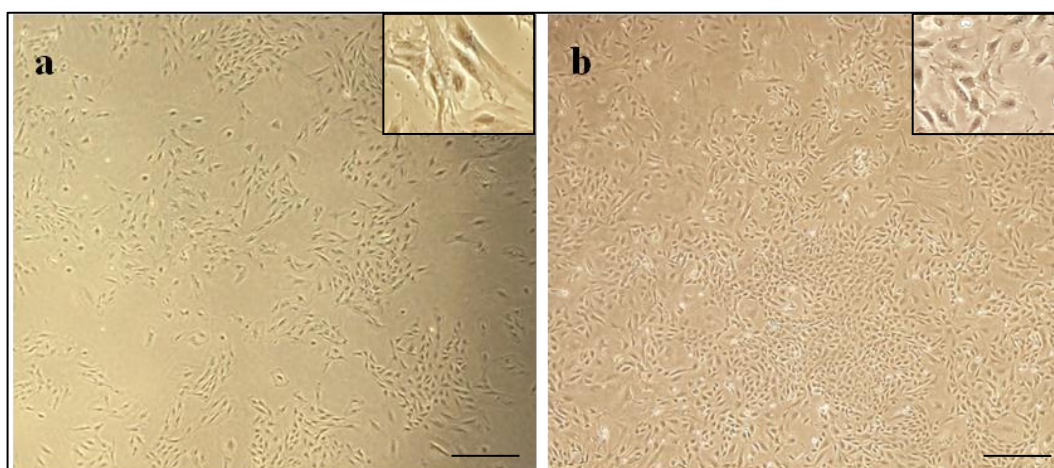


Figure 4.4. Bright field images of (a) passage zero rBMSCs and (b) passage zero rat knee chondrocytes taken with 4X objective. Small figures at the right corner demonstrate higher magnification images. Scale bars represent 500 μm .

4.3. TRANSFECTION AND TRANSDUCTION STUDIES

During transduction, protamine sulfate (PS) was used as a cationic polymer, because it was observed that PS did not have a cytotoxic effect on rBMSCs, even at high concentrations (100 $\mu\text{g}/\text{mL}$); instead, it showed proliferative effect (Figure D.1). Therefore, 50 $\mu\text{g}/\text{mL}$ PS concentration was chosen for the transduction process (3 hours of pre-incubation + 24 hours of viral media incubation).

4.3.1. Determination of Transfection Efficiency by Fluorescence Microscopy

HEK293T is a highly transfectable derivative of human embryonic kidney cell line, which is genetically engineered to produce the simian virus 40 (SV40) large tumor (T)-antigen [141]. This cell line stably expresses SV40 T-antigen, increasing the replication of plasmids with SV40 origin of replication inside the transfected cell [142]. For that reason, HEK293T cells were used for the production of lentiviral particles. It was observed that almost all of the cells were successfully transfected 48 hours after transfection with pEGFP plasmid vector, which was visualized by EGFP expression (Figure 4.5 b). Therefore, it could be said that the transfection efficiency was approximately 90 per cent. Even, the half of the cells

were already expressing EGFP at 24 hours of transfection (Figure 4.5 a) suggesting that transfection was quite efficient.

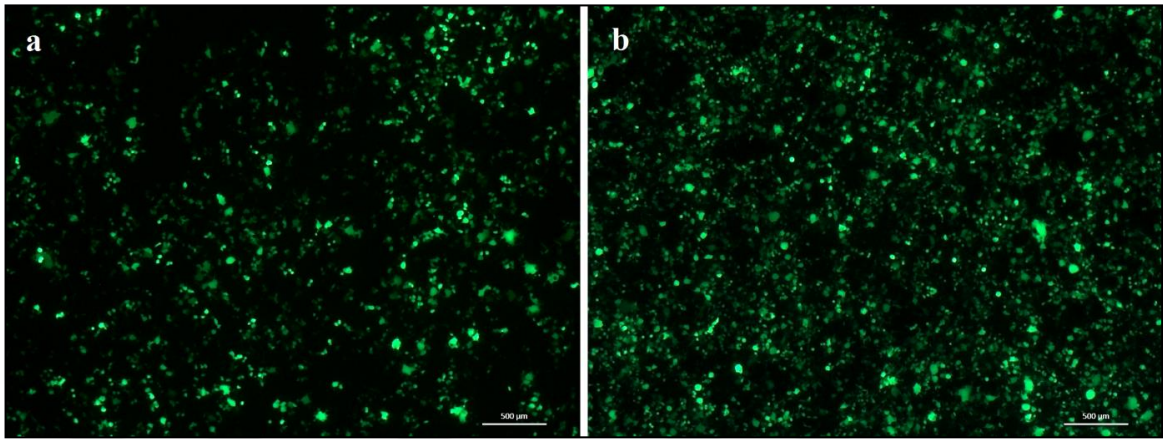


Figure 4.5. Fluorescence microscopy of HEK-293T cells (a) 24 hours, (b) 48 hours after transfection with pEGFP plasmid vector. Scale bars represent 500 μm .

4.3.2. Determination of Transduction Efficiency by Fluorescence Microscopy

After 48 hours of plasmid delivery into HEK-293T cells, the lentiviral particles were collected, and then supplied to rBMSCs. Since EGFP was used as a control plasmid, it was possible to verify the effectiveness of the viruses on the cells. Among lentiviral plasmid vectors, HIV-1-based ones, like we used in this study, were shown to be more effective in transducing MSCs [46]. Figures 4.6 - 4.8 belong to the fluorescence microscopy images of EGFP transduced cells after 24 hours, 4 days, and 7 days of incubation, respectively. As can be observed in Figure 4.6 a-f, rBMSCs in all groups started to express EGFP after 24 hours of transduction. It could clearly be observed that almost all of the cells were successfully transduced at the end of 4 days (Figure 4.7 a-f), and cells continued to proliferate for a week (Figure 4.8 a-f) without any loss in fluorescent signal. There was no significant difference among the cells in terms of transduction efficiency. All of the groups were transduced with almost the same efficiency.

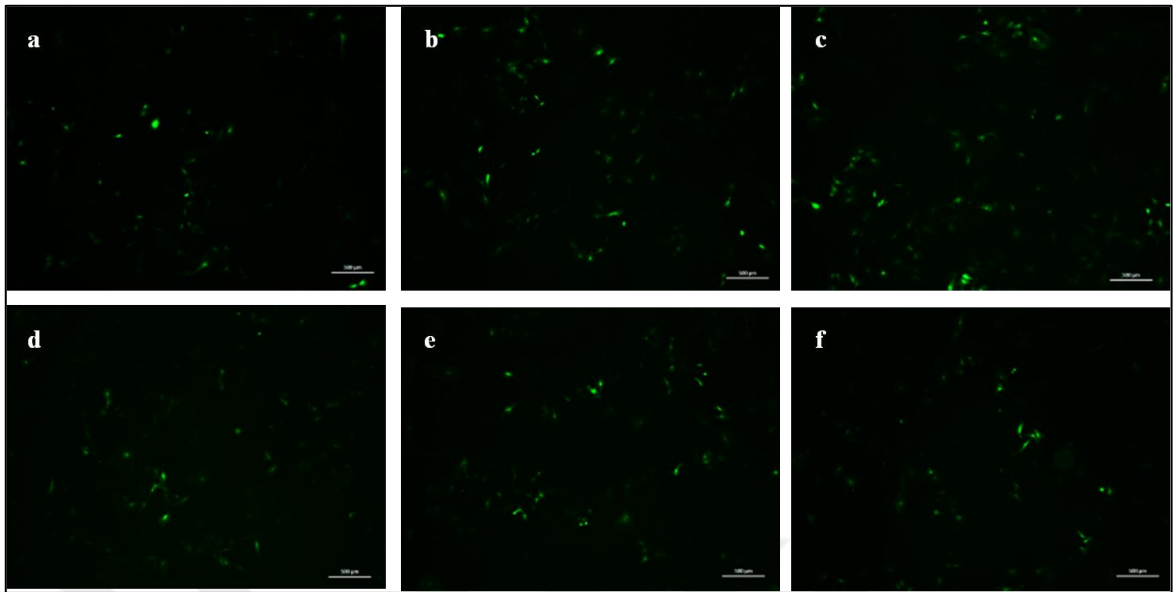


Figure 4.6. rBMSCs after 24 hours of transduction with lentiviral particles encoding EGFP; (a) group 1X, (b) group 1.5X, (c) group 2X, (d) group 1ML, (e) group 1.5ML, (f) group 2ML. Scale bars represent 500 μm .

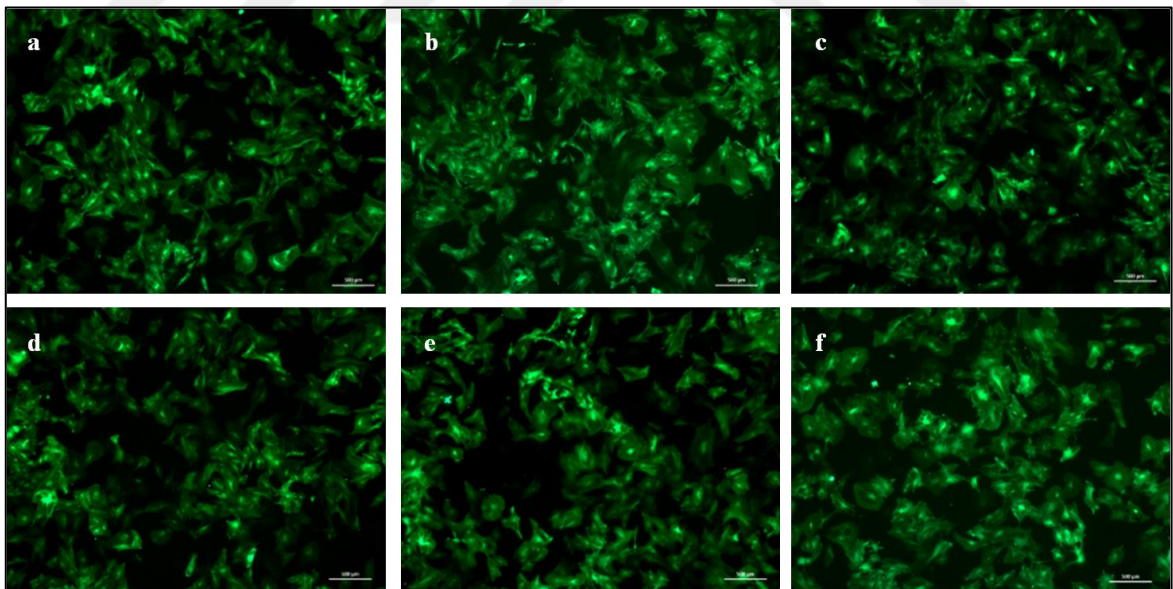


Figure 4.7. rBMSCs after 4 days of transduction with lentiviral particles encoding EGFP; (a) group 1X, (b) group 1.5X, (c) group 2X, (d) group 1ML, (e) group 1.5ML, (f) group 2ML. Scale bars represent 500 μm .

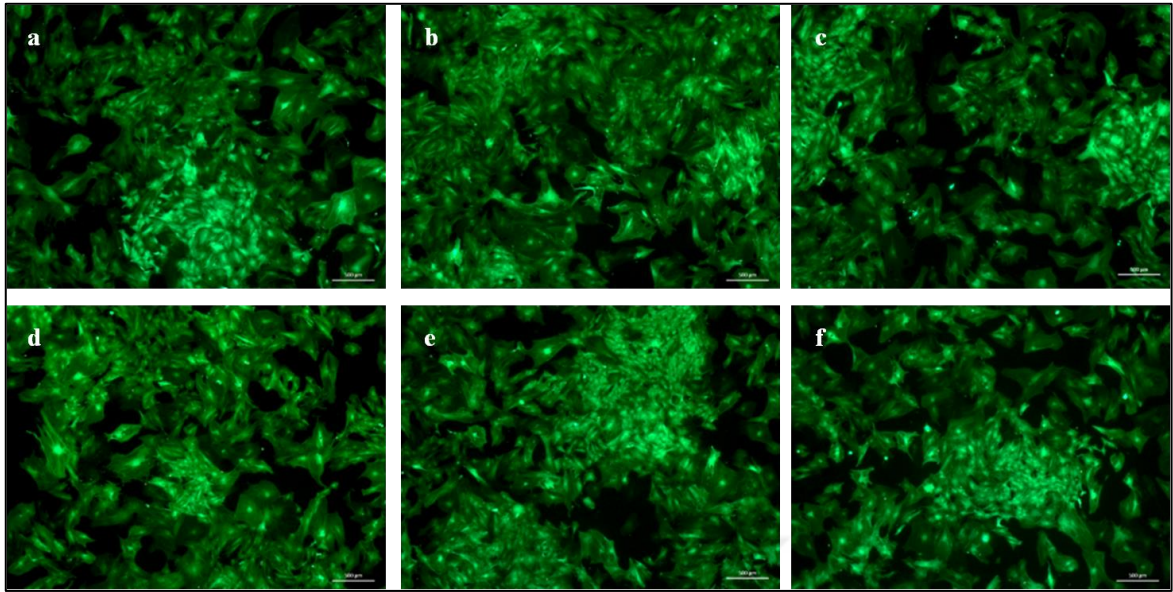


Figure 4.8. rBMSCs after 7 days of transduction with lentiviral particles encoding EGFP; (a) group 1X, (b) group 1.5X, (c) group 2X, (d) group 1ML, (e) group 1.5ML, (f) group 2ML. Scale bars represent 500 μm .

4.3.3. Flow Cytometry Analysis For the Verification of Transduction Efficiency

In order to validate the efficiency of transduction, rBMSCs transduced with lentiviral particles encoding EGFP were also analyzed with a flow cytometer (BD Biosciences) when they reached to the full confluency. The results were shown as flow graphs in Figure 4.9, and in Table 4.1 as a summary. Although both 2X and 2ML were almost equally efficient to transduce the rBMSCs with pEGFP, the transduction efficiency was slightly better with 2ML (99.56 per cent).

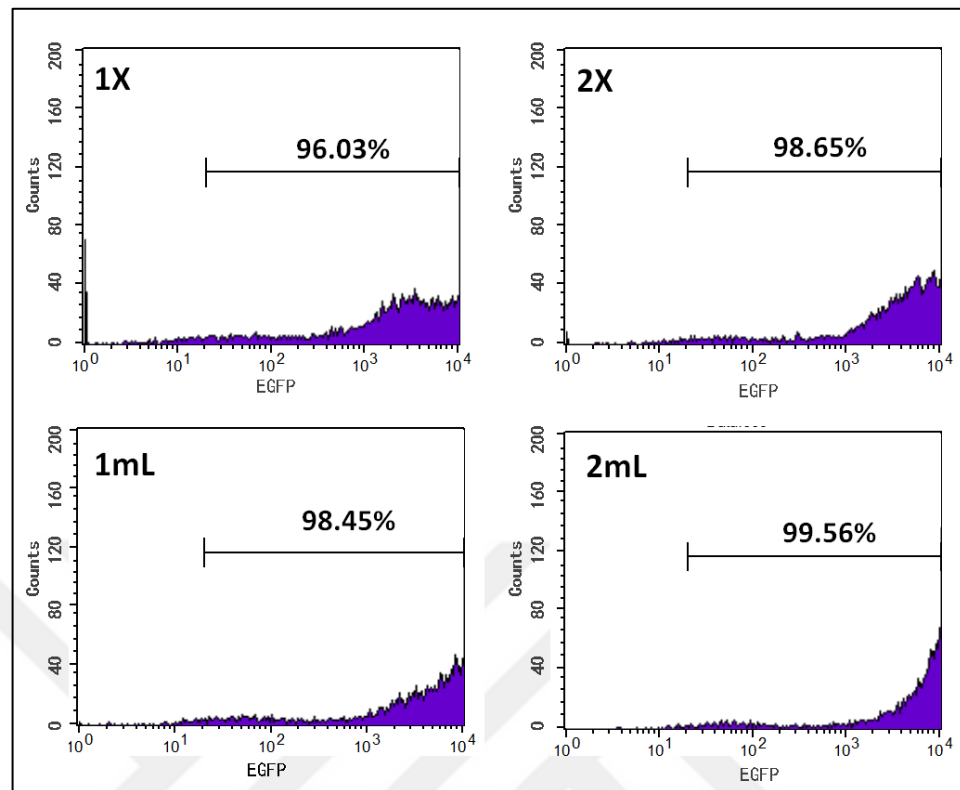


Figure 4.9. Flow cytometry analyses of rBMSCs transduced with lentiviral particles encoding EGFP (1X, 2X, 1ML and 2ML groups)

Table 4.1. Summary of flow cytometry results showing rBMSCs transduced with lentiviral particles encoding EGFP

EGFP- positive cells (%)	1X	2X	1ML	2ML
		96.03%	98.65%	98.45%

Meanwhile, the 2ML group cells were examined with flow cytometer for the expression surface markers to check if they could maintain their MSC properties. The flow graphs were shown in Figure 4.10 and summarized in Table 4.2. It was observed that rBMSCs could maintain their MSC phenotype even after transduction with viruses encoding TGM2_v2, as shown by 1.1 fold increase in the expression of rat MSC surface markers CD90 and CD29 [143]; in other words, transduction did not cause a reduction in stemness of these cells. In addition, transduced cells remained negative for endothelial marker CD31 and

hematopoietic marker CD45, which were shown by 1.4 fold and 5 fold decrease with respect to control cells.

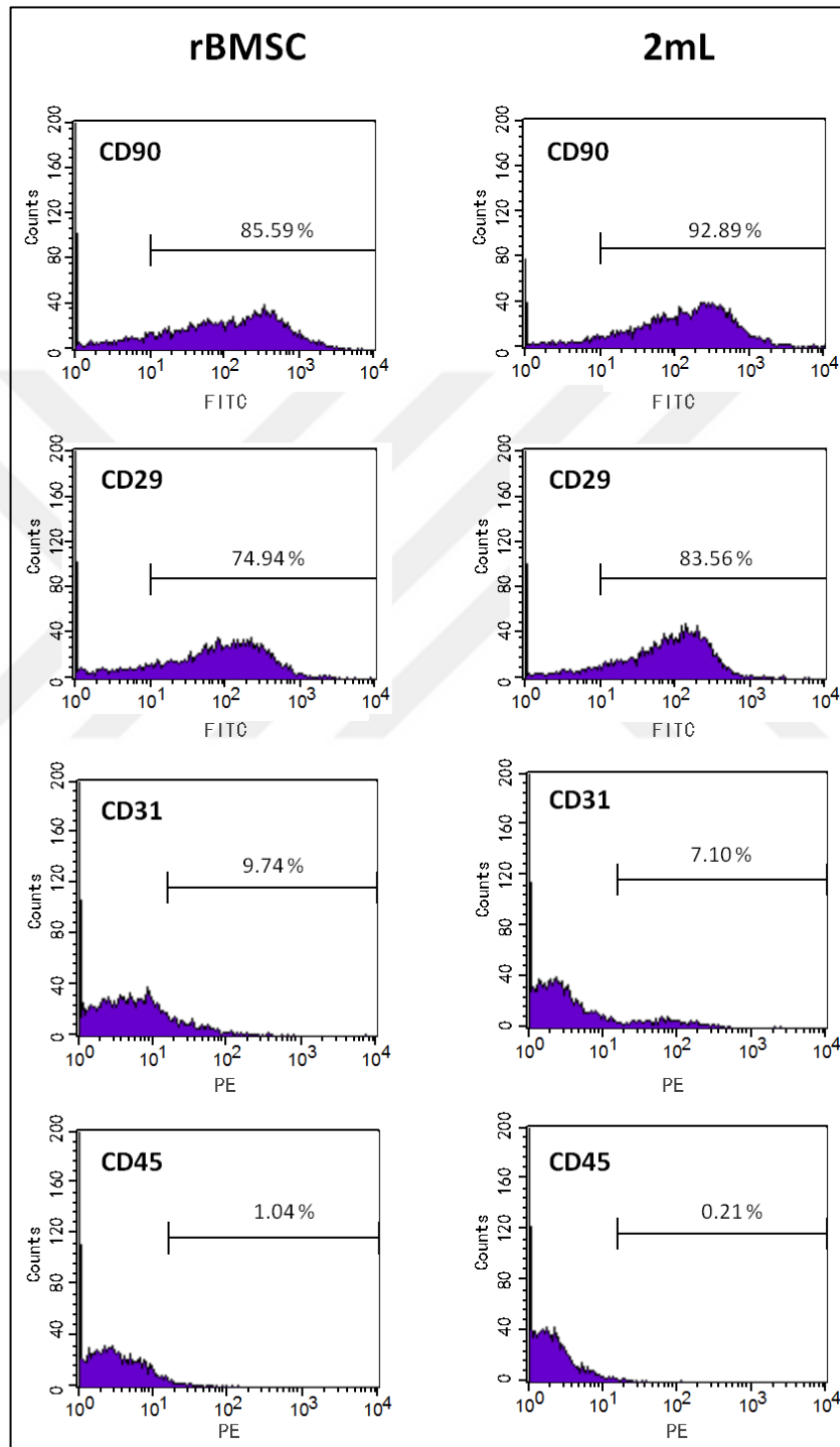


Figure 4.10. Flow cytometry results showing the stemness of rBMSCs after TGM2_v2 transduction (2ML group only)

Table 4.2. Positivity of mesenchymal stem cell markers of transduced rBMSCs (2ML only)

	CD31 (% positive cells)	CD45 (% positive cells)	CD90 (% positive cells)	CD29 (% positive cells)
Control rBMSCs	9.74	1.04	85.59	74.94
Transduced rBMSCs (2ML)	7.10	0.21	92.89	83.56

4.4. CHARACTERIZATION OF TRANSDUCED CELLS

Before characterization, the cells were selected with Blasticidin in order to eliminate the non-transduced ones from the cell culture flask. For this purpose, a kill curve was plotted for Blasticidin. As shown in Figure C.1, the cell viability decreased with the increasing Blasticidin concentration. According to this result, it was decided to use 5 $\mu\text{g}/\text{mL}$ of Blasticidin for selection of the cells after transduction.

4.4.1. TGM2_v2 Gene Expression Analysis for the Verification of Transduction Efficiency

In order to measure transgene expression at the mRNA level, real-time PCR was performed after 4 days following cell seeding on culture plates. The results were calculated by ΔC_T method using 18SrRNA reference gene. Figure 4.11 represents the relative expression levels of human TGM2_v2 gene in transduced rBMSCs (P5) (1X, 1.5X, 2X, 1ML, 1.5ML, and 2ML) and non-transduced cells (MSC). This graph could directly refer to transduction efficiency since the non-transduced rBMSCs have no human TGM2_v2 expression. The differences between the gene expression in control group (MSC) and those in other groups were found significant as expected because the control group normally has no TGM2_v2 gene. The lowest transduction efficiency was observed in 1X and 1ML, and no significant difference was detected between them, although there was a 40-fold increase in TGM2_v2 expression with respect to negative control. Among the viral media group, efficiency increased as the concentration of media increased, as expected; however, in viral pellet group, the trend was a little bit different. The transduction efficiency significantly increased

from 1X to 1.5X (1.8-fold), but the 1.2-fold decrease from 1.5X to 2X viral concentration was not significant. Still, a 1.5-fold increase in efficiency was recorded from 1X to 2X, which was found insignificant. There was a 2.5-fold significant increase in gene expression from 1ML to 1.5ML in viral media group, and a 2-3 fold increase from 1ML to 2ML was found significant. In 2ML group, a 120-fold increase in TGM2_v2 expression was recorded with respect to negative control suggesting that the highest efficiency was obtained with 2ML viral media usage in transduction of rBMSCs.

To sum up, the expression of TGM2_v2 was significantly higher in viral suspension groups (1ML to 2ML) than viral pellet groups (1X to 2X) indicating that transduction efficiency was better with the viral suspension usage rather than viral pellet, being the highest in the most concentrated viral suspension, 2ML. As viral pellet groups are more concentrated in terms of viral particle when compared to viral suspension groups, our result suggested that use of high virus particle concentrations may decrease the efficiency of gene transfer in rBMSCs. In agreement, transduction of human bone marrow derived MSCs with HIV-1 lentiviral particles caused cytotoxicity with increased viral titers (MOIs > 2) [144], possibly due to the VSV-G envelope of the plasmid vector [145]. Similarly, use of high MOI (>10) for the transduction of rat MSCs with adenoviral particles resulted in cell damage in a dose-dependent manner [146].

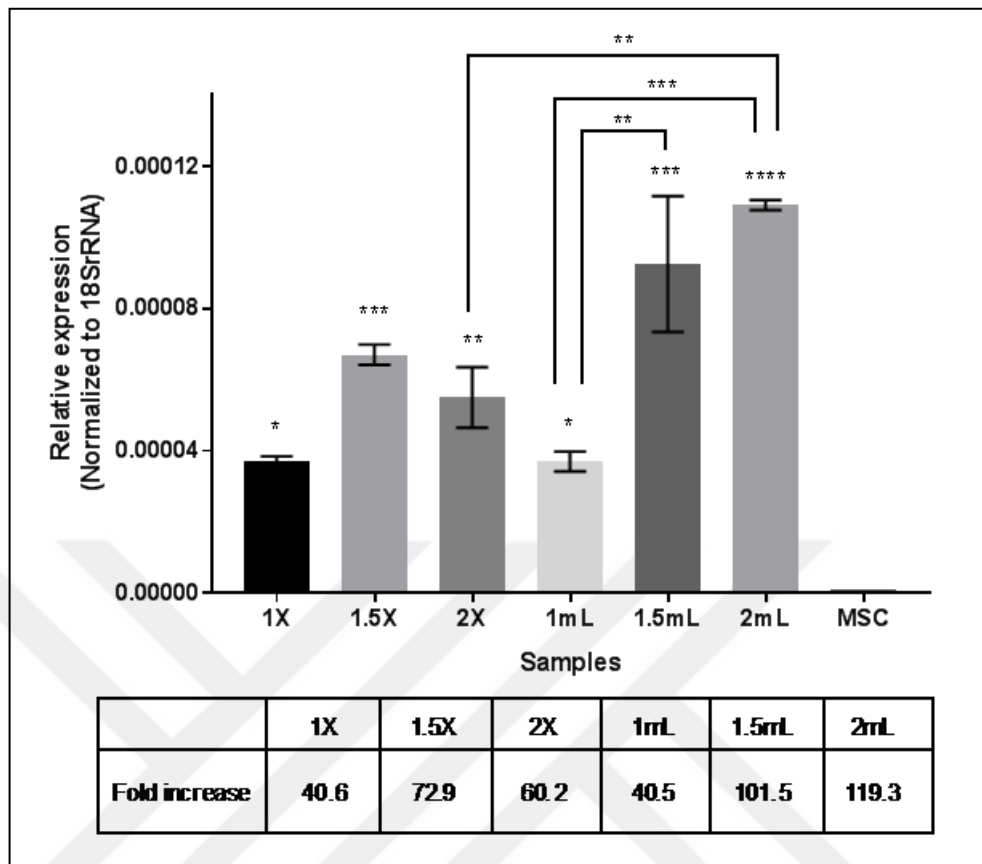


Figure 4.11. Relative expression of hTGM2_v2 in transduced P5 rBMSCs (viral pellets: 1X, 1.5X, 2X; viral suspensions: 1mL, 1.5mL, 2mL) and non-transduced P5 rBMSCs (MSC) as negative control. Values were normalized with housekeeping gene 18SrRNA, and denoted as fold increase with respect to negative control (* $p < 0.05$, ** $p < 0.005$, *** $p < 0.0005$, **** $p < 0.0001$).

Agarose gel electrophoresis was also performed at the end of real-time PCR in order to check the accuracy of the reaction. It was observed that except hTGM2 in negative control, all the DNA groups were successfully amplified (Figure 4.12). Since the MSC group was not transduced and the cells were rat MSCs, the absence of human TGM2 in this group was expected. According to the agarose gel electrophoresis result it can be proved that transduction of rBMSCs with hTGM2_v2 was successfully achieved. The difference in transduction efficiencies between different viral titers could not be distinguished from this figure.

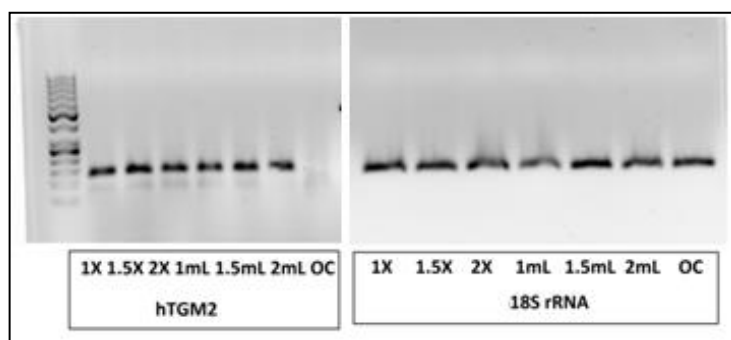


Figure 4.12. Agarose gel electrophoresis of real-time PCR products (hTGM2 and h18SrRNA: 142 bp). OC: non-transduced rBMSCs as negative control.

4.4.2. Western Blotting for the Observation of TG2-S Protein Expression

To analyze the expression of TG2-S in the transduced cells at the protein level, Western blotting was performed using rat β -actin protein as internal control (Figure 4.13). TG2-S protein expression was clearly visible in all groups, in comparison with the negative control (MSC). Decrease in TG2-S expression was recorded among viral pellet groups, 1X, 1.5X, 2X, while an increasing trend in TG2-S expression was observed among the viral suspension group with increasing viral concentration as indicated by densitometry analysis (normalized to β -actin) showing 10 per cent, 14 per cent and 16 per cent increase in TG2-S expression in 1ML, 1.5ML, 2ML groups, respectively. This trend among the viral suspension groups were in consistency with the real-time PCR results of TGM2_v2 gene expression. In contrast, the western blot analysis indicate a decrease in protein expression from 1X to 2X, although the gene expression increased with increasing viral pellet concentration, which suggests a malfunction in the process of translation from mRNA to protein. This could be the result of cell damage due to the high virus concentration, which was in consistency with the evidence showing cytotoxicity with increasing viral titers [144][146], as described in the previous section. Together with real-time PCR results, these data suggested that 2 mL transduction method was more efficient for rBMSCs for the expression of the human TGM2_v2 both in mRNA and protein level.

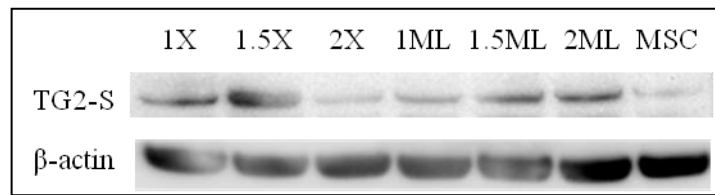


Figure 4.13. Western blot with TG2 antibody (62 kDa) and β -actin antibody (42 kDa).

MSC: non-transduced rBMSCs as negative control.

4.4.3. Cell Viability Assay to Examine Cell Proliferation

After transduction, the cells were examined under bright field microscope throughout the culture time to check the cell viability. All of the transduced cells proliferated as healthy as non-transduced cells suggesting that transduction did not affect cell viability. This finding was quite promising for the future experiments, because in contrast to our result, the expression of TG2-S in fibroblasts was found to be related with cell death [129]. In order to compare the effect of transduction method on cell proliferation, MTS assay was carried out with 2X and 2ML groups on 1, 7, and 14 days after cell seeding on 12-well plates (Figure 4.14). The cell number graph was plotted using a calibration curve that was previously prepared for rBMSCs (Figure B.1). The viability profiles were almost equal within 2 weeks; however the viability of 2ML group was significantly ($p < 0.0001$) 1.3 fold better than that of 2ML on the day 7, and the 1.2 fold difference between 2X and 2ML on the day 14 was found significant ($p < 0.0001$). This initial difference in cell number could be due to the role of TG2 in enhancing cell adhesion-mediated survival signaling [108], hence the number of cells attaching on culture plates after initial seeding increased in the higher TG2-S expressing group.

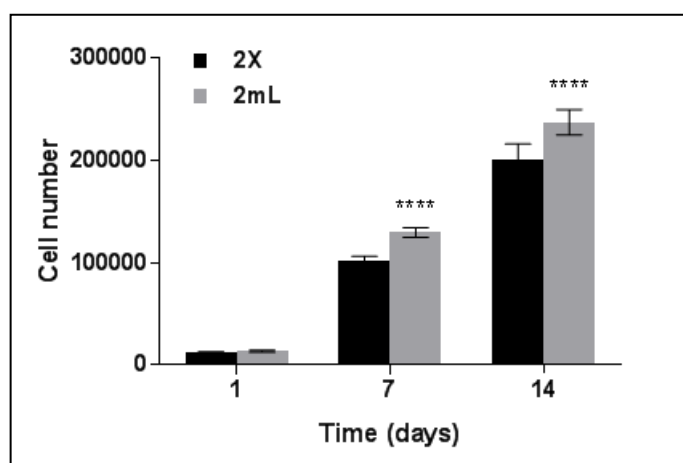


Figure 4.14. Comparison of cell viabilities of transduced (2X and 2ML) cells after 1, 7, and 14 days of incubation in growth media (no chondrogenic induction). Initial cell seeding density: 20 000 cells/well (**** $p < 0.0001$).

Another 2-week-MTS assay was performed to see the effect of chondrogenic differentiation media on the cells. For this purpose, only 2ML group was used to compare with the control group (MSC), and the graph showing cell number was plotted using the calibration curve that was previously prepared (Figure B.1). It was clearly observed that differentiation media significantly decreased the rate of proliferation in both 2ML and control group after day 7, which could suggest chondrogenic differentiation (Figure 4.15), since proliferating cells could not maintain differentiation within the same level; first they need to stop mitosis, then continue differentiation [147]. The decrease in proliferation continued on day 14 of incubation, which was significantly 2 fold and 4 fold for 2ML and MSC group, respectively. The proliferation profiles of 2ML and MSC group cells were similar, except that initial transduced cell attachment was almost one third of the control cells, which was found quite significant ($p < 0.0001$). Therefore, the proliferation of transduced cells was significantly lower than that of non-transduced ones throughout 2 weeks without chondrogenic stimulation. Likewise, when chondrogenic induction was applied, the cell number in 2ML group on day 7 was significantly lower (2 fold) than that of control ($p < 0.0001$). However, the difference in cell numbers observed between 2ML and MSC groups on day 14 without chondrogenic stimulation was found insignificant. Once more, this can be related with either the initial cell number or chondrogenic differentiation of 2ML group cells.

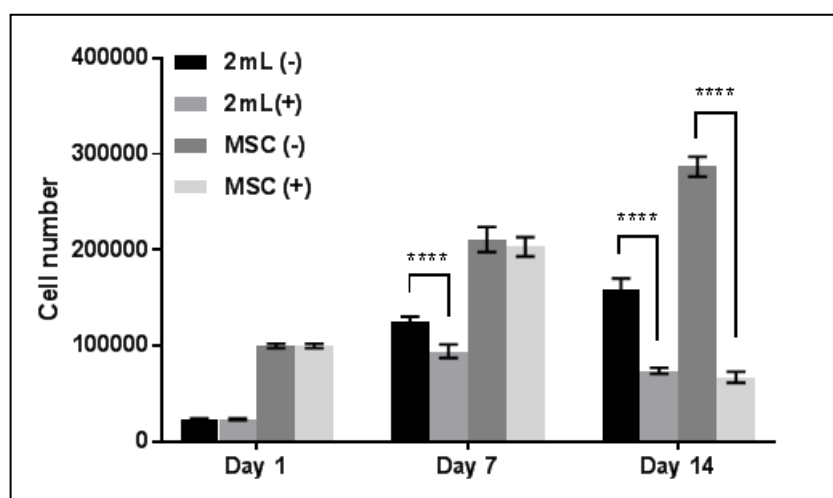


Figure 4.15. Effect of chondrogenic differentiation medium on the viabilities of transduced (2ML) and non-transduced (MSC) rBMSCs after 1, 7, and 14 days of incubation; (+): chondrogenic induction; (-): no induction (**** $p < 0.0001$). Initial cell seeding density: 100 000 cells/well.

4.5. CHARACTERIZATION OF THE SCAFFOLDS

PBSu is one of the biodegradable aliphatic polyesters, which has been used since 1993 and under investigation for different applications. It is synthesized from succinic acid and 1,4-butanediol which can be extracted from either fossil reserves or through fermentation [148]. PBSu biodegradation products are mainly water and carbon dioxide, which means that it can be metabolized by living organisms, making this polymer an attractive one for research [149]. The number of studies that use PBSu or its copolymers is increasing. In 2008, a scaffold prepared from poly(1,4-butylene succinate) extended with 1,6-diiocyanato-hexane (PBSu–DCH) was proposed to be used in bone tissue engineering [150]. Another study showed that chitosan/polybutylene succinate fibre-based scaffolds (C-PBS) that were seeded with bovine articular chondrocytes can be potentially used in cartilage tissue engineering [70]. Based on this information, we decided to investigate PBSu as the scaffold material in our research due to the limited number of studies utilizing PBSu in cartilage tissue engineering.

4.5.1. Fluorescence Microscopy of the Cell-Seeded PBSu Scaffolds to Observe Cell Attachment and Morphology

EGFP-transduced rBMSCs of all viral pellet and viral suspension groups were seeded on 2 per cent, 4 per cent, 6 per cent, and 8 per cent PBSu scaffolds in order to observe cell behaviors on the scaffolds, such as attachment, migration, and proliferation. Both the transduction groups and scaffold concentrations were tested in this part of the study. After 35 days of cell seeding, fluorescent images of the cell seeded scaffolds were captured with fluorescence microscope (Axio Vert.A1, Carl Zeiss). Figures 4.16 to 4.19 belong to 2 per cent to 8 per cent scaffolds, respectively. The cells that were attached at the bottom of the flasks were out of focus and observed as green blurs (Figure 4.16 a; Figure 4.17 c, e; Figure 4.18 e). The cells inside the pores of the scaffolds could be distinguished by their localization along the inner walls of the pores, forming spherical groups (Figure 4.16 a, c; Figure 4.17 c, d; Figure 4.18 c, e, f). Most of the cells were able to attach and proliferate in the pores of the scaffolds, especially 2X, 1.5ML and 2ML group cells. The lowest cell viability was observed in group 1X and 1ML. Among 1X group cells, the best result was obtained with 6 per cent scaffolds (Figure 4.18 a). When 1.5X group was observed, it could be said that 4 per cent scaffold was the most suitable one (Figure 4.17 b). Group 2X cells were considerably better in attachment onto the scaffolds, except the 8 per cent PBSu scaffold (Figure 4.19 c). There were nice clusters of them inside the pores of the 2 per cent, 4 per cent, and 6 per cent scaffolds (Figure 4.16 c, 4.17 c, 4.18 c). It could clearly be seen that 1.5ML group cells were able to attach and proliferate on all of the scaffolds, almost with the same efficiency (Figure 4.16 e, 4.17 e, 4.18 e, 4.19 e). When 2ML group cells were observed in detail, as they will be the main cells of choice in the following differentiation analyses, it could be seen that the best cell proliferation and attachment were achieved on 8 per cent scaffolds, as evident by the cells in the pores (Figure 4.19 f). Similarly, the cells attached inside the pores of 6 per cent scaffolds (Figure 4.18 f) better than they did in 2 per cent (Figure 4.17 f) and 4 per cent (Figure 4.17 f).

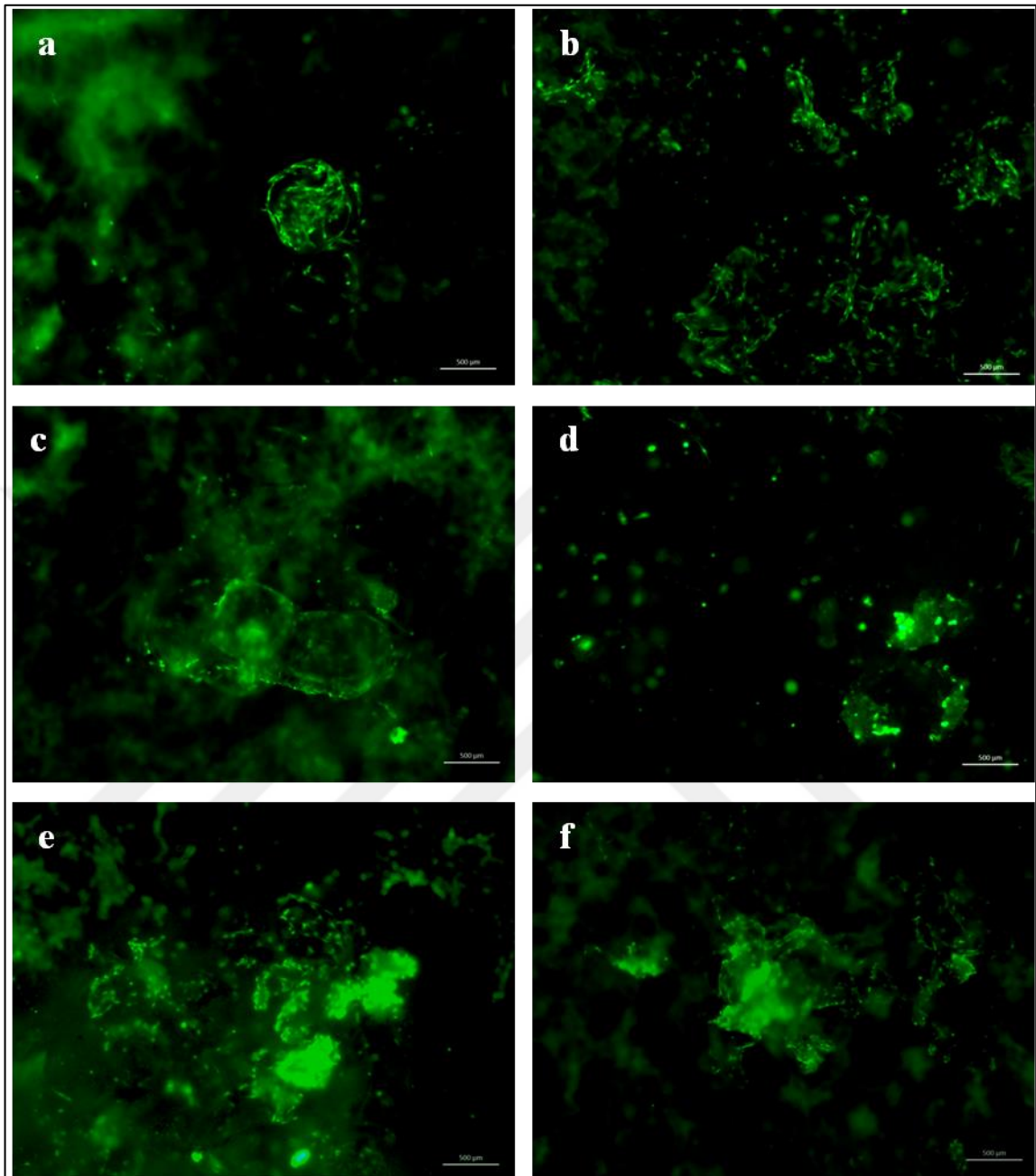


Figure 4.16. Fluorescence microscopy of rBMSCs transduced with lentiviruses encoding EGFP on 2% PBSu scaffolds 35 days after cell-seeding. (a) 1X group, (b) 1.5X group, (c) 2X group, (d) 1ML group, (e) 1.5ML group, (f) 2ML group. Scale bar: 500 μm , objective: 5X.

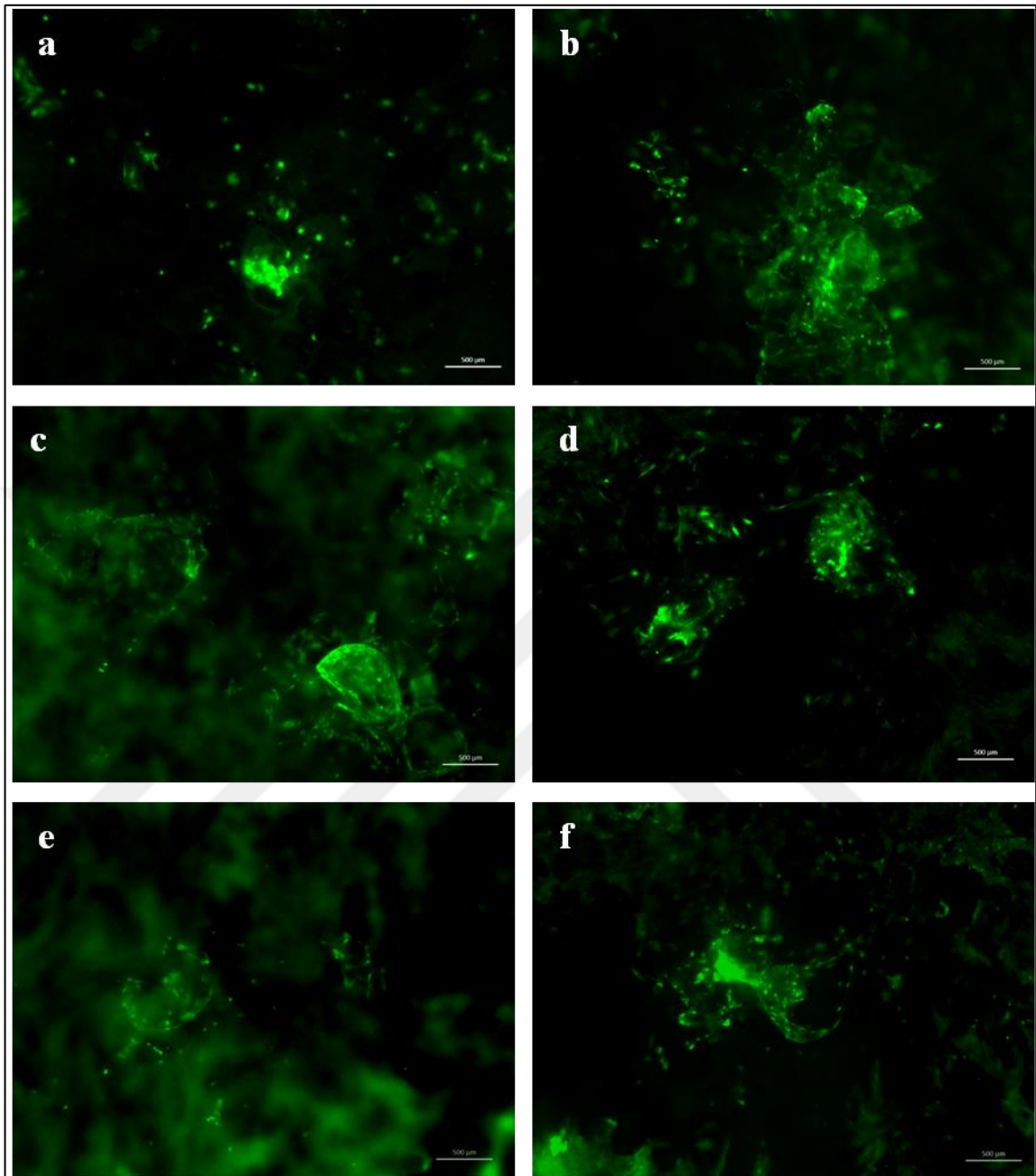


Figure 4.17. Fluorescence microscopy of rBMSCs transduced with lentiviruses encoding EGFP on 4% PBSu scaffolds 35 days after cell-seeding. (a) 1X group, (b) 1.5X group, (c) 2X group, (d) 1ML group, (e) 1.5ML group, (f) 2ML group. Scale bar: 500 μm , objective: 5X.

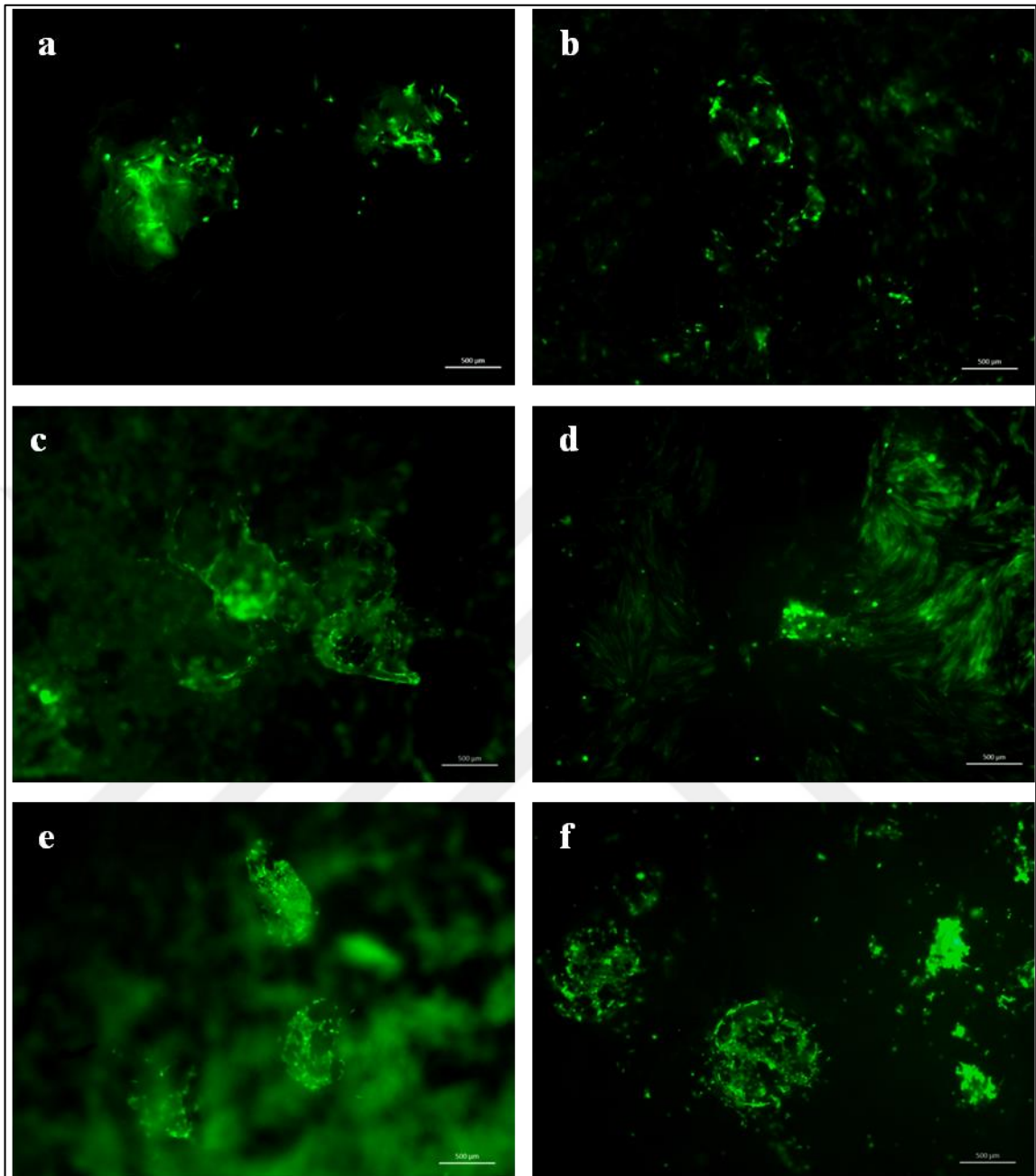


Figure 4.18. Fluorescence microscopy of rBMSCs transduced with lentiviruses encoding EGFP on 6% PBSu scaffolds 35 days after cell-seeding. (a) 1X group, (b) 1.5X group, (c) 2X group, (d) 1ML group, (e) 1.5ML group, (f) 2ML group. Scale bar: 500 μm , objective: 5X.

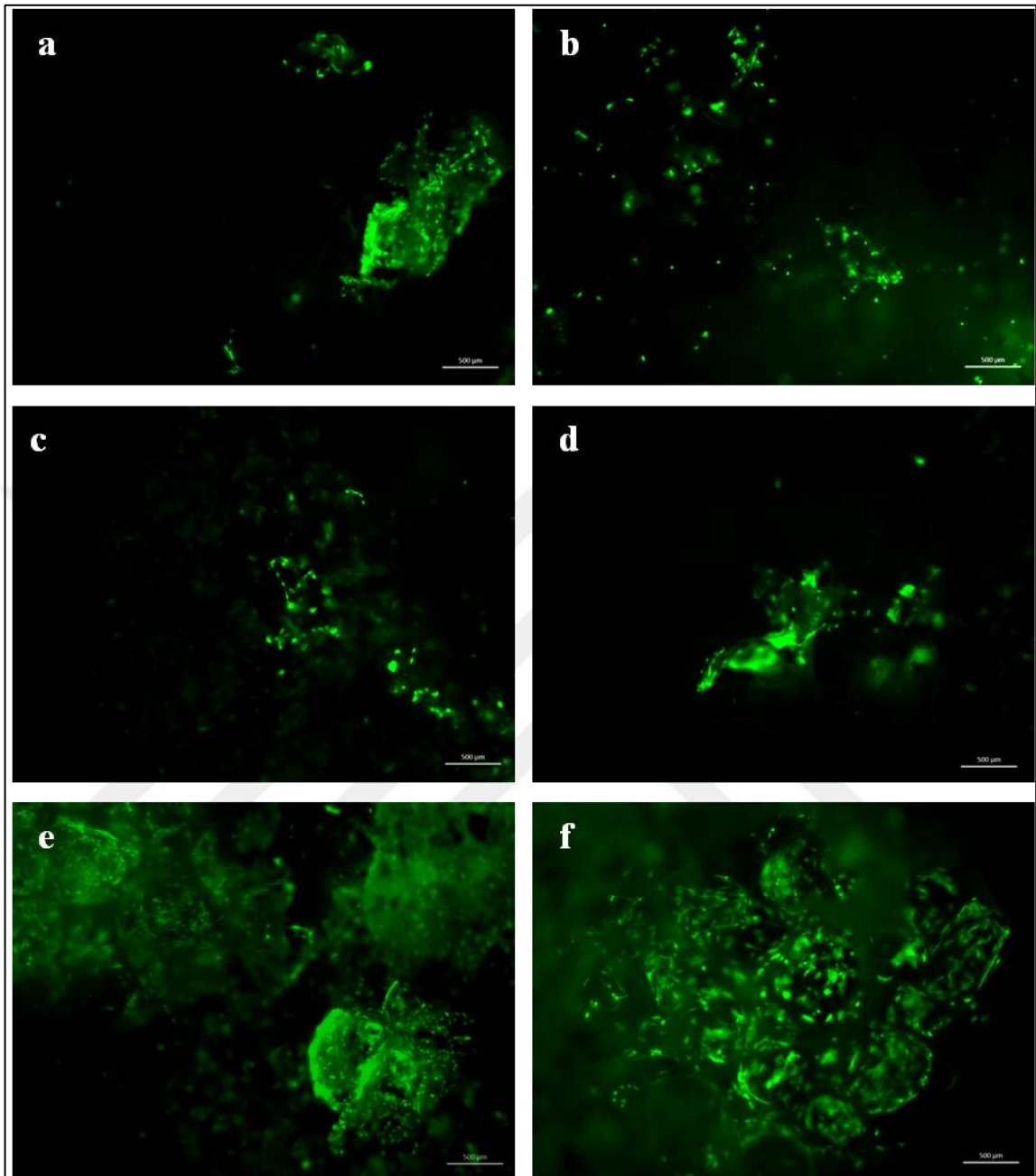


Figure 4.19. Fluorescence microscopy of rBMSCs transduced with lentiviruses encoding EGFP on 8% PBSu scaffolds 35 days after cell-seeding. (a) 1X group, (b) 1.5X group, (c) 2X group, (d) 1ML group, (e) 1.5ML group, (f) 2ML group. Scale bar: 500 μm , objective: 5X.

The fluorescence microscopy images of the transduced cells on scaffolds were summarized in terms of cell attachment in Table 4.3. The best attachment was graded as (+++), whereas the worst one was graded as (+). According to that table, the best cell attachment was observed in 2ML group, followed by 1.5ML and 2X groups. The 1X group cells displayed an overall moderate attachment on PBSu scaffolds, which was slightly better in 1.5X and 1ML groups. These results suggested that TGM2_v2 transduction increased the ability of rBMSCs to adhere onto the scaffolds in a dose-dependent manner, which is probably due to the role of TG2 in integrin-mediated cell adhesion as described in section 1.3.1.

Table 4.3. Grading of the attachment* of transduced cells on PBSu scaffolds at day 35 according to Figures 4.16 to 4.19.

	1X	1.5X	2X	1ML	1.5ML	2ML
2% PBSu	++	++	+++	+	+++	+++
4% PBSu	+	++	+++	++	++	+++
6% PBSu	+	+	+++	++	+++	+++
8% PBSu	+	+	+	+	+++	+++

* moderate attachment: +, good attachment: ++, best attachment:+++

4.5.2. SEM of the Scaffolds for Topographical Analysis

Analysis of PBSu scaffold topographies (porosity, homogeneity, etc.) were accomplished by SEM. It was observed that as the percent concentration of PBSu increased, porosity decreased and poor pore homogeneity was observed (Figure 4.20). Distorted pore structures were quite visible in 8 per cent and 10 per cent scaffolds (Figure 4.20 e and f); whereas fine pore structures were observed in 4 per cent and 6 per cent (Figure 4.20 c and d). Scaffolds with 1 per cent and 2 per cent PBSu were too porous (Figure 4.20 a and b) such that it might pose problems such as quick degradation of scaffolds. Porosity is one of the key criteria for scaffold design. If a scaffold does not have sufficient porosity for both cell migration and exchange of culture media, it cannot be used for tissue regeneration [151]. For that reason, 4 per cent and 6 per cent PBSu were found potentially suitable for cell seeding.

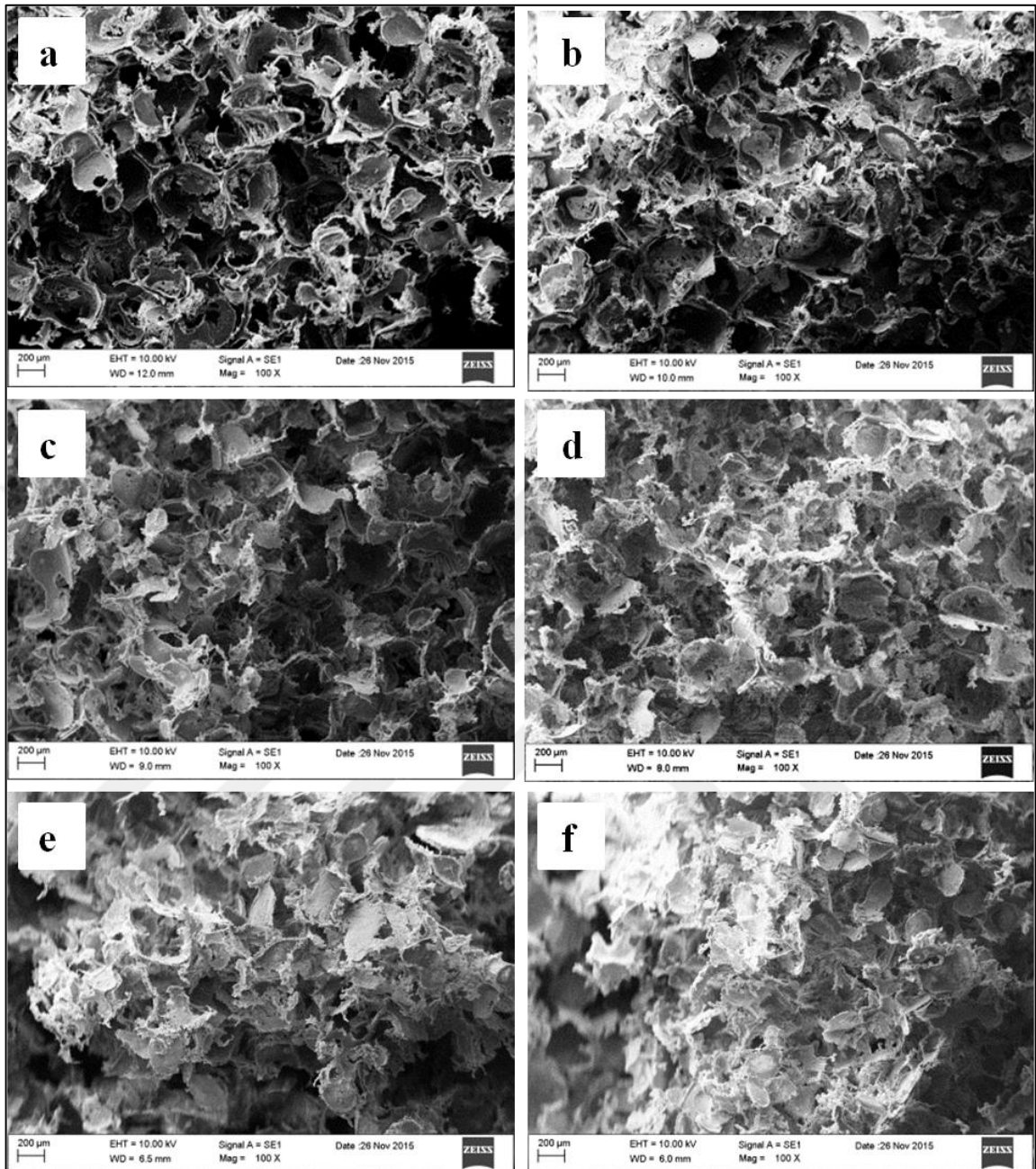


Figure 4.20. SEM micrographs of (a) 1%, (b) 2%, (c) 4%, (d) 6%, (e) 8%, (f) 10% PBSu scaffolds. Magnification: 100X, scale bar: 200 µm.

PBSu scaffolds were found too fragile and had a tendency towards break up. Therefore, it was decided to prepare its blend with a polymer that is more rigid than PBSu. Similar to PBSu, PLLA is biodegradable at a controllable rate, and its biodegradation products are basically water and carbon dioxide, which are non-toxic for living organisms [152]. On the other hand, PLLA is much less ductile than PBSu [153]. Blending PBSu with PLLA would

result in a scaffold biomaterial that is neither too brittle, nor too flexible for cartilage tissue engineering. For this reason, PBSu:PLLA blend scaffolds prepared in 1:1 (w/w) ratio were used for the following part of this study.

The SEM of 4 per cent and 6 per cent PBSu:PLLA blend scaffolds (1:1 w/w) were shown in Figure 4.21. PBSu:PLLA scaffolds were found more suitable for cell-seeding rather than PBSu alone, as they presented better surface and pore characteristics. The scaffolds with 6 per cent PBSu:PLLA (Figure 4.21 b) had better and more homogeneous pore shapes than 4 per cent (Figure 4.21 a). As a result, 6 per cent PBSu:PLLA scaffolds were chosen as the most suitable ones for the cell culture experiments, which was supported by our previous study [154].

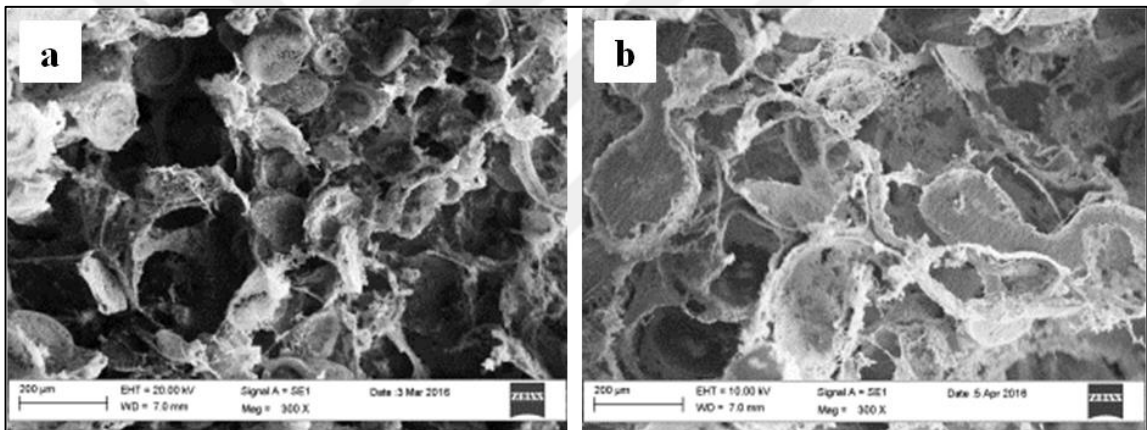


Figure 4.21. Scanning electron micrographs of a) 4% and b) 6% PBSu:PLLA scaffolds. Magnification: 300X, scale bar: 200 µm.

After choosing 6 per cent PBSu:PLLA scaffold for the following experiments, cell seeding was performed. The cell-seeded scaffolds were analyzed using SEM at day 1, 14 and, 21 after incubation in growth medium (Figure 4.22). Since it was chosen according to previous experiments, 2ML group was used as the representative of transduced rBMSCs, together with the control cells (non-transduced rBMSCs and rat chondrocytes). On the first day of incubation, not much cells were observed on the scaffolds (Figure 4.22 a, d, g); however, after 14 days of incubation, the cells grew and migrated inside the pores (Figure 4.22 b, e, h). On the 21st day of incubation, the cells almost covered the surfaces of pores as cell sheets,

as can be observed in Figure 4.22 c, f, i. No significant difference was detected between the cell types when cell morphology was considered.

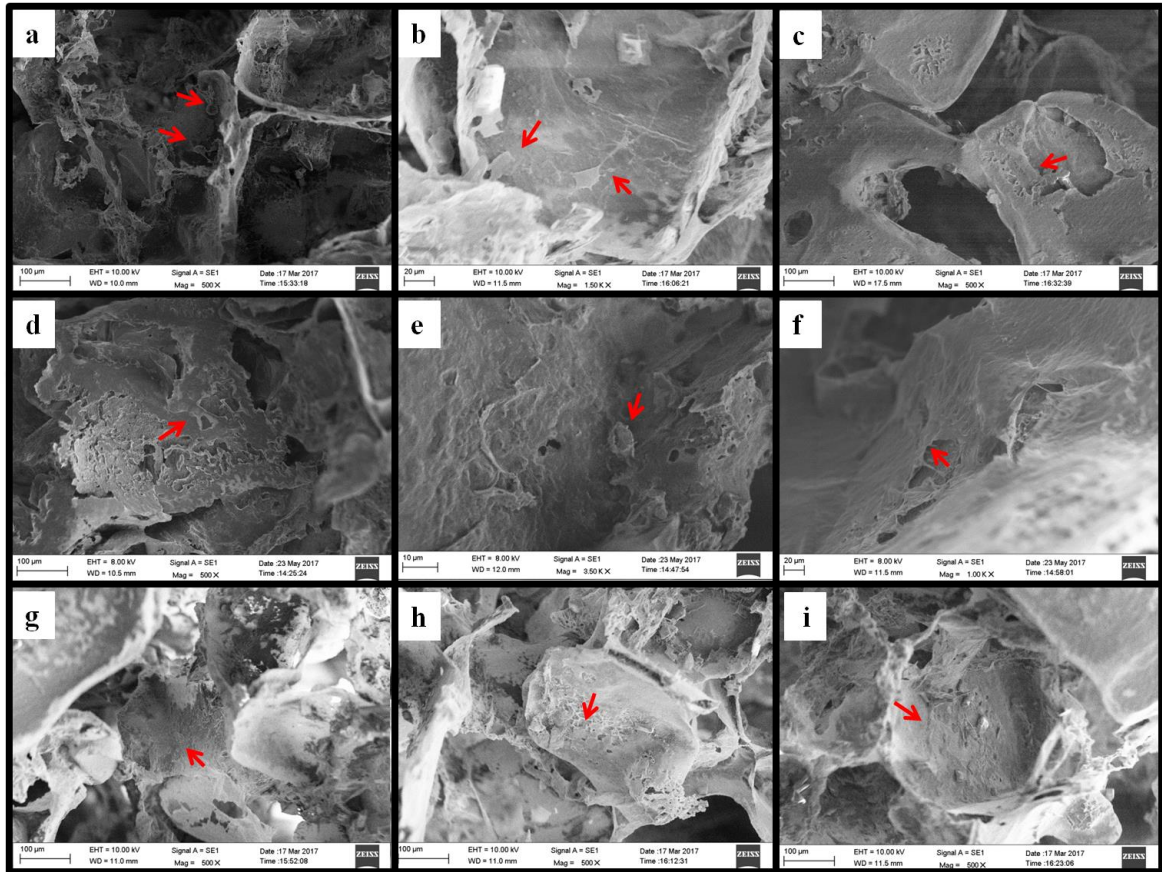


Figure 4.22. Scanning electron micrographs of cell-seeded PBSu:PLLA (6%) scaffolds at day 1 (a, d, g), day 14 (b, e, h), and day 21 (c, f, i). SEM of 2ML groups (a-c), non-transduced rBMSC group (d-f), chondrocyte group (g-i). Some of the cells were shown with arrows.

4.5.3. Cell Viability on Scaffolds to Observe Cell Proliferation

Cell attachment and proliferation of 2X and 2ML cells on PBSu:PLLA (6 per cent) scaffolds were analyzed by MTS assay on the 1st, 7th, and 14th days of cell seeding. Bar graph showing cell numbers was plotted for 2X, 2ML, and MSC groups using the calibration curve that was previously prepared (Figure B.1). No chondrogenic induction was applied so that only the effect of scaffolds on cell viability could be observed. According to figure 4.23, the transduced cells could not attach to the scaffolds as good as non-transduced ones, since the

cell numbers calculated for 2X and 2ML groups on day 1 were significantly lower (~1.5 fold) than the control group (MSC). Accordingly their cell proliferation rates were much lower than that of MSC in the following days. On day 7, there was a decrease in cell numbers observed for both 2X and 2ML groups (~2 fold for both), but cell number recorded in 2ML was significantly 1.5 fold higher than that of 2X. Among the transduced cells, 2ML group had a significantly better profile than 2X group throughout 14 days, which can be deduced from the 2-fold cell number increment on day 14. This could also suggest that 2ML group could adapt themselves to the scaffold environment after 7 days, whereas 2X group possibly detached from the scaffold. Together with the mRNA and protein expression results, it can be concluded that usage of 2 mL lentiviral media for rBMSC transduction was better than using viral pellets. Therefore, the cells that were transduced with 2 mL viral media were found suitable for seeding on scaffolds in the following part of this study.

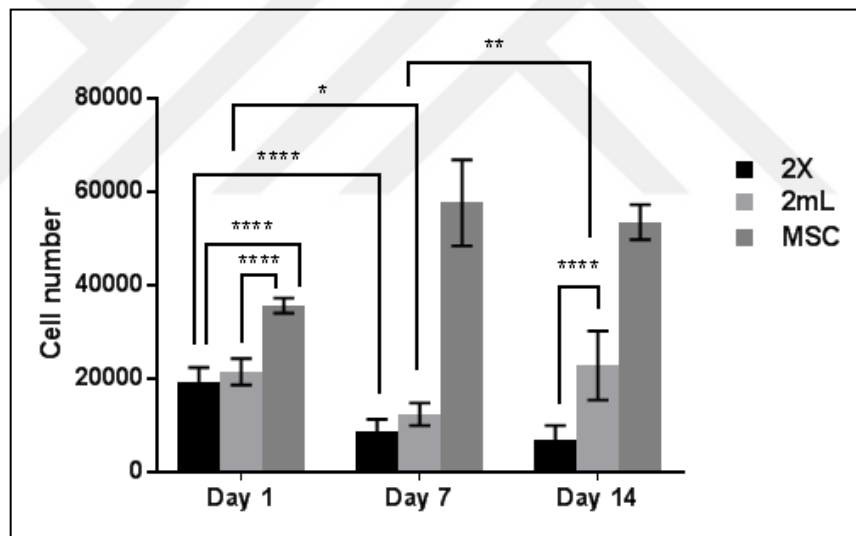


Figure 4.23. Viability of transduced (2X, 2ML), and non-transduced (MSC) cells on 6% PBSu:PLLA scaffolds (1:1 w/w) after 1, 7, and 14 days of incubation in growth media (* $p < 0.05$, ** $p < 0.005$, **** $p < 0.0001$). Initial cell-seeding density: 50 000 cells/scaffold.

Similarly, the cell-seeded scaffolds were analyzed in terms of cell attachment and proliferation by MTS assay on day 1, 14, and 21 of incubation in chondrogenic media. Figure 4.24 showing cell number values was plotted using the calibration curves that were previously prepared for rBMSCs and chondrocytes (Figure B.1 and B.2). It was observed that 2ML group cells had significantly better (1.5-2 fold) cell attachment on day 1 than

chondrocytes and rBMSCs on day 1, which was an expected result due to the ECM crosslinking activity of TG2-S in 2ML group. After 14 days of incubation in growth media, the cell number recorded for 2ML group was significantly lower than CH, whereas it was significantly higher than the number observed for MSC group. On the other hand, when chondrogenic induction was applied on day 14, it was observed that cell numbers recorded for 2ML and MSC group decreased 1.5 fold, while the number calculated in CH increased. A 4.5 fold difference in proliferation between 2ML and CH on day 14 was found significant. This result could indicate that since chondrocytes were already differentiated, they could adapt themselves to proliferation, but 2ML group cells and non-transduced rBMSCs started to differentiate, thus they decreased their rates of proliferation. After 21 days of incubation in growth media, 2ML group displayed an increase in cell number, which was slightly less than the CH group. Yet the difference between them was found insignificant, suggesting that 2ML and CH groups had similar proliferation profiles without chondrogenic induction. In contrast, the cell number recorded for chondrogenically induced MSC group on day 21 was significantly lower than that of 2ML group both with (3 fold) and without (10 fold) chondrogenic induction. It can be concluded that transduction of rBMSCs with TGM2_v2 increased the cell attachment onto the scaffolds throughout 21 days, which was consistent with the finding that MSCs that are genetically engineered to overexpress TG2 displayed an increase cell attachment on 3D matrices [103]. Besides, chondrogenic induction resulted in decrease of rBMSC (either transduced or non-transduced) proliferation, as expected.

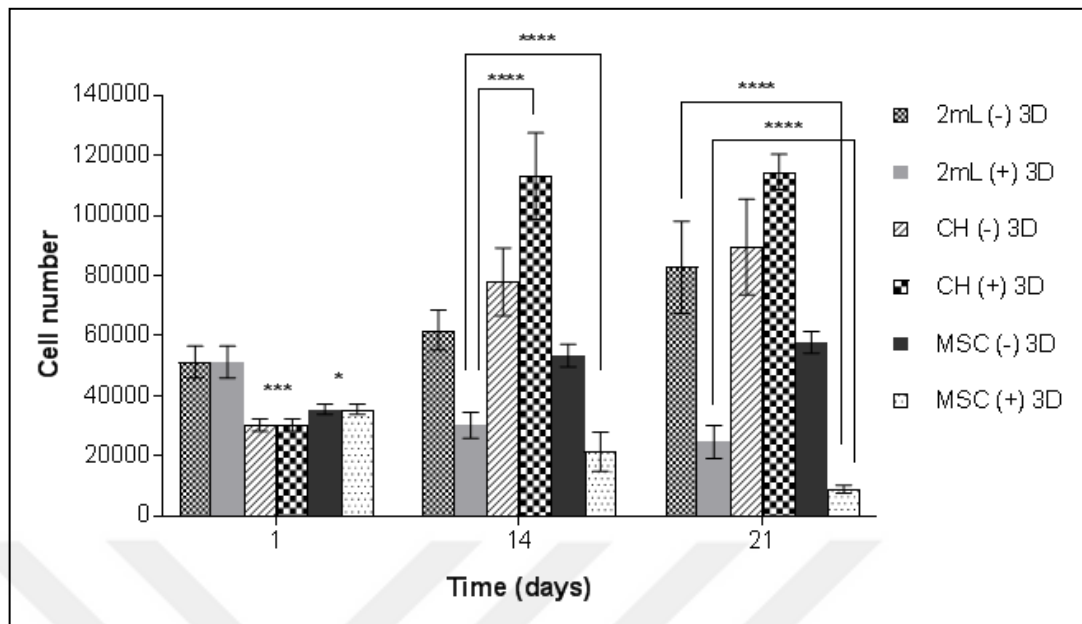


Figure 4.24. Cell viabilities on 6% PBSu:PLLA scaffolds at day 1, 14, and 21. (-): no chondrogenic induction, (+): chondrogenic induction; 3D: on scaffold; 2ML: transduced rBMSCs, CH: rat chondrocytes, MSC: non-transduced rBMSCs (* $p < 0.05$, *** $p < 0.0005$, **** $p < 0.0001$).

4.6. EXPRESSION OF CARTILAGE-SPECIFIC GENES

Real-time PCR was performed on day 1, 14, and 21 in order to check and compare the chondrogenic gene expression among the experimental groups. Figure 4.25 belongs to mRNA expressions of Sox9, Col2a1, Agc, Col1a1, and Col10a1 relative to 18SrRNA expression. As mentioned before, Col2a1 and Agc are the leading markers of chondrocyte differentiation. Sox9 is a transcription factor that is necessary for the differentiation of chondrocytes, as well as the prevention of hypertrophy formation by the chondrocytes during proliferation [155]. Therefore, collaborate expression of these 3 markers is a sign of chondrogenic differentiation.

When Sox9 (Figure 4.25 a) graph was examined it could be observed that when the 2ML, MSC, and CH group cells were seeded on scaffolds, the expression of Sox9 was much higher compared to those on cell culture plates throughout 21 days of incubation, suggesting that using PBSu:PLLA scaffolds increased the chondrogenic capacities of the cells. In addition, the highest expression profile of Sox9 was observed among 2ML group on scaffolds at day

1, even higher (2 fold) than the chondrocytes, indicating that these cells started chondrogenic differentiation earlier than the other cell types. Likewise, 2ML group cells on scaffold (2ML 3D) displayed a 2 fold higher Sox9 expression profile than the CH group throughout 21 days of incubation without chondrogenic stimulation. When the cells on scaffolds were examined in detail, it was observed that Sox9 expression was decreasing at least 4 fold from day 1 to 21, except chondrogenically induced chondrocytes (CH + 3D) in which Sox9 expression increased 2 fold from day 14 to 21. Among the cells seeded on TCP, Sox9 expression slightly increased in chondrogenically induced 2ML and CH groups from day 1 to 21, but a slightly decreasing trend was observed in chondrogenically induced MSC group. Similarly, Sox9 expression in non-induced MSC and CH groups on TCP decreased 2-3 fold from day 1 to 21, while in non-induced 2ML group on TCP there was a 6 fold increase from day 1 to 14, and then a sharp decrease (>10 fold) from day 14 to 21. Knowing that Sox9 is an early marker of chondrogenesis that is responsible for the transcriptional activation of cartilage specific proteins such as collagen type II and aggrecan [156], it can be concluded that transduction of rBMSCs with TGM2_v2 resulted in a boost in chondrogenic differentiation capacity of these cells.

The overall Col2a1 expression (Figure 4.23 b) was quite high in chondrocytes throughout 21 days (>10 fold), both on scaffolds and TCP, especially in chondrogenically induced ones on scaffolds (CH + 3D), whereas Col2a1 expression in other groups were relatively very low. Among them, the best expression profile was again obtained with 2ML+3D when compared to the positive control (CH+3D), although the expression of Col2a1 was not as high as Sox9 expression, which could indicate an early sign of chondrogenic differentiation since collagen type II and aggrecan synthesis begins after Sox9 expression [114]. There was a 2 fold decrease in expression from day 14 to 21 in 2ML+3D group, which was found insignificant indeed, and a similar but a 10 fold lower Col2a1 expression profile was observed for MSC 3D group when chondrogenic induction was applied. These results suggest that both transduced (2ML group) and non-transduced rBMSCs (MSC group) were possibly in their early stages of chondrogenic differentiation, and addition of chondrogenic differentiation, as well as TGM2_v2 transduction, accelerated the process.

In consistency with the results above, initial Agc expression in 2ML 3D group was the highest among the other groups (Figure 4.25 c), and the 3 fold difference between non-induced 2ML 3D and MSC 3D groups was found significant. In addition, Agc expression

displayed a decreasing trend among all groups from day 1 to 21 (>2 fold), except CH 3D group showing at least 2 fold increase in *Agc* expression. This is in consistency with *Sox9* results, since *Sox9* is known to enhance the transcription of *Agc* through its promoter/enhancer activity [158]. After day 14, *Agc* expression was still the highest in 2ML groups, which continued throughout 21 days of incubation. At day 21, the 3 fold difference between non-induced 2ML 3D and MSC 3D groups was found significant, just as the 7 fold difference between non-induced 2ML 3D and CH 3D groups.

Col1a1 was found to be expressed at similar levels among all the groups, but at least 2 fold higher than the cartilage specific ones (*Sox9*, *Col2a1*, *Agc*) (Figure 4.25 d). This is due to the fact that *Col1a1* is a commonly expressed protein among the connective tissue cells [159]. MSCs from bone marrow express high amount of collagen type I before they start to express collagen type II during chondrogenesis [160]. Different from the other groups, *Col1a1* expression was found to decrease from day 14 to 21 in both non-induced 2ML on TCP (2-3 fold) and in chondrogenically induced 2ML 3D group (~1.5 fold), which could mean that chondrogenic differentiation may have started in these groups. A similar decreasing trend from day 14 to 21 was observed for the non-induced CH on TCP (3 fold) and chondrogenically induced CH 3D groups (~1.5 fold), in accordance with the evidence stating that arresting of collagen type I synthesis followed by the onset of collagen type II expression is an indicator of chondrocyte maturation [21]. Still, the highest expression levels were observed within 2ML groups (all four), suggesting that these cells may differentiate into other cell types of connective tissue such as bone and fibrocartilage in which *Col1a1* expression is dominant to other collagen types [161] [32], and this requires further investigation.

Being a late hypertrophy marker, *Col10a1* was found to be expressed at relatively very low levels in all groups (Figure 4.25 e); however, the highest expression was detected in 2ML groups, especially in those on TCP and without any chondrogenic induction at day 14, decreasing almost 4 fold throughout 21 days. This trend was similar for MSC 3D with chondrogenic induction, in which a 3 fold increase was observed from day 1 to 14, and a 4-5 fold decrease was recorded for day 21. Only in 2ML 3D group with chondrogenic induction displayed an approximately 1.5 fold increasing level of *Col10a1* expression throughout 21 days of incubation. These results could support the fact that TG2 is expressed in chondrocytes that mature into hypertrophy [162]. However, in some cases, collagen type X

expression could occur before the expression of type II collagen during chondrogenic differentiation [163]. Yet, these results could be neglected for our study when cartilage tissue engineering is concerned, since the relative expression was quite low in comparison to the expressions of cartilage specific genes.



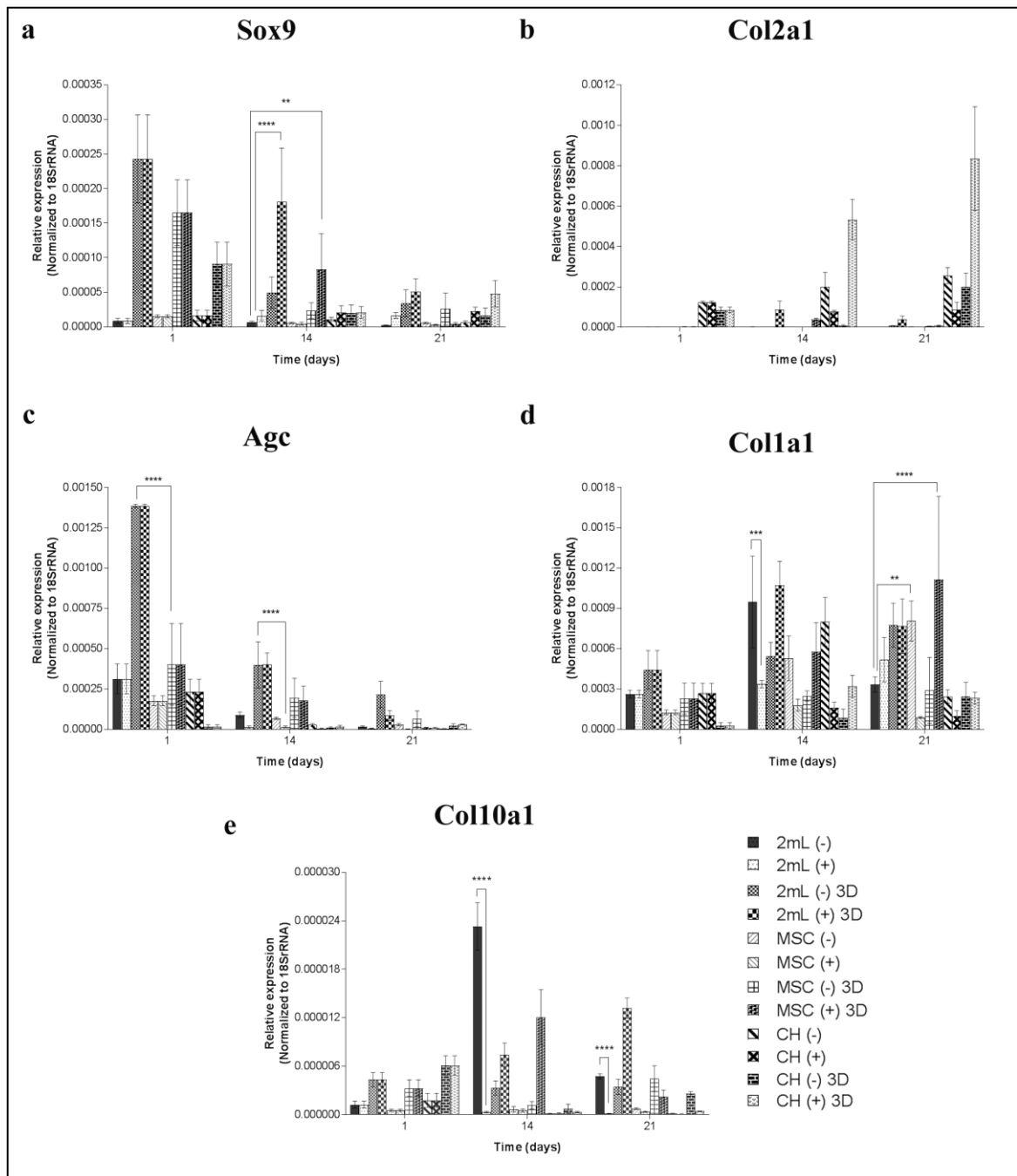


Figure 4.25. Relative expressions of a) Sox9, b) Col2a1, c) Agc, d) Col1a1, e) Col10a1 with respect to 18S rRNA housekeeping gene. 2ML: transduced rBMSCs, MSC: non-transduced rBMSCs, CH: rat chondrocytes, (-): no chondrogenic induction, (+): chondrogenic induction on the 4th day of incubation, 3D: 6% PBSu:PLLA scaffold groups, others on TCP. Sox9, Col2a1, and Agc are chondrocytic markers, while Col1a1 is an indicator of fibroblastic or osteocytic phenotype, and Col10a1 is the marker of hypertrophy (** $p < 0.005$, *** $p < 0.0005$, **** $p < 0.0001$).

4.7. IMMUNOCHEMISTRY OF THE CELL-SEEDED SCAFFOLDS

4.7.1. TG2 Deposition Into the Scaffolds

Expression and deposition of TG2 by the cells on the scaffolds throughout 3 weeks was detected by immunostaining with anti-TG2 antibody. It was observed that the expression of TG2 by transduced rBMSCs (2ML group) gradually increased from day 1 to 21 (Figure 4.26 a-c) and surprisingly, TG2 expression was present in rat chondrocytes as well (Figure 4.26 d-f). This could be correlated with the finding that TG2 is present in cartilage tissue [94]. No TG2 expression was detected in non-transduced rBMSCs (Figure 4.26 g-i), suggesting that rBMSCs normally do not have TG2 expression, and the expression in transduced cells belong to TG2-S.

Similarly, TG2 expression was not detected in non-transduced rBMSCs when chondrogenic stimulation was applied (Figure 4.27 e, f) neither on day 14 nor on day 21. Both the expression and deposition of TG2 was found to increase when chondrogenic induction was applied to transduced rBMSCs (Figure 4.27 a, b), as well as chondrocytes (Figure 4.27 c, d), suggesting that the expression of TG2-S by the transduced rBMSCs was enhanced with chondrogenic induction, as endogenous TG2 expression is known to be induced by TGF- β signaling [128] [129], as explained in section 1.3.1.

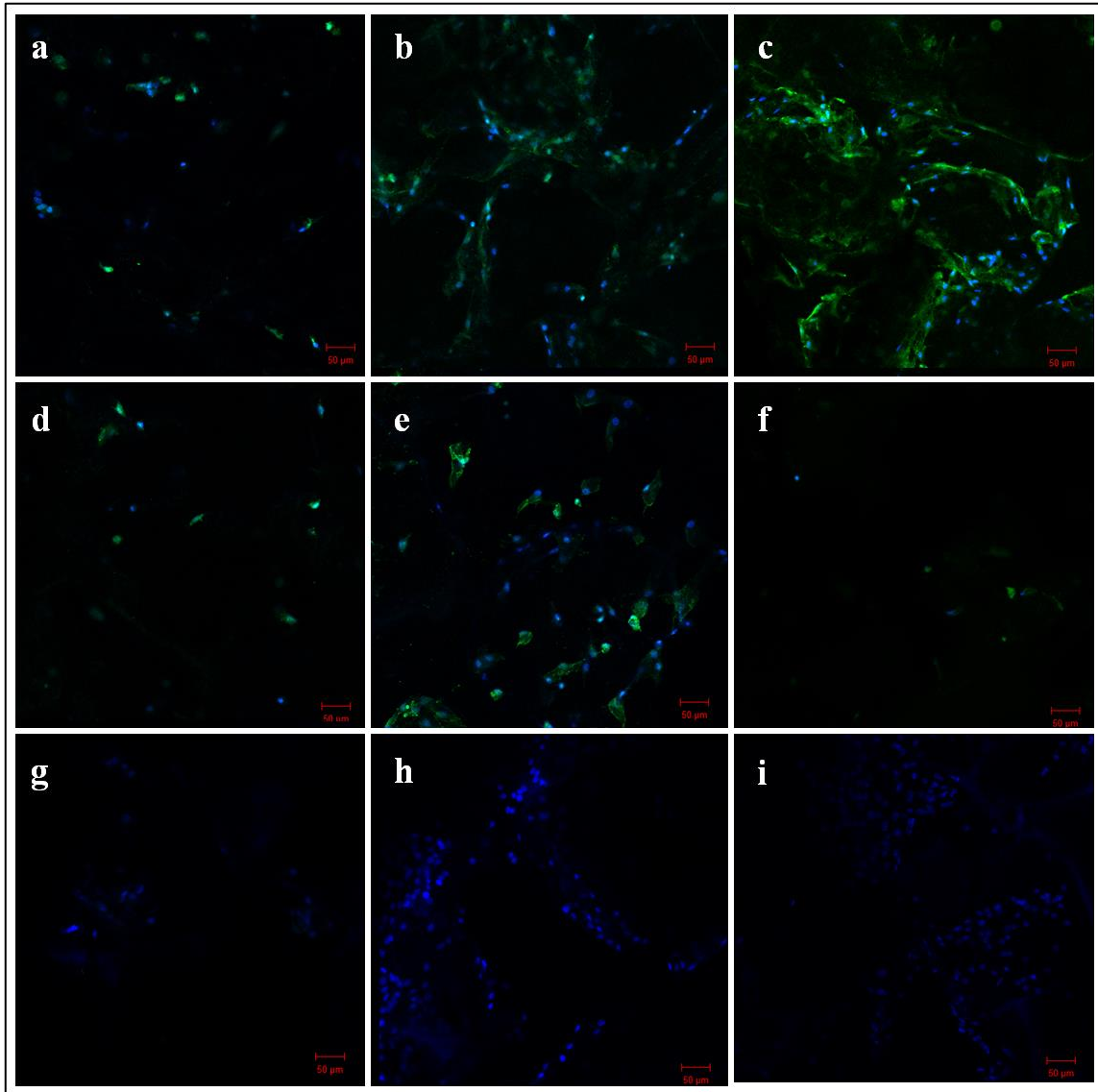


Figure 4.26. Confocal microscope images of transduced rBMSCs (2ML group) (a-c), chondrocytes (d-f), and non-transduced rBMSCs (g-i) on 6% PBSu:PLLA scaffolds on day 1 (a, d, g), day 14 (b, e, h), and day 21 (c, f, i) showing TG2 deposition (objective: 10X, scale bar: 50 μ m). Green: TG2; blue: DAPI. No chondrogenic induction was applied.

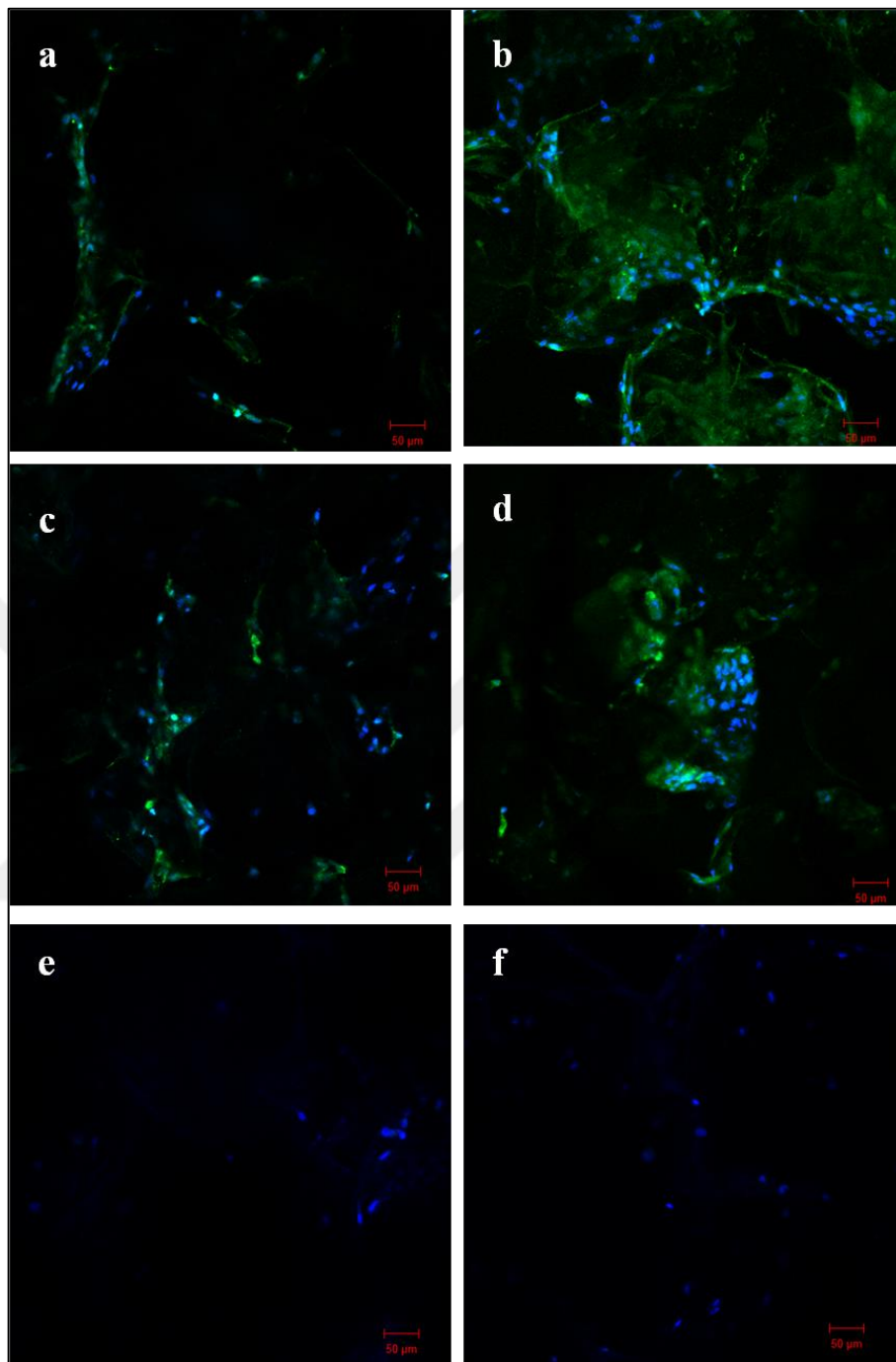


Figure 4.27. Confocal microscope images of transduced rBMSCs (2ML group) (a,b), chondrocytes (c, d), and non-transduced rBMSCs (e, f) on 6% PBSu:PLLA scaffolds on day 14 (a, c, e), and day 21 (b, d, f) showing TG2 deposition (objective: 10X, scale bar: 50 μm). Green: TG2; blue: DAPI. Chondrogenic induction was applied on the 4th day of incubation.

4.7.2. Immunocytochemistry of ECM and Nuclei

4.7.2.1. Collagen Type II Staining for Chondrogenic Matrix Protein Expression

Collagen type II production is a marker of chondrogenesis, which should be addressed while carrying out chondrogenic differentiation of stem cells. After 14 days of incubation in growth media, the ECM of the transduced (2X and 2ML groups) and non-transduced rBMSCs were labeled with collagen type II antibody so as to observe whether spontaneous chondrogenic differentiation could be obtained without any induction (Figure 4.28). It was observed that there was collagen type II deposition in the ECM of both 2X and 2ML groups (Figure 4.28 a and b), meanwhile there was no sign of differentiation in non-transduced cells (Figure 4.28 c). It means that the expression of TG2-S had a positive effect on these cells in terms of chondrogenic differentiation.

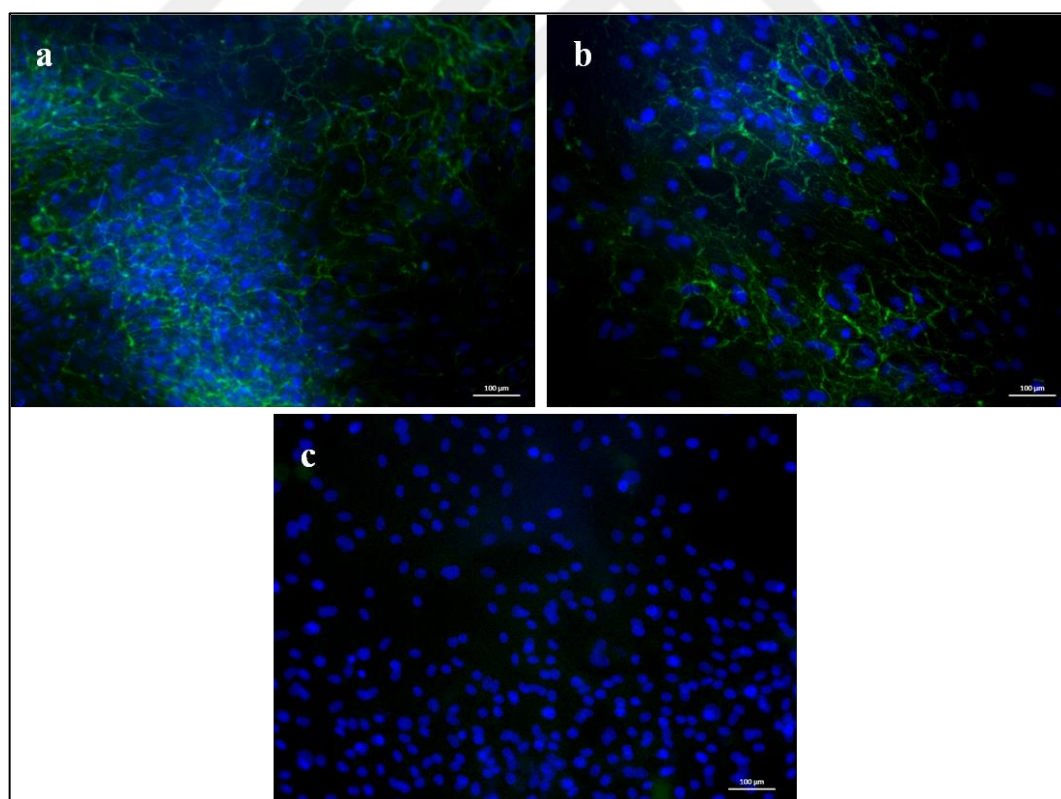


Figure 4.28. Immunofluorescence images of transduced (a: 2X, b: 2ML) and non-transduced (c) rBMSCs on day 14 (objective: 20X, scale bar: 100 μm). Green: collagen type II; blue: DAPI. No chondrogenic induction was applied.

In order to check the presence of chondrogenic ECM after chondrogenic induction, immunostaining of collagen type II was performed on day 21 (Figure 4.29). It was observed that the transduced rBMSCs (2ML group) could express collagen type II with (Figure 4.29 d) and without chondrogenic induction (Figure 4.29 b) after 21 days of incubation. Likewise, non-transduced rBMSCs could produce collagen type II on day 21 without chondrogenic induction (Figure 4.29 a), and the expression of collagen type II increased with chondrogenic stimulation (Figure 4.29 c). In addition, transduced rBMSCs tended to form clusters without chondrogenic induction (Figure 4.29 b), which could be the result of too much cell number at the end of 21 days in culture, since no such structures were observed in differentiated cells (Figure 4.29 d).

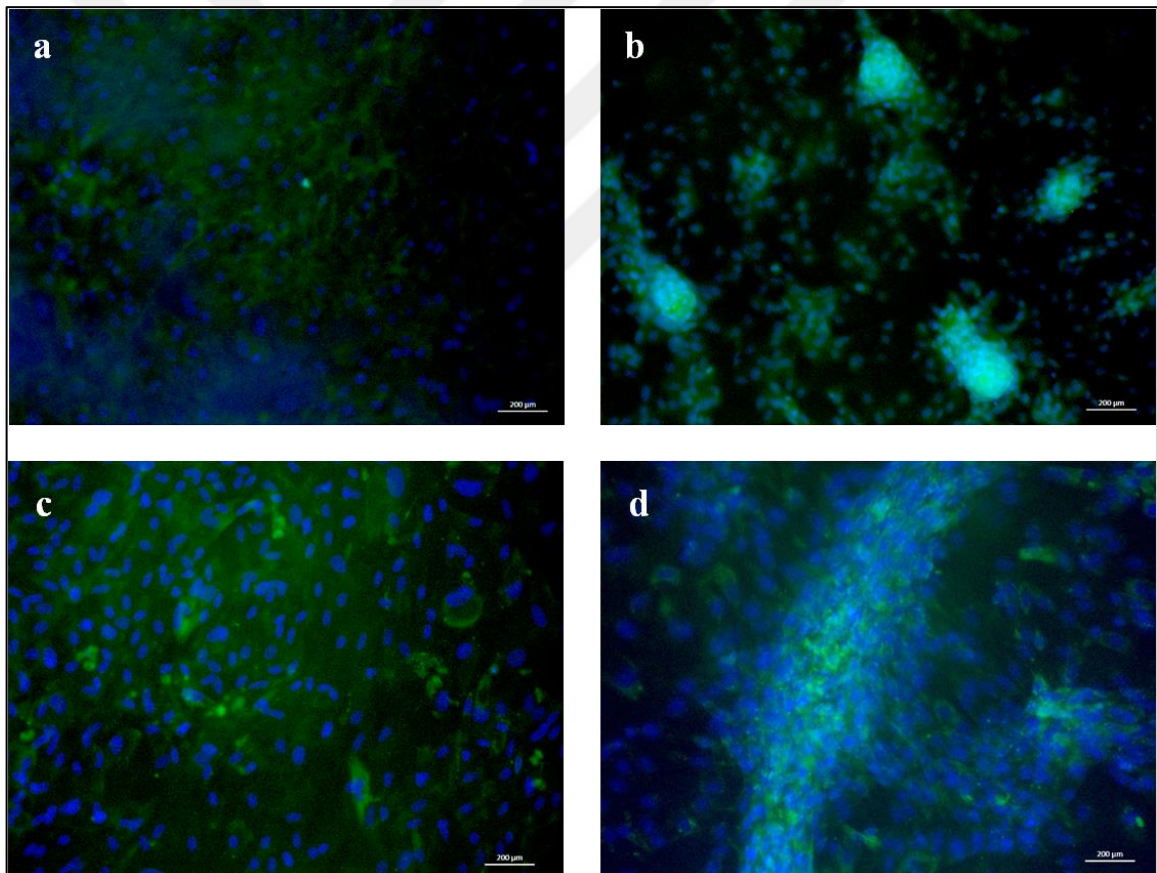


Figure 4.29. Immunofluorescence images of non-transduced and transduced (2ML group) rBMSCs on day 21 (objective: 10X, scale bar: 200 µm). Green: collagen type II; blue: DAPI. (a) rBMSC; no induction, (b) 2ML; no induction, (c) rBMSC; chondrogenic induction, (d) 2ML; chondrogenic induction

4.7.2.2. Collagen Type I Staining for Osteogenic/Fibrogenic Matrix Expression

To distinguish between osteogenic and chondrogenic differentiation, the samples were immunolabeled with collagen type I which is one of the major proteins specific to bone and fibrocartilage cells [159]. It was observed that (Figure 4.30) without chondrogenic differentiation, the transduced rBMSCs (2ML group) expressed collagen type I on day 21 (Figure 4.30 a), but no collagen type I expression was observed in non-transduced cells (Figure 4.30 b). It means that these cells had potential of osteogenic differentiation after 21 days in culture; however, it could be prevented with the chondrogenic induction medium (Figure 4.30 c). On the other hand, the addition of chondrogenic medium resulted in collagen type I expression by the non-transduced cells (Figure 4.30 d), which could be due to the tendency of MSCs towards osteogenic lineage [143]. These results were in contrast with real-time PCR results showing that in chondrogenically induced transduced cells (2ML group) and MSC group collagen type I expression has increased on day 21; however, the differences were not significant. Therefore, it would not be accurate to compare the mRNA expressions to the protein expressions.

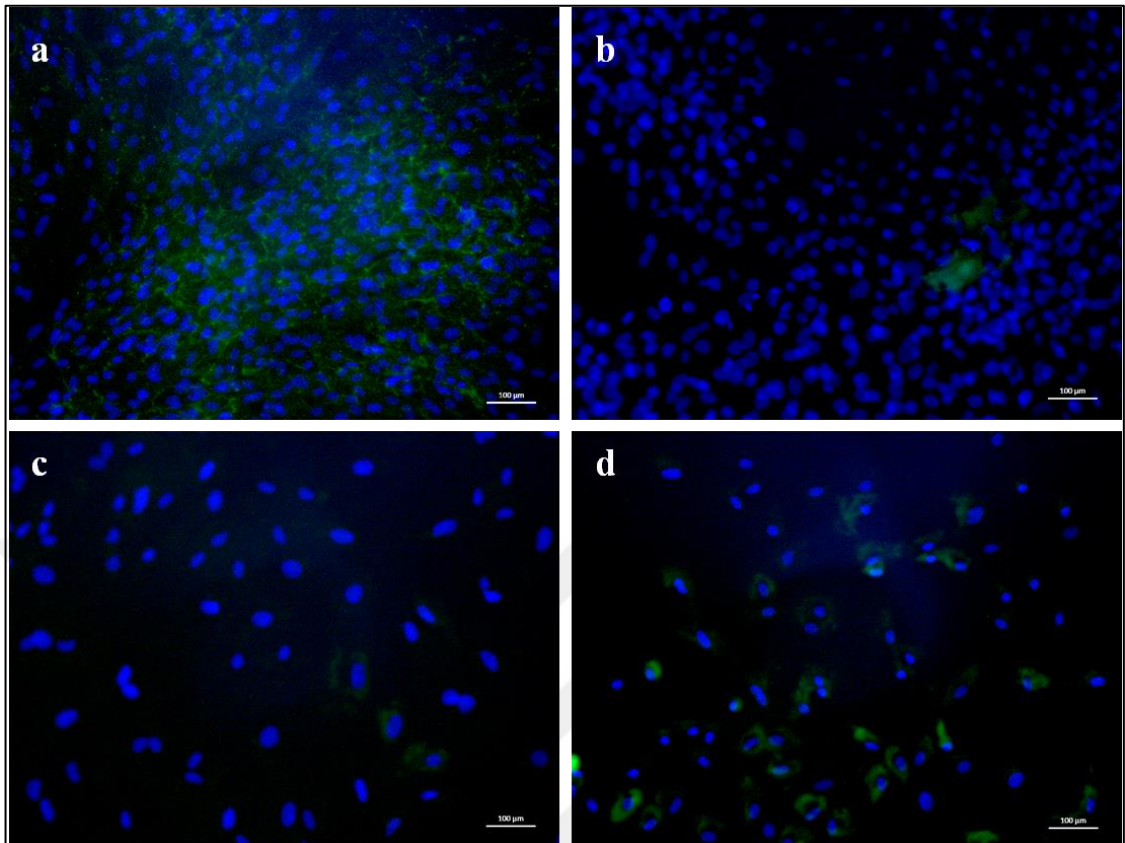


Figure 4.30. Immunofluorescence images of transduced (2ML) and non-transduced rBMSCs on day 21 (objective: 20X, scale bar: 100 μm). Green: collagen type I; blue: DAPI. (a) 2ML; no induction, (b) rBMSC; no induction, (c) 2ML; chondrogenic induction, (d) rBMSC; chondrogenic induction

4.7.2.3. *Collagen Type II and Aggrecan Staining of the Cell-Seeded Scaffolds for Chondrogenic Differentiation Analysis*

In order to observe chondrogenic ECM production on PBSu:PLLA (6 per cent) scaffolds, the cell-seeded scaffolds were stained with anti-collagen type II and anti-aggrecan antibodies. Similar to collagen type II, aggrecan is another marker of chondrogenesis, indicating that it should be produced by the cells as soon as chondrogenic differentiation begins [157]. Figures 4.31 - 4.33 show collagen type II and aggrecan staining of the cell seeded scaffolds on day 1, day 14, and day 21. Images of the stained scaffolds were taken with confocal microscope (LSM 700, Carl Zeiss, Germany) at 20X objective.

The expression of collagen type II and aggrecan proteins were slightly visible in all cell types on the scaffolds on day 1 (Figure 4.31 a, b, c), but after 14 days of incubation, collagen type II could clearly be detected, especially in 2ML group without chondrogenic induction (Figure 4.32 a). In addition, these cells had rounded shapes in contrast to the non-transduced ones (Figure 4.32 c), as in the native cartilage tissue. Likewise, this expression continued throughout 21 days of incubation (Figure 4.33 a), being much better than the groups with chondrogenic induction (Figure 4.33 b). As expected, collagen type II and aggrecan production was clearly observed in the positive control cells (chondrocytes with induction) (Figure 4.30 f; Figure 4.33 f), being much stronger than the other cells. In contrast, small amount of signal was detected in non-transduced cells, with and without induction (Figure 4.30 c, d; Figure 4.33 c, d). Together with real-time PCR results showing the increase in expression of cartilage specific genes in transduced rBMSCs, this supports our theory that TGM2_v2 transduction supplied the rBMSCs with an ability of spontaneous chondrogenic differentiation without the addition of differentiation factors.

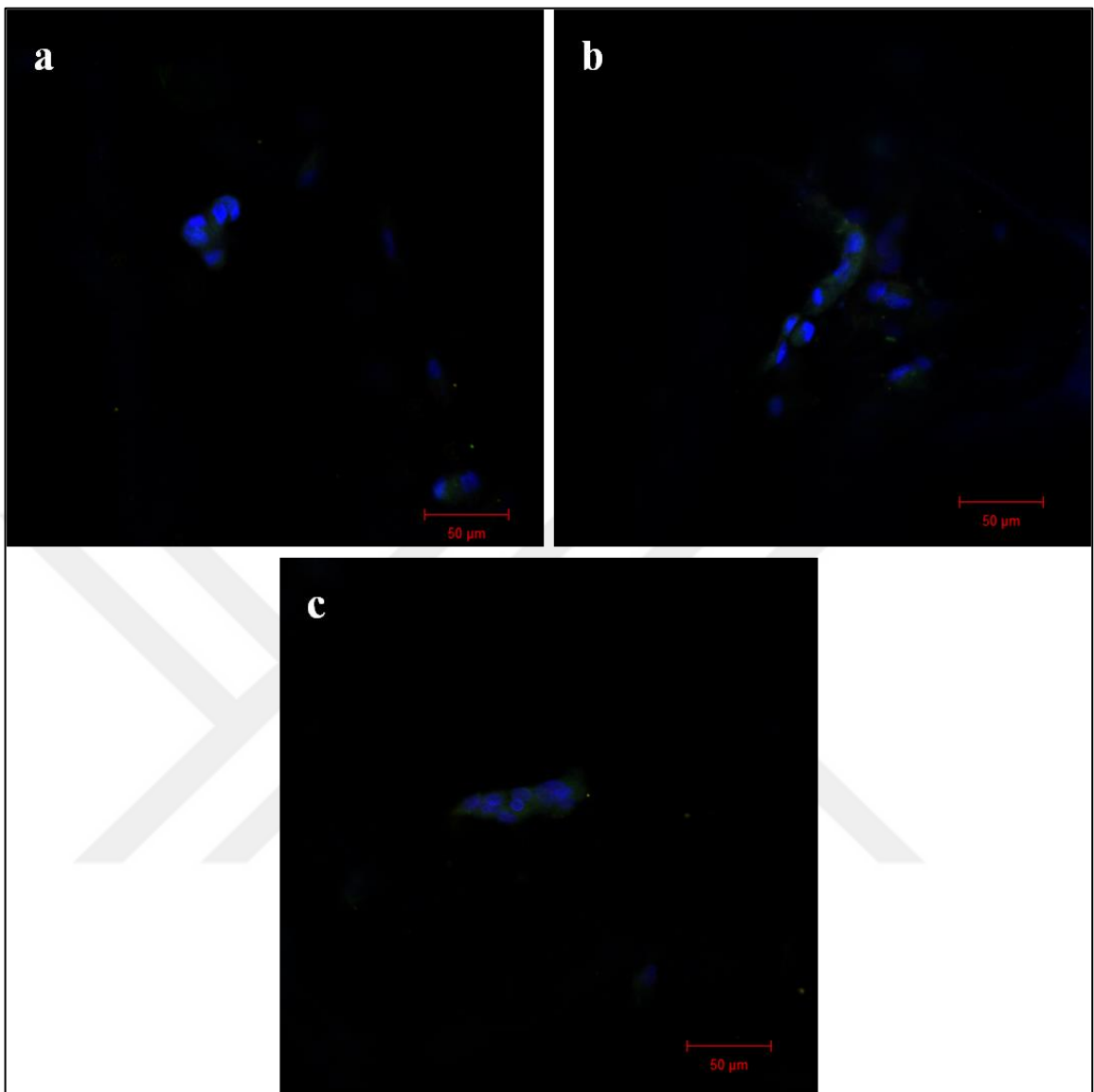


Figure 4.31. Confocal microscopy of the cell-seeded scaffolds at day 1; (a) transduced rBMSCs (2ML group), (b) non-transduced rBMSCs, (c) rat chondrocytes (positive control). Blue: nuclei, green: collagen type II, red: aggrecan. Objective: 20X, scale bar: 50 μm.

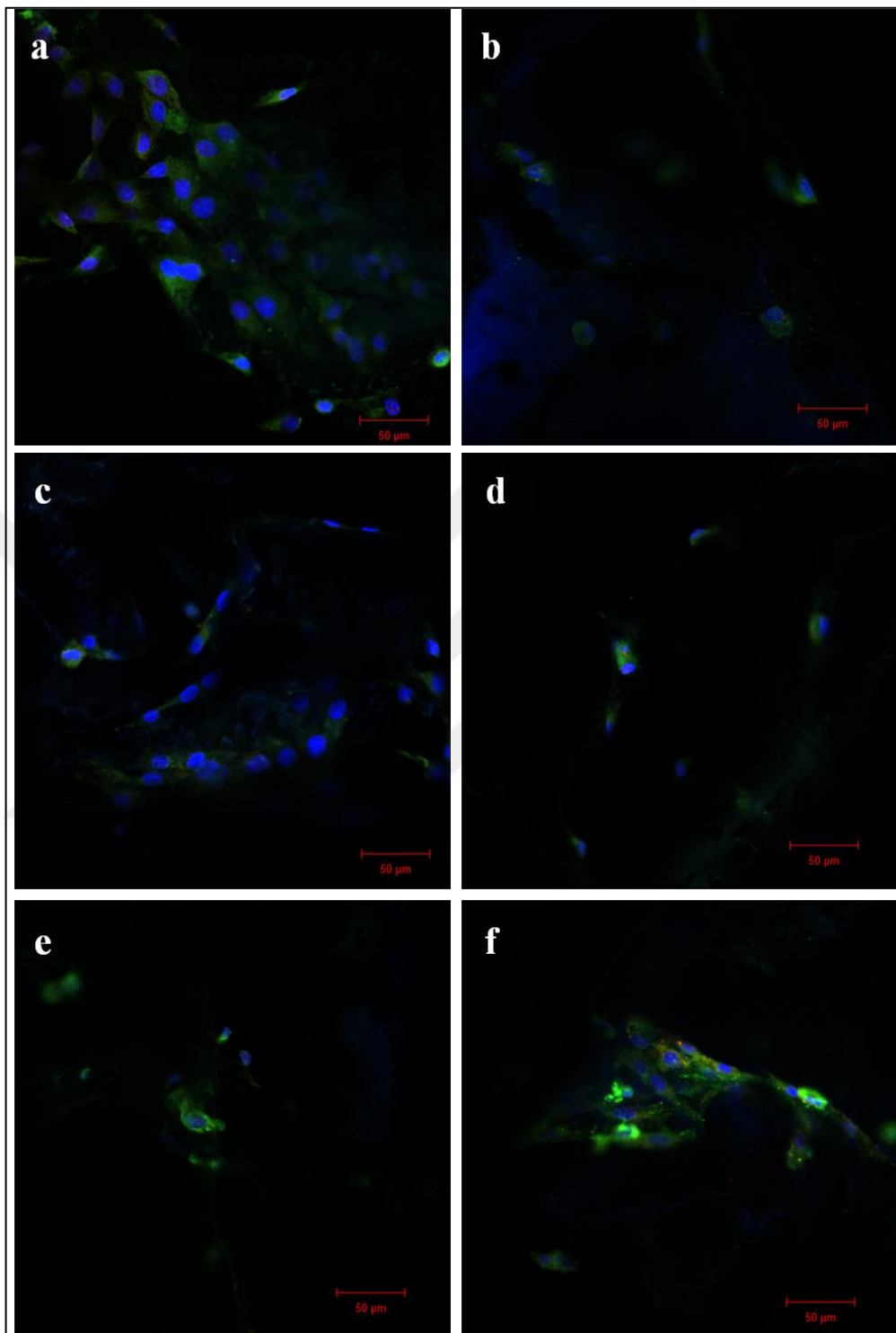


Figure 4.32. Confocal microscopy of the cell-seeded scaffolds at day 14; (a,b) transduced rBMSCs (2ML group), (c, d) non-transduced rBMSCs, (e, f) rat chondrocytes as positive control; (a, c, e) cells without chondrogenic induction, (b, d, f) cells with chondrogenic induction. Blue: nuclei, green: collagen type II, red: aggrecan. Objective: 20X, scale bar: 50 μ m.

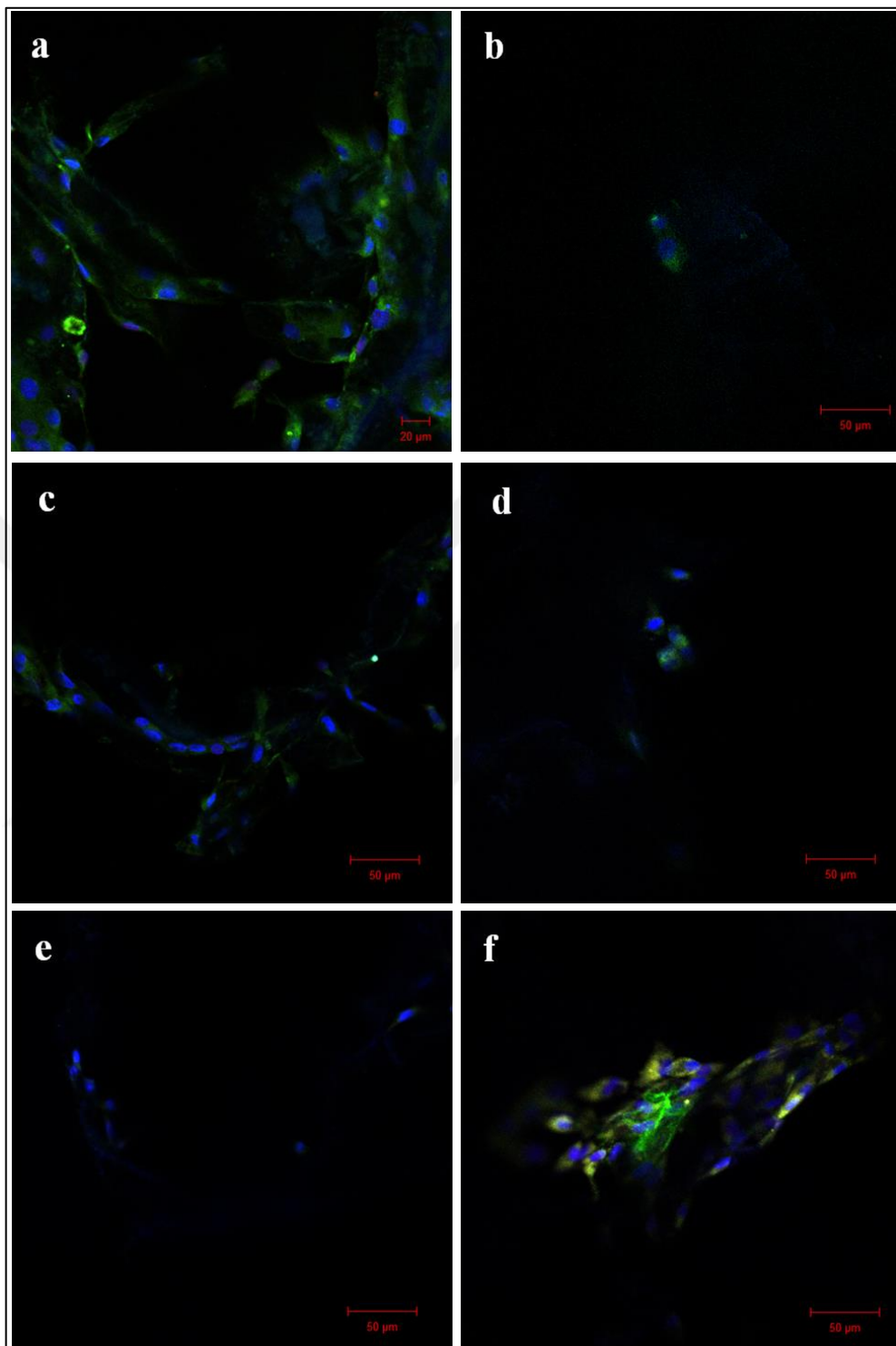


Figure 4.33. Confocal microscopy of the cell-seeded scaffolds at day 21; (a,b) transduced rBMSCs (2ML group), (c, d) non-transduced rBMSCs, (e, f) rat chondrocytes as positive control; (a, c, e) cells without chondrogenic induction, (b, d, f) cells with chondrogenic induction. Blue: nuclei, green: collagen type II, red: aggrecan. Objective: 20X, scale bar: 20 μm (a) and 50 μm (others).

4.7.2.4. Collagen Type I and Collagen Type X Staining of the Cell-Seeded Scaffolds for Osteogenic/Fibrogenic and Hypertrophic Differentiation Analysis

The cell-seeded scaffolds were labeled with anti-collagen type I and anti-collagen type X antibodies to understand whether there were any differentiation towards fibrocartilage or osteogenic lineage, and hypertrophic cartilage, respectively. The confocal microscopy images of the scaffolds were shown in Figure 4.34 - 4.36. Neither type I nor type X collagen was produced on day 1 (Figure 4.34 a, b, c) in any sample. Consistent with the results of real-time PCR, collagen type I expression could be detected in all types of cells on the scaffolds after day 14 (Figure 4.35 a, c, d, e), except chondrogenically induced transduced rBMSCs (2ML group) and chondrocytes (Figure 4.35 b and f) but not as high as the mRNA level. The strongest collagen type I signal was obtained in non-transduced and non-induced rBMSCs (Figure 4.35 c). Collagen type I production was found quite decreased, even negligible, after 21 days of incubation in all cell types, except chondrogenically induced non-transduced rBMSCs (Figure 4.36 d). The increase of collagen type I expression from day 14 to 21 in non-transduced but chondrogenically induced rBMSCs verifies our findings in immunostaining (Section 4.7.2.2). These results were in contrast with real-time PCR results which showed that 2ML groups had more collagen type I mRNA expression than the non-transduced rBMSCs, which could be related with the evidence defining that mRNA expression level of a gene does not always correlate with its protein expression level due to the alternative splicing and post-translational modifications [163]. Expression of collagen type X was not visible in any of the groups, indicating that hypertrophy was not present (Figure 4.34 - 4.36), in accordance with the results of real-time PCR. Knowing that short form of TG2 has reduced ECM crosslinking capacity, it can be concluded that TG2-S expression increased the ability of chondrogenic differentiation, but prevented further hypertrophic and osteogenic differentiation of rBMSCs. Therefore, rBMSCs transduced with the viral particles encoding TGM2_v2 could be accepted as suitable cells for cartilage tissue engineering with 3D PBSu:PLLA scaffolds.

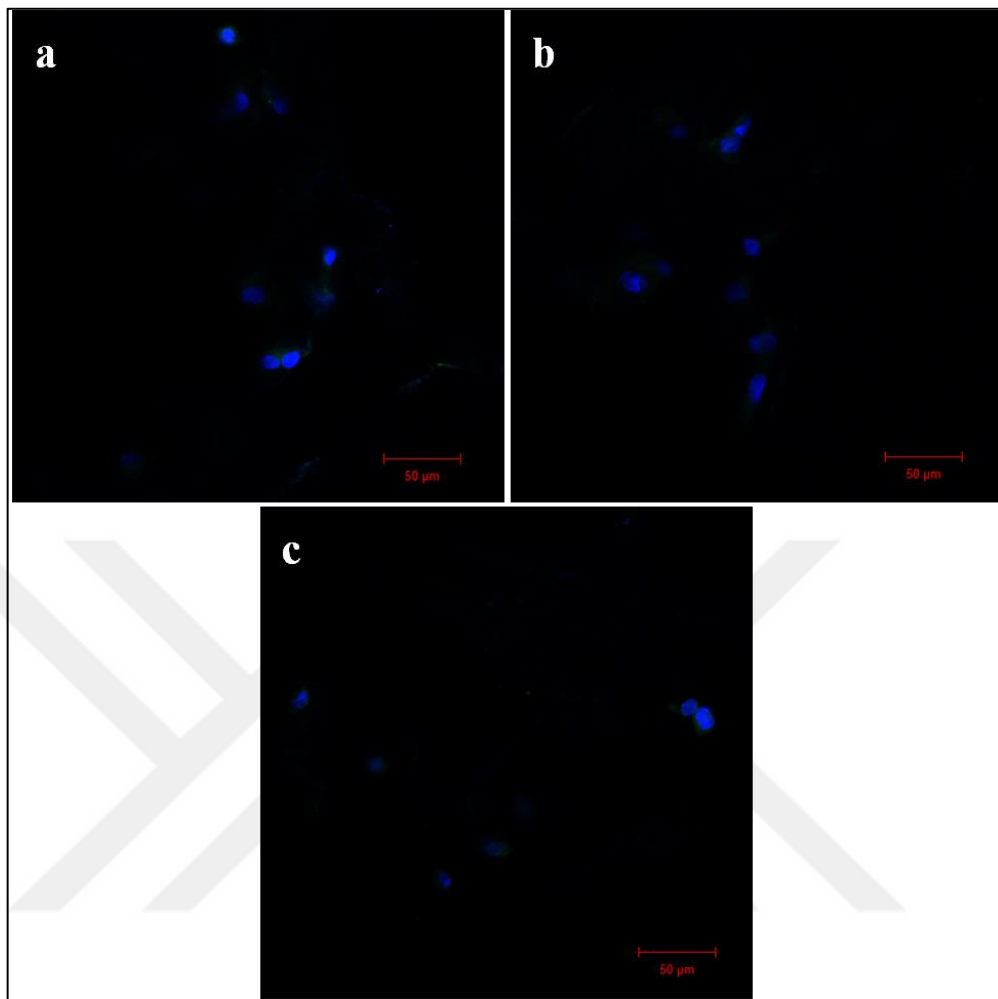


Figure 4.34. Confocal microscopy of the cell-seeded scaffolds at day 1; (a) transduced rBMSCs (2ML group), (b) non-transduced rBMSCs, (c) rat chondrocytes. Blue: nuclei, green: collagen type I, orange: collagen type X. Objective: 20X, scale bar: 50 μm.

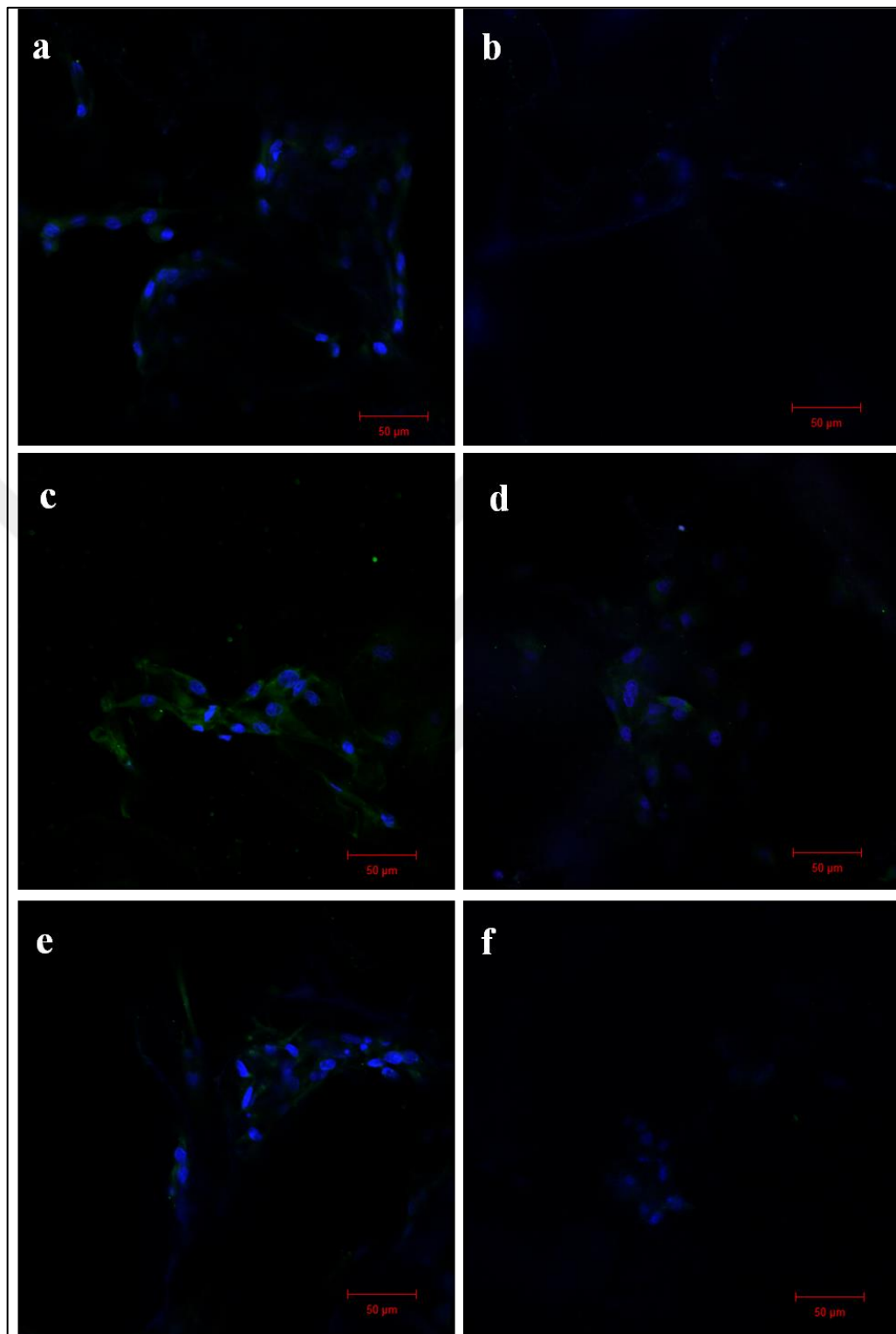


Figure 4.35. Confocal microscopy of the cell-seeded scaffolds at day 14; (a, b) transduced rBMSCs (2ML group), (c, d) non-transduced rBMSCs, (e, f) rat chondrocytes; (a, c, e) cells without chondrogenic induction, (b, d, f) cells with chondrogenic induction. Blue: nuclei, green: collagen type I, orange: collagen type X. Objective: 20X, scale bar: 50 μm .

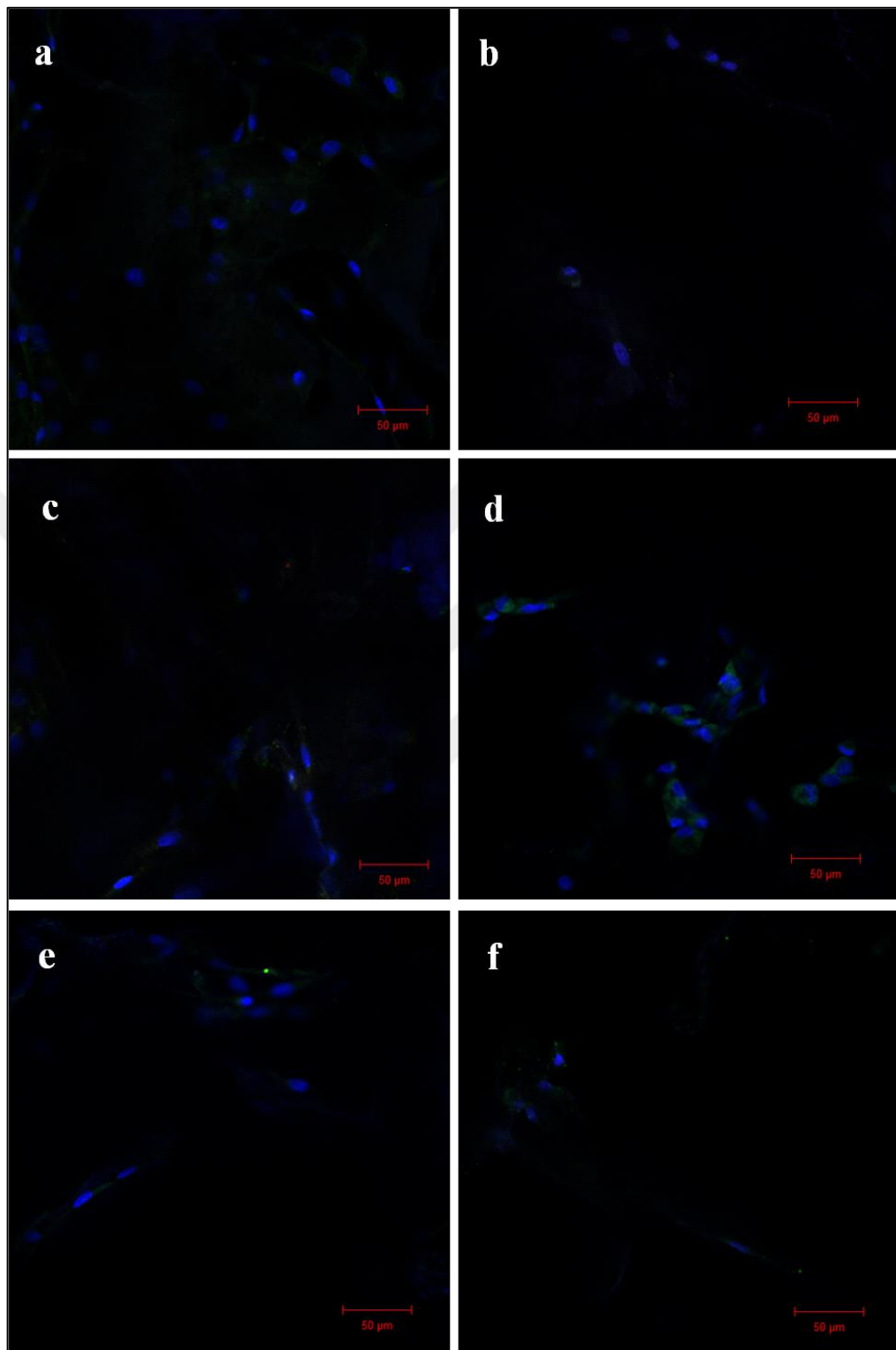


Figure 4.36. Confocal microscopy of the cell-seeded scaffolds at day 21; (a, b) transduced rBMSCs (2ML group), (c, d) non-transduced rBMSCs, (e, f) rat chondrocytes; (a, c, e) cells without chondrogenic induction, (b, d, f) cells with chondrogenic induction. Blue: nuclei, green: collagen type I, orange: collagen type X. Objective: 20X, scale bar: 50 μm .

To determine whether the fluorescent staining was observed due to the background that was created by the secondary antibodies or due to auto-fluorescence, the cells were stained with only secondary antibodies. Figure F.1 belongs to the negative control for TG2 deposition experiments, and Figure F.2 belongs to the negative control of immunostaining experiments of the cell-seeded scaffolds. As can be observed in Figure F.1 that the scaffolds had no auto-fluorescence. Likewise, secondary antibodies did not cause any background fluorescence in the scaffolds (Figure F.2).

4.8. ALCIAN BLUE STAINING FOR CHONDROGENIC DIFFERENTIATION

4.8.1. Deposition of sGAG by the Cells on TCP

In ECM of cartilage tissue, sulphated glycosaminoglycan (sGAG) molecules are found as covalently linked to aggrecan proteoglycans [164]. Therefore, the synthesis and deposition of sGAG in the ECM of cells is another sign of the chondrogenic differentiation. Alcian blue staining is a technique used to determine the sGAG content of a sample. Blue color indicates the presence of acid mucins, proteoglycans, and hyaluronic acids, while red color indicates the presence of neutral mucins, glycogens, and glycoproteins. Nuclei are stained in pale blue. In brief, the blue staining represents the deposition of sGAG in ECM. As a positive control, rat knee chondrocytes were used (Figures 4.37 e – 4.40 e).

Positivity in Alcian Blue staining implies that all of the transduced cells were capable of depositing sGAG in their ECM (Figures 4.37 a-d – 4.40 a-d). At day 4, the highest sGAG deposition was observed within 2X group both with and without chondrogenic induction (Figure 4.37 b and Figure 4.38 b). Production of sGAG was quite low in other transduced cells (Figure 4.37 a, c, d) in comparison to the non-transduced cells (Figure 4.37 f) without chondrogenic induction. After the addition of chondrogenic differentiation media, sGAG deposition was observed especially in 2X and 2ML groups (Figure 4.38 b and d), as well as non-transduced rBMSCs (Figure 4.38 f). More glycoprotein structures rather than sGAG were observed in 1X and 1ML groups (Figure 4.38 a and c) as pink color.

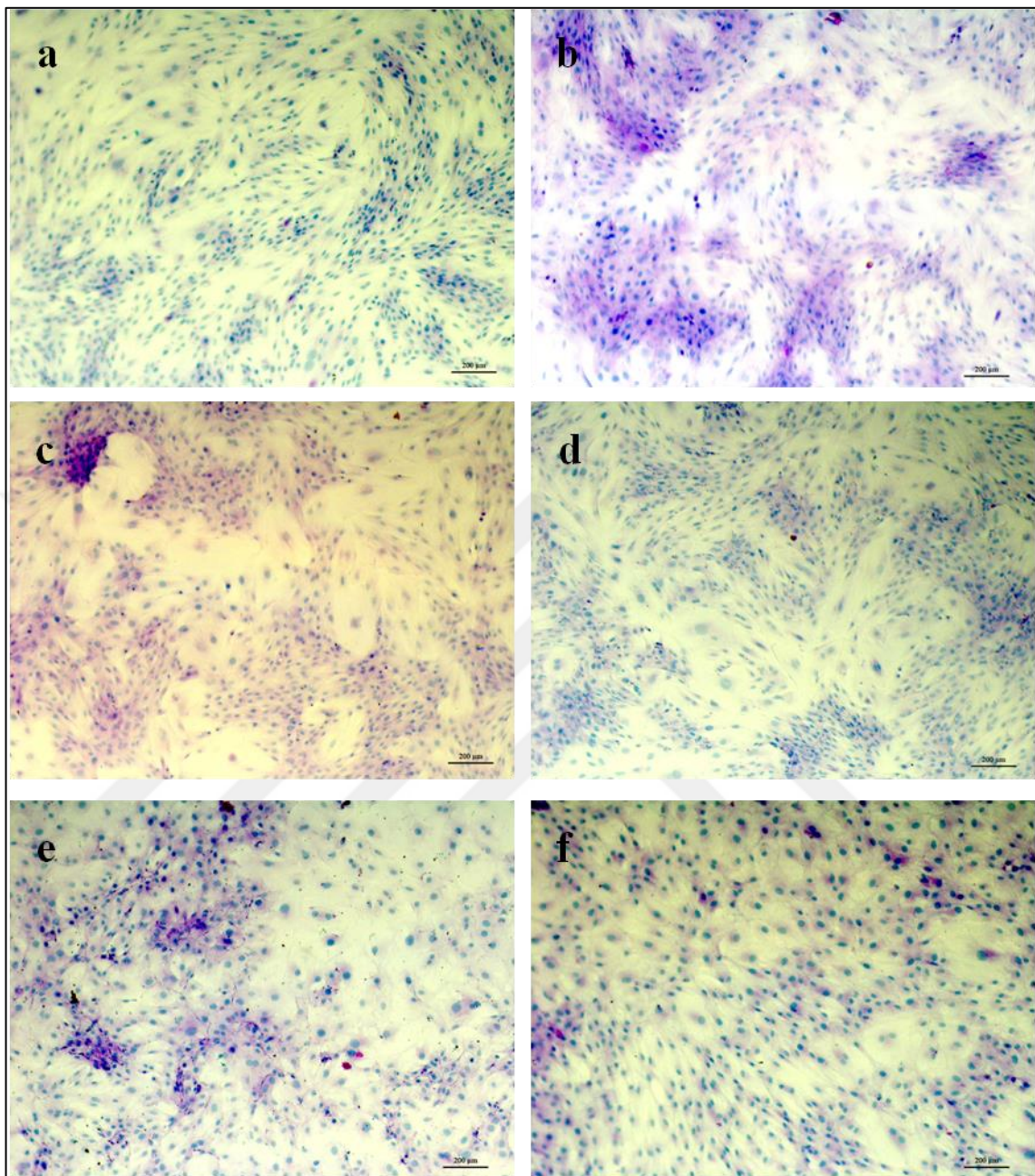


Figure 4.37. Alcian Blue staining results of transduced rBMSCs (a-d), chondrocytes (e), and non-transduced rBMSCs (f), after 4 days of incubation in normal growth medium; (a) 1X group, (b) 2X group, (c) 1ML group, (d) 2ML group. Scale bar: 200 μm .

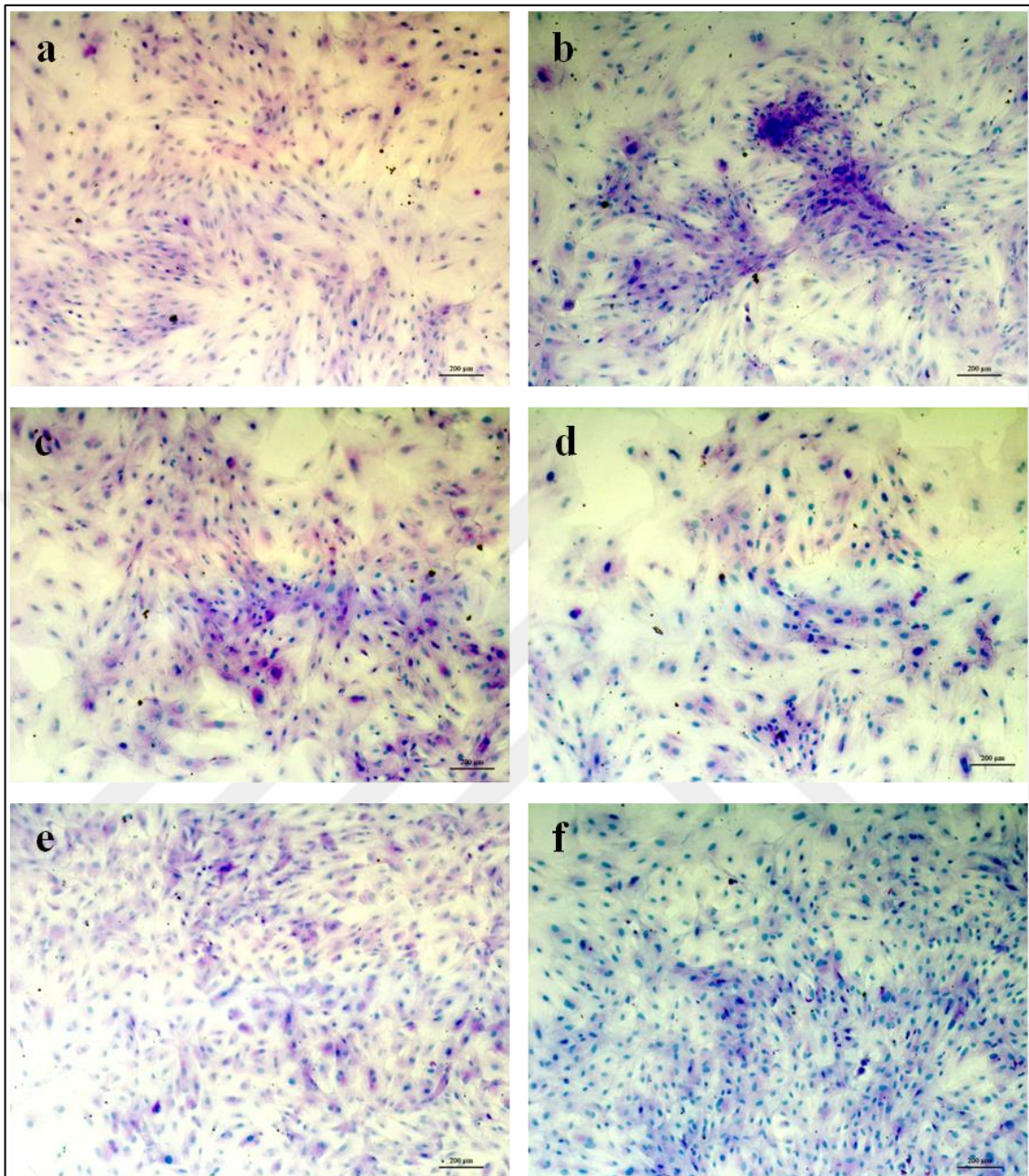


Figure 4.38. Alcian Blue staining results of transduced rBMSCs (a-d), chondrocytes (e), and non-transduced rBMSCs (f), and after day 4 of chondrogenic induction; (a) 1X group, (b) 2X group, (c) 1ML group, (d) 2ML group. Scale bar: 200 μm.

After 10 days, all types of transduced cells (Figure 4.39 a-d), except non-transduced cells (Figure 4.39 f) produced sGAG without chondrogenic induction. Transduced rBMSCs (2ML group) deposited the highest amount of sGAG in normal growth medium (Figure 4.39 d). Furthermore, it can be observed that these 2ML group cells tended to form clusters, as observed in collagen type II immunostaining, and could deposit chondrogenic ECM at these spots without any induction when compared to the non-transduced ones (Figure 4.39 f). Similarly, sGAG deposition was detected in transduced cells (both 2X and 2ML groups) on day 10 after chondrogenic induction (Figure 4.40 a-d), meanwhile it was lower than sGAG deposition in 2X and 2ML groups without chondrogenic induction. Less cells were observed in both of the positive (chondrocytes) and negative control (non-transduced) cells (Figure 4.40 e and f) which could suggest that the cells had no more space to grow on TCP after 10 days of incubation, but the problem is prevented using scaffolds.

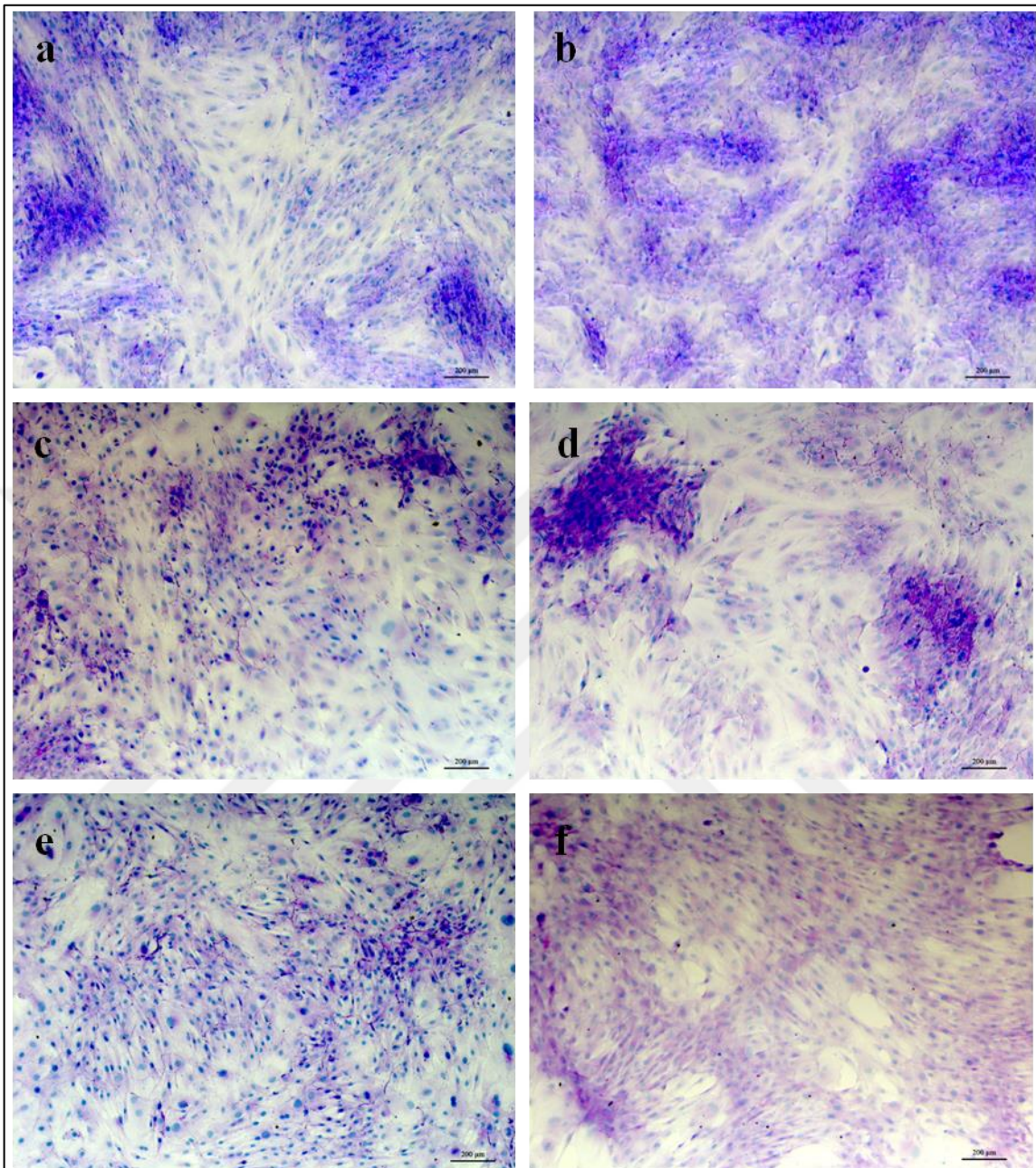


Figure 4.39. Alcian Blue staining results of transduced rBMSCs (a-d), chondrocytes (e), non-transduced rBMSCs (f), after 10 days of incubation in normal growth medium; (a) 1X group, (b) 2X group, (c) 1ML group, (d) 2ML group. Scale bar: 200 μ m.

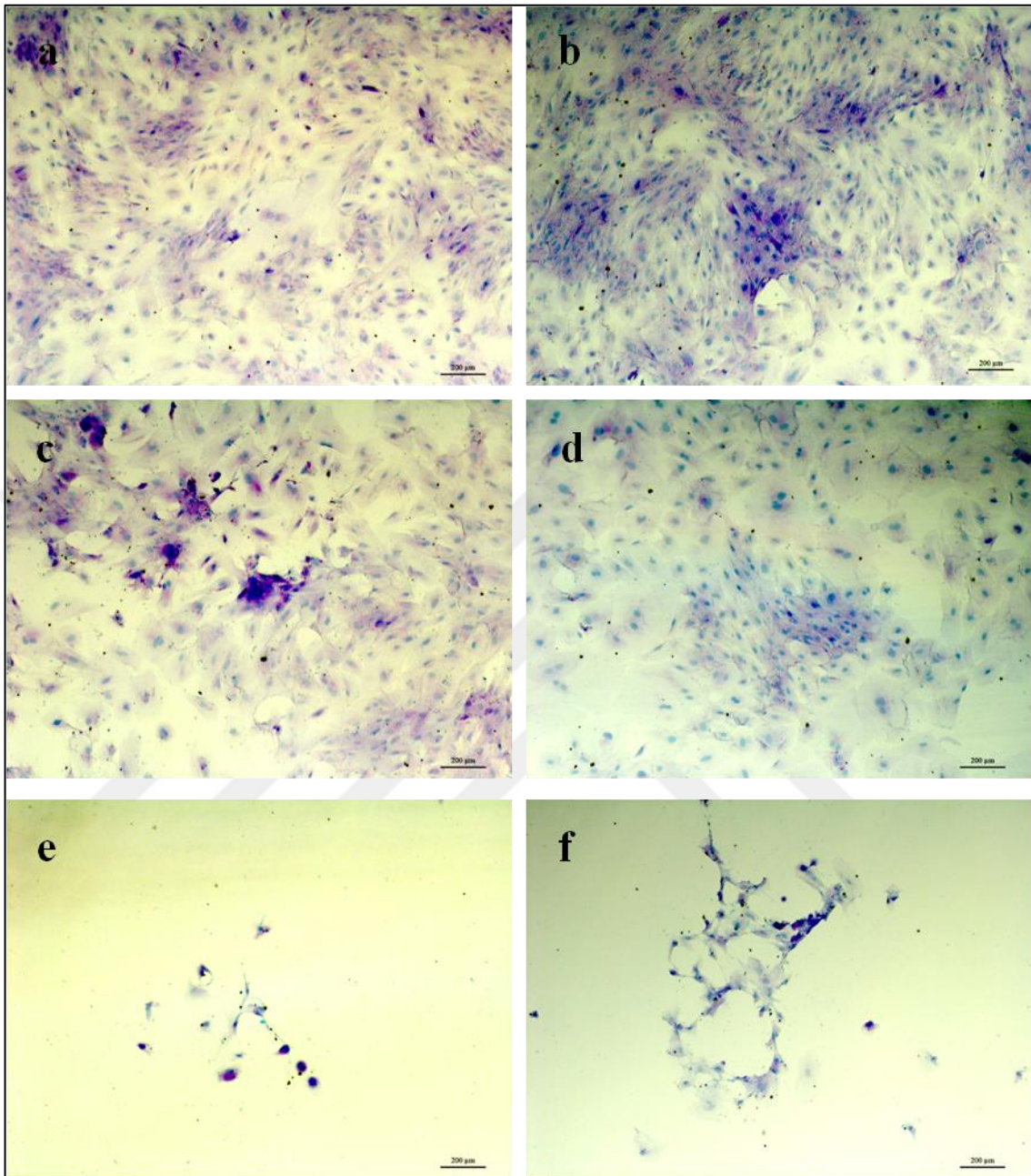
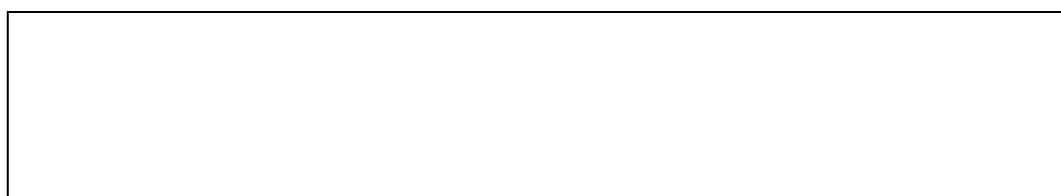


Figure 4.40. Alcian Blue staining results of transduced rBMSCs (a-d), chondrocytes (e), and non-transduced rBMSCs (f), after 10 days of incubation in chondrogenic differentiation medium; (a) 1X, (b) 2X, (c) 1ML, (d) 2ML. Scale bar: 200 μm.

It was found that TG2 provided mesenchymal-like characteristics in different cell types, which is done mainly by GTP-binding domain [136][137][139]. Since TG2-S is deficient in GTP-binding, MSCs that express TG2-S would be promoted towards differentiation. As a confirmation of this hypothesis, results of Alcian Blue staining and immunostaining collectively showed that the transduction of rBMSCs with TGM2_v2 provided the cells a potential of spontaneous chondrogenic differentiation. Moreover, no major difference was detected between the transduction methods (2X viral pellet or 2 mL viral suspension) in terms of chondrogenic matrix production and deposition.

4.8.2. Deposition of sGAG by the Cells on PBSu:PLLA Scaffolds

In order to observe sGAG deposition inside the scaffolds throughout 3 weeks of incubation, the cell-seeded scaffolds were stained with Alcian Blue, as well. Only 2ML groups were used as the representative of transduced rBMSCs, and rat chondrocytes were used as a positive control (Figure 4.39, CH column). Blue color intensity was quantified using Adobe Photoshop (Figure 4.40). It was observed that the empty scaffolds tended to disintegrate their form at the end of 21 days, because there were no ECM molecules to hold the polymer pieces together. After 14 days of incubation in growth media, 2ML group displayed a denser blue color compared to the other cell types (MSC and CH), indicating more sGAG deposition without chondrogenic induction. Similarly, more matrix deposition was observed in 2ML group than MSC group after 21 days of incubation in chondrogenic differentiation media, confirmed by blue color density graph (Figure 4.40). Moreover, though data could not be shown here, 2ML groups seemed more firm during handling at day 21, which could be correlated with the ECM crosslinking ability of TG2 [120]. The densest blue color was observed in the CH group on day 21 without chondrogenic induction, as expected. These results indicated that TG2-S production by rBMSCs affected the deposition of chondrogenic ECM in a positive manner, regardless of chondrogenic stimulation.



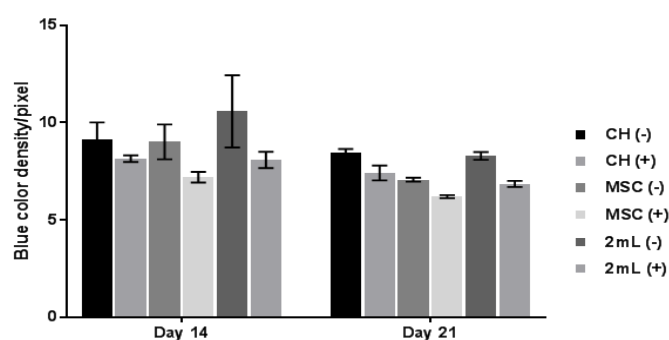
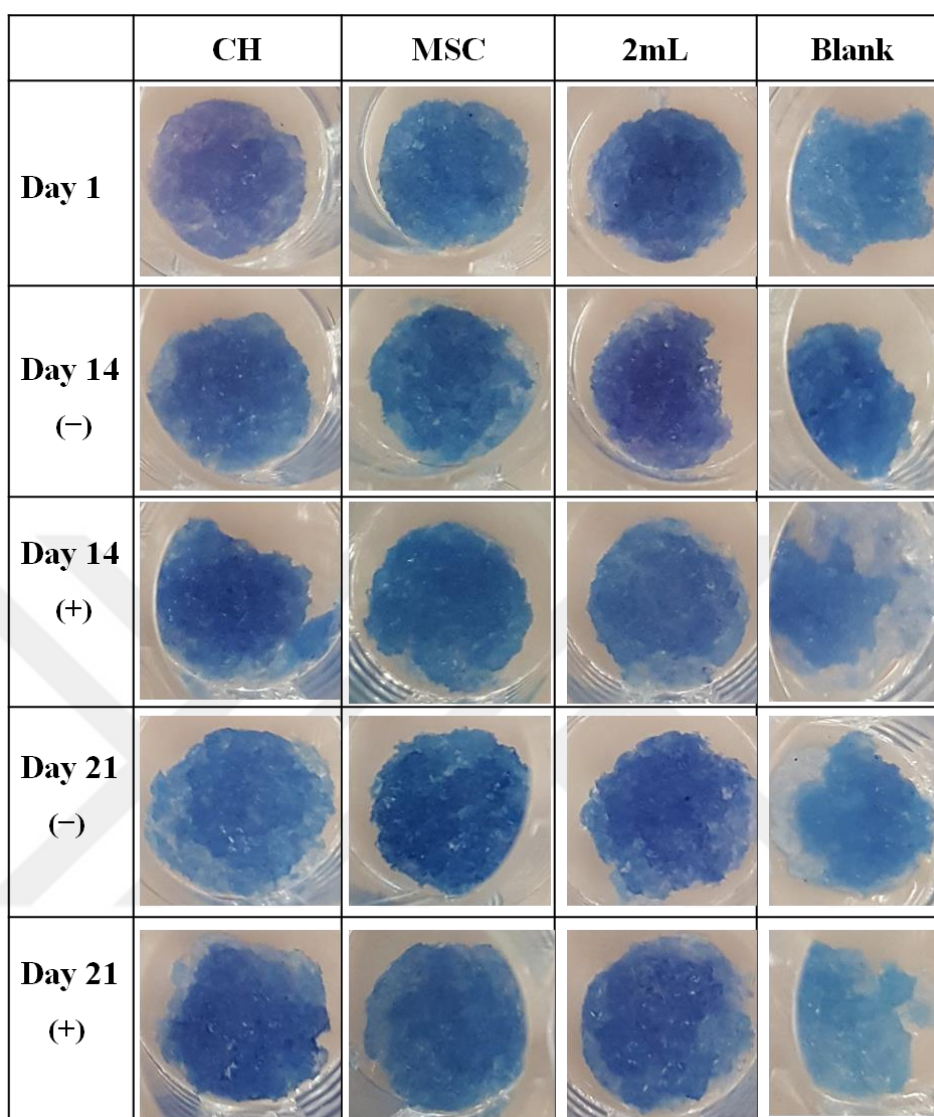


Figure 4.41. Alcian Blue staining of cell-seeded 6% PBSu:PLLA scaffolds on day 1, 14, and 21. CH: rat chondrocytes, MSC: non-transduced rBMSCs, 2mL: Transduced rBMSCs, Blank: empty scaffold, (-): no chondrogenic induction, (+): chondrogenic induction on the 4th day of incubation. The graph at the bottom shows blue color density per pixel.

4.9. ALIZARIN RED STAINING FOR OSTEOGENIC DIFFERENTIATION

In addition to chondrogenic potential, the 2X and 2ML groups were analyzed in terms of osteogenic potential. For this purpose, Alizarin Red staining was carried out to examine the calcium deposits in the ECMs (Figure 4.42), which is a sign of osteogenic differentiation [165]. Human osteoblasts were used as the positive control (Figure 4.42 f) in which the calcium deposits were dominantly observed in pinkish red color. The dark red clusters in Figure 4.42 b indicate that 2X groups started differentiation towards the osteogenic lineage after 14 days in culture. Less dense clusters were also observed in 1X group (Figure 4.42 a), 1ML group (Figure 4.42 c), and MSC group (Figure 4.42 e), yet it is known that MSCs have tendency towards osteogenesis [166]. On the other hand, calcium deposits were not much apparent in 2ML group (Figure 4.42 d), suggesting that TGM2_v2 transduction prevented osteogenic differentiation of rBMSCs, which supports our findings in immunostaining.

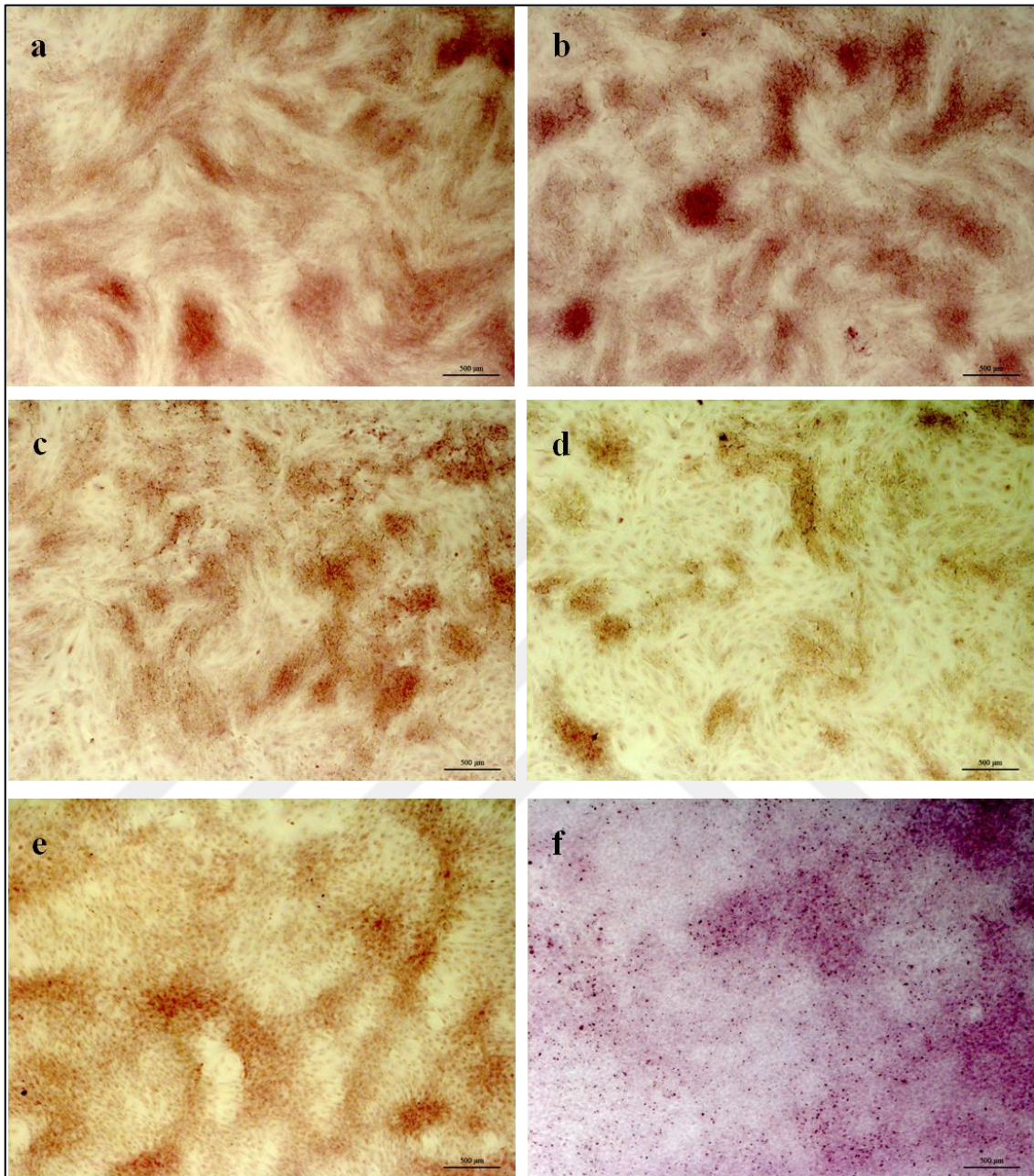


Figure 4.42. Alizarin Red staining of transduced (a: 1X, b: 2X, c: 1ML, d: 2ML) and non-transduced rBMSCs (e) on day 14 of incubation taken by bright field microscope (objective: 5X, scale bar: 500 μm). No chondrogenic induction was applied. Human osteoblasts (f) were used as positive control of osteogenic differentiation.

4.10. MECHANICAL ANALYSIS OF THE CELL-SCAFFOLD CONSTRUCTS

The Young's moduli (compressive moduli) of the cell-seeded PBSu: PLLA scaffolds were calculated after testing the materials with Instron Universal Testing System (ITW, USA) to evaluate the strength of the constructs against compressive force. Testing was performed on wet groups in order to accurately compare them with the original cartilage tissue. Compressive modulus of rat femoral condylar cartilage was found to be 0.7 MPa [167]. It was observed that after 18 days of incubation in chondrogenic differentiation media, the construct that was produced by PBSu:PLLA scaffolds seeded with rat chondrocytes displayed a similar value as 0.78 MPa (Table 4.4). Following the control cells (rat chondrocytes), the closest value to the modulus of original cartilage tissue was presented by the non-transduced rBMSCs at day 46 without chondrogenic induction (0.63 MPa). A much higher value was observed with 2ML groups on day 18 without the chondrogenic induction (1.46 MPa), which could also indicate that this construct may also be used in bone tissue engineering after being extensively studied in this field.

Table 4.4. Compressive moduli of the cell-seeded PBSu:PLLA (6%) scaffolds. The modulus of the empty scaffold was measured as 0.3232 MPa. 2ML: 2ML transduced rBMSCs, MSC: non-transduced rBMSCs, CH: rat chondrocytes.

	No chondrogenic induction			Chondrogenic induction		
	2ML	MSC	CH	2ML	MSC	CH
Day 18	1.4601 MPa	0.4216 MPa	0.4455 MPa	0.1443 MPa	0.5072 MPa	0.7725 MPa
Day 46	0.3845 MPa	0.6308 MPa	0.4698 MPa	0.3186 MPa	0.3697 MPa	0.1563 MPa

5. CONCLUSION

Articular cartilage degeneration has always been a serious problem affecting the people of almost every age due to the tissue's lack of ability of self-healing, and it is increasing day by day as we choose to live less active because of the developing technology [168]. Therefore, the need for joint surgeries and implants are growing rapidly. Cartilage tissue engineering is utilized as the best alternative to such invasive methods, which aims to regenerate a defected cartilage tissue so that the joint functions can totally be restored. The design of the most suitable cell/scaffold construct for the regeneration of joint cartilage is still under investigation. The choice of a biocompatible scaffold and a cell source that is capable of cartilage tissue formation under suitable environmental conditions should be done carefully such that the construct would be prepared and implanted in the easiest and the least invasive way, without causing any side-effects or further degeneration of the tissue. For this purpose, we developed a construct using TG2-S-transduced MSCs and 3D porous PBSu:PLLA scaffolds which were shown to be biocompatible cell carriers for cartilage tissue regeneration [69] [70]. In agreement, our 3D porous 6 per cent PBSu:PLLA scaffolds were shown to be suitable cell carriers when cartilage regeneration is concerned. MSC from rat bone marrow were chosen to due to their high tendency of chondrogenic differentiation as well as the ease of isolation [130]. In this study, we demonstrated that TG2-S transduction provided rBMSCs the ability to differentiate towards chondrogenic lineage without any addition of chondrogenic stimulants, which can reduce the need for the addition of expensive growth and differentiation factors in the culture medium. In addition, the problem of hypertrophy with the cell-seeded cartilage implants after knee surgeries [169] could be reduced since TGM2_v2 transduction prevented hypertrophy. The usage of lentiviral media for the transduction of rBMSCs was found more efficient than lentiviral pellet use. To conclude, our construct could serve as a good candidate for further cartilage tissue engineering studies, reducing the need for expensive external chondrogenic inducers like differentiation factors. Our paper presents an innovative view of cartilage tissue engineering using TGM2_v2-transduced MSCs on PBSu:PLLA scaffolds. Further research is necessary to verify whether these constructs could be used as cartilage substitutes.

6. FUTURE PROSPECTS

Our construct showed promising results in terms of cartilage tissue regeneration, however further experiments should be carried out to maximize the effectiveness of the future product of tissue engineering. First of all, mechanical testing should be performed with repeating measurements using sensitive instruments that are designed for testing the strength of tissue substitutes against compressive, tensile, and shear forces. The potential of the transduced rBMSC-seeded scaffolds in regeneration of elastic cartilage and fibrocartilage could be investigated. In addition, an osteochondral tissue engineering construct could be created by using biphasic scaffolds, in which TGM2_v2 transduced rBMSCs or chondrocytes are seeded on the cartilage interface, while seeding TGM2 transduced rBMSCs or osteoblasts on the bone-facing surface. TGM2 transduced cells would express the long form of TG2 which has high crosslinking activity, resulting in osteogenic differentiation. TG2 variants other than second isoform could be tested for their effects in the chondrogenic differentiation and stemness of the cells, as alternatively spliced variants of TG2 other than TG2-S are also GTP-binding deficient. The transduced cells could be used with various types of polymer scaffolds having different pore sizes and tested for cartilage tissue engineering. Different PBSu:PLLA scaffold compositions could be investigated, such as 1:2 and 2:1. Further chondrogenic differentiation analyses should be performed to confirm our results. Lastly, long term *in vivo* experiments could be performed to observe the potential of our constructs in cartilage regeneration, and observe their effects on the site of implantation.

REFERENCES

1. Nukavarapu SP, Dorcemus DL. Osteochondral tissue engineering: current strategies and challenges. *Biotechnol Adv.* 2013;31(5):706–21.
2. Kuo CK, Li W-J, Mauck RL, Tuan RS. Cartilage tissue engineering: its potential and uses. *Curr Opin Rheumatol.* 2006;18(1):64–73.
3. Oseni A, O, Crowley C, Boland MZ, Butler PE, Seifalian AM. Cartilage tissue engineering : the application of nanomaterials and stem cell technology. In: D. Eberli editor, *Tissue Eng Tissue Organ Regeneration*, pages 233–66. IntechOpen, London, 2011.
4. Poole CA. Articular cartilage chondrons: form, function and failure. *J Anat.* 1997;191:1–13.
5. LeBaron RG, Athanasiou KA. Ex vivo synthesis of articular cartilage. *Biomaterials.* 2000;21(24):2575–87.
6. Black J, Hastings G. *Handbook of biomaterial properties*. Chapman & Hall, London, 1998.
7. Meyer U, Wiesmann HP. *Bone and cartilage engineering*. Springer, Berlin 2006.
8. Plumb MS, Aspden RM. The response of elderly human articular cartilage to mechanical stimuli in vitro. *Osteoarthritis Cartilage.* 2005;13(12):1084–91.
9. Khan IM, Francis L, Theobald PS, Perni S, Young RD, Prokopovich P, et al. In vitro growth factor-induced bio engineering of mature articular cartilage. *Biomaterials.* 2013;34(5):1478–87.
10. Williams RJ. Articular cartilage repair: clinical approach and decision making. *Oper Tech Orthop.* 2006;16(4):218–26.
11. Getgood A, Bhullar TPS, Rushton N. Current concepts in articular cartilage repair. *Orthop Trauma.* 2009;23(3):189–200.
12. Athanasiou KA, Rosenwasser MP, Buckwalter JA, Malinin TI, Mow VC. Interspecies

- comparisons of in situ intrinsic mechanical properties of distal femoral cartilage. *J Orthop Res.* 1991;9(3):330–40.
13. Temenoff JS, Mikos AG. Review: tissue engineering for regeneration of articular cartilage. *Biomaterials.* 2000;21(5):431–40.
 14. Poole AR, Kojima T, Yasuda T, Mwale F, Kobayashi M, Lavery S. Composition and structure of articular cartilage: a template for tissue repair. *Clin Orthop Relat Res.* 2001;1:S26–33.
 15. Cohen B, Lai WM, Mow VC. A transversely isotropic biphasic model for unconfined compression of growth plate and chondroepiphysis. *J Biomech Eng.* 1998;120(4):491–6.
 16. Darling EM, Athanasiou KA. Rapid phenotypic changes in passaged articular chondrocyte subpopulations. *J Orthop Res.* 2005;23(2):425–32.
 17. Yang L, Carlson SG, McBurney D, Horton WE. Multiple signals induce endoplasmic reticulum stress in both primary and immortalized chondrocytes resulting in loss of differentiation, impaired cell growth, and apoptosis. *J Biol Chem.* 2005;280(35):31156–65.
 18. Dedivitis RA, Abrahão M, Simões MDJ, Mora OA, Cervantes O. Aging histological changes in the cartilages of the cricoarytenoid joint. *Acta Cirúrgica Brasileira,* 2004;19(2):136–40.
 19. Demoor M, Ollitrault D, Gomez-Leduc T, Bouyoucef M, Hervieu M, Fabre H, et al. Cartilage tissue engineering: Molecular control of chondrocyte differentiation for proper cartilage matrix reconstruction. *Biochim Biophys Acta.* 2014;1840(8):2414–40.
 20. Alberts B, Johnson A, Lewis J, Raff M, Roberts K, Walter P. *Molecular biology of the cell*, Garland Science, New York, 2008.
 21. Gentili C, Cancedda R. Cartilage and bone extracellular matrix. *Curr Pharm Des.* 2009;15:1334–48.
 22. Iozzo R V. Matrix proteoglycans: from molecular design to cellular function. *Annu*

- Rev Biochem.* 1998;67(1):609–52.
23. Chen FH, Rousche KT, Tuan RS. Technology Insight: adult stem cells in cartilage regeneration and tissue engineering. *Nat Clin Pract Rheumatol.* 2006;2(7):373–82.
 24. Gomes RR, Farach-Carson MC, Carson DD. Perlecan functions in chondrogenesis: insights from in vitro and in vivo models. *Cells Tissues Organs.* 2004;176(1–3):79–86.
 25. Kuno K, Okada Y, Kawashima H, Nakamura H, Miyasaka M, Ohno H, et al. ADAMTS-1 cleaves a cartilage proteoglycan, aggrecan. *FEBS Lett.* 2000;478(3):241–5.
 26. Kämäräinen O-P, Solovieva S, Vehmas T, Luoma K, Leino-Arjas P, Riihimäki H, et al. Aggrecan core protein of a certain length is protective against hand osteoarthritis. *Osteoarthr Cartil.* 2006;14(10):1075–80.
 27. Kadler KE, Hill A, Canty-Laird EG. Collagen fibrillogenesis: fibronectin, integrins, and minor collagens as organizers and nucleators. *Curr Opin Cell Biol.* 2008;20(5):495–501.
 28. Ackermann B, Steinmeyer J. Collagen biosynthesis of mechanically loaded articular cartilage explants. *Osteoarthritis Cartilage.* 2005;13(10):906–14.
 29. Felson DT, Lohmander LS. Whither osteoarthritis biomarkers? *Osteoarthr Cartil.* 2009;17(4):419–22.
 30. Buckwalter JA. Articular cartilage: injuries and potential for healing. *J Orthop Sports Phys Ther.* 1998;28(4):192–202.
 31. Hunziker EB. Biologic repair of articular cartilage. *Clin Orthop Relat Res.* 1999;367(367):S135–46.
 32. Madry H, van Dijk CN, Mueller-Gerbl M. The basic science of the subchondral bone. *Knee Surg Sports Traumatol Arthrosc.* 2010;18(4):419–33.
 33. Laupattarakasem W, Laopaiboon M, Laupattarakasem P, Sumananont C. *Arthroscopic debridement for knee osteoarthritis*, John Wiley & Sons, Ltd., New Jersey, 2009.

34. Steadman JR, Briggs KK, Rodrigo JJ, Kocher MS, Gill TJ, Rodkey WG. Outcomes of microfracture for traumatic chondral defects of the knee: average 11-year follow-up. *Arthroscopy*. 2003;19(5):477–84.
35. Haene R, Qamirani E, Story RA, Pinsker E, Daniels TR. Intermediate outcomes of fresh talar osteochondral allografts for treatment of large osteochondral lesions of the talus. *J Bone Joint Surg Am*. 2012;94(12):1105–10.
36. Beris AE, Lykissas MG, Papageorgiou CD, Georgoulis AD. Advances in articular cartilage repair. *Injury*. 2005;36S:S14-23.
37. Henderson I, Francisco R, Oakes B, Cameron J. Autologous chondrocyte implantation for treatment of focal chondral defects of the knee—a clinical, arthroscopic, MRI and histologic evaluation at 2 years. *Knee*. 2005;12(3):209–16.
38. Brittberg M. Autologous chondrocyte implantation—technique and long-term follow-up. *Injury*. 2008;39S1:S40-9.
39. Kon E, Verdonk P, Condello V, Delcogliano M, Dhollander A, Filardo G, et al. Matrix-assisted autologous chondrocyte transplantation for the repair of cartilage defects of the knee—systematic clinical data review and study quality analysis. *Am J Sports Med*. 2009;37:156S–166S.
40. Bhattacharjee M, Coburn J, Centola M, Murab S, Barbero A, Kaplan DL, et al. Tissue engineering strategies to study cartilage development, degeneration and regeneration. *Adv Drug Deliv Rev*. 2015;84:107–22.
41. French MM, Rose S, Canseco J, Athanasiou KA. Chondrogenic differentiation of adult dermal fibroblasts. *Ann Biomed Eng*. 2004;32(1):50–6.
42. Bigdeli N, Karlsson C, Strehl R, Concaro S, Hyllner J, Lindahl A. Coculture of human embryonic stem cells and human articular chondrocytes results in significantly altered phenotype and improved chondrogenic differentiation. *Stem Cells*. 2009;27(8):1812–21.
43. Wei Y, Wei Y, Zeng W, Wan R, Wang J, Zhou Q, et al. Chondrogenic differentiation of induced pluripotent stem cells from osteoarthritic chondrocytes in alginate matrix. *Eur Cells Mater*. 2012;23:1–12.

44. Pittenger MF, Marshak DR. Mesenchymal stem cells of human adult bone marrow. In: D.R. Marshak, R.L. Gardner, D.Gottlieb editors, *Stem Cell Biology*, pages: 349-351. Cold Spring Harbor Laboratory Press, New York, 2001.
45. Csaki C, Schneider PRA, Shakibaei M. Mesenchymal stem cells as a potential pool for cartilage tissue engineering. *Ann Anat.* 2008;190:395-412.
46. Von Der Mark K, Gauss V, Von Der Mark H, Müller P. Relationship between cell-shape and type of collagen synthesized as chondrocytes lose their cartilage phenotype in culture. *Nature.* 1977;267:531-2.
47. Wang Y, Blasioli DJ, Kim H-J, Kim HS, Kaplan DL. Cartilage tissue engineering with silk scaffolds and human articular chondrocytes. *Biomaterials.* 2006;27:4434-42.
48. Chung C, Burdick JA. Engineering cartilage tissue. *Adv Drug Deliv Rev.* 2008;60:243-62.
49. Lee MW, Kim DS, Yoo KH, Kim HR, Jang IK, Lee JH, et al. Human bone marrow-derived mesenchymal stem cell gene expression patterns vary with culture conditions. *Blood Res.* 2013;48(2):107-14.
50. Wagner W, Feldmann RE, Seckinger A, Maurer MH, Wein F, Blake J, et al. The heterogeneity of human mesenchymal stem cell preparations-evidence from simultaneous analysis of proteomes and transcriptomes. *Exp Hematol.* 2006;34:536-48.
51. Wang Y, Bian Y-Z, Wu Q, Chen G-Q. Evaluation of three-dimensional scaffolds prepared from poly(3-hydroxybutyrate-co-3-hydroxyhexanoate) for growth of allogeneic chondrocytes for cartilage repair in rabbits. *Biomaterials.* 2008;29(19):2858-68.
52. Hiramatsu K, Sasagawa S, Outani H, Nakagawa K, Yoshikawa H, Tsumaki N. Generation of hyaline cartilaginous tissue from mouse adult dermal fibroblast culture by defined factors. *J Clin Invest.* 2011;121(2):640-57.
53. Gan L, Kandel RA. In vitro cartilage tissue formation by co-culture of primary and passaged chondrocytes. *Tissue Eng.* 2007;13(4):831-42.

54. Jiang J, Nicoll SB, Lu HH. Co-culture of osteoblasts and chondrocytes modulates cellular differentiation in vitro. *Biochem Biophys Res Commun*. 2005;338(2):762–70.
55. Tsuchiya K, Chen G, Ushida T, Matsuno T, Tateishi T. The effect of coculture of chondrocytes with mesenchymal stem cells on their cartilaginous phenotype in vitro. *Mater Sci Eng C*. 2004;24(3):391–6.
56. Ozturk N, Girotti A, Kose GT, Rodríguez-Cabello JC, Hasirci V. Dynamic cell culturing and its application to micropatterned, elastin-like protein-modified poly(N-isopropylacrylamide) scaffolds. *Biomaterials*. 2009;30(29):5417–26.
57. Hutmacher DW. Scaffolds in tissue engineering bone and cartilage. *Biomaterials*. 2000;21(24):2529–43.
58. Liao S, Chan CK, Ramakrishna S. Stem cells and biomimetic materials strategies for tissue engineering. *Mater Sci Eng C*. 2008;28(8):1189–202.
59. Puppi D, Chiellini F, Piras AM, Chiellini E. Polymeric materials for bone and cartilage repair. *Prog Polym Sci*. 2010;35(4):403–40.
60. Lee KY, Peters MC, Mooney DJ. Controlled drug delivery from polymers by mechanical signals. *Adv Mater*. 2001;13(11):837–9.
61. Nan A, Ghandehari H. Structure, properties, and characterization of polymeric biomaterials. In: R.I. Mahato editor, *Biomaterials for Delivery and Targeting of Proteins and Nucleic Acids*, pages: 1-44. CRC Press, New York, 2005.
62. Köse GT, Korkusuz F, Ozkul A, Soysal Y, Ozdemir T, Yildiz C, et al. Tissue engineered cartilage on collagen and PHBV matrices. *Biomaterials*. 2005;26(25):5187–97.
63. Marler JJ, Upton J, Langer R, Vacanti JP. Transplantation of cells in matrices for tissue regeneration. *Adv Drug Deliv Rev*. 1998;33(1–2):165–82.
64. Wong JY, Kuhl TL, Israelachvili JN, Mullah N, Zalipsky S. Direct measurement of a tethered ligand-receptor interaction potential. *Science*. 1997, 7;275(5301):820-2.
65. Stoop R. Smart biomaterials for tissue engineering of cartilage. *Injury*. 2008;39S1:S77-87.

66. Cima LG, Vacanti JP, Vacanti C, Inger D, Mooney D, Langer R. Tissue engineering by cell transplantation using degradable polymer substrates. *J Biomech Eng T ASME*. 1991;113:143–51.
67. Vacanti CA, Langer R, Schloo B, Vacanti JP. Synthetic polymers seeded with chondrocytes provide a template for new cartilage formation. *Plast Reconstr Surg*. 1991;88(5):753–9.
68. Ma PX, Langer R. Morphology and mechanical function of long-term in vitro engineered cartilage. *J Biomed Mater Res*. 1999;44(2):217–21.
69. Li W-J, Jiang YJ, Tuan RS. Chondrocyte phenotype in engineered fibrous matrix is regulated by fiber size. *Tissue Eng*. 2006;12(7):1775–85.
70. Oliveira JT, Crawford A, Mundy JL, Sol PC, Correlo VM, Bhattacharya M, et al. Novel melt-processable chitosan-polybutylene succinate fibre scaffolds for cartilage tissue engineering. *J Biomater Sci Polym Ed*. 2011;22(4–6):773–88.
71. Pérez DD, Lunz JSC, Santos ERF dos, Oliveira GE de, Jesus EFO de, Souza FG de. Poly (butylene succinate) scaffolds prepared by leaching. *MOJ Polym Sci*. 2017;1(6):8–11.
72. Hariraksapitak P, Suwantong O, Pavasant P, Supaphol P. Effectual drug-releasing porous scaffolds from 1,6-diisocyanatohexane-extended poly(1,4-butylene succinate) for bone tissue regeneration. *Polymer (Guildf)*. 2008;49(11):2678–85.
73. Oliveira JT, Correlo VM, Sol PC, Costa-Pinto AR, Malafaya PB, Salgado AJ, et al. Assessment of the suitability of chitosan/polybutylene succinate scaffolds seeded with mouse mesenchymal progenitor cells for a cartilage tissue engineering approach. *Tissue Eng Part A*. 2008;14(10):1651–61.
74. Oliveira JM, Rodrigues MT, Silva SS, Malafaya PB, Gomes ME, Viegas C a, et al. Novel hydroxyapatite/chitosan bilayered scaffold for osteochondral tissue-engineering applications: Scaffold design and its performance when seeded with goat bone marrow stromal cells. *Biomaterials*. 2006;27(36):6123–37.
75. Jung Y, Park MS, Lee JW, Kim YH, Kim S-H, Kim SH. Cartilage regeneration with highly-elastic three-dimensional scaffolds prepared from biodegradable poly(L-

- lactide-co-epsilon-caprolactone). *Biomaterials*. 2008;29(35):4630–6.
76. Tan H, Chu CR, Payne KA, Marra KG. Injectable in situ forming biodegradable chitosan-hyaluronic acid based hydrogels for cartilage tissue engineering. *Biomaterials*. 2009;30(13):2499–506.
 77. Park H, Choi B, Hu J, Lee M. Injectable chitosan hyaluronic acid hydrogels for cartilage tissue engineering. *Acta Biomater*. 2013;9(1):4779–86.
 78. Gaissmaier C, Koh JL, Weise K. Growth and differentiation factors for cartilage healing and repair. *Injury*. 2008;39S1:S88-96.
 79. Masuda K, An HS. Growth factors and the intervertebral disc. *Spine J*. 2004;4:330S–340S.
 80. Hwang NS, Kim MS, Sampattavanich S, Baek JH, Zhang Z, Elisseeff J. Effects of three-dimensional culture and growth factors on the chondrogenic differentiation of murine embryonic stem cells. *Stem Cells*. 2006;24:284–91.
 81. Holland TA, Mikos AG. Advances in drug delivery for articular cartilage. *J Control Release*. 2003;86:1–14.
 82. Nawata M, Wakitani S, Nakaya H, Tanigami A, Seki T, Nakamura Y, et al. Use of bone morphogenetic protein 2 and diffusion chambers to engineer cartilage tissue for the repair of defects in articular cartilage. *Arthritis Rheum*. 2005;52(1):155–63.
 83. Vinatier C, Mrugala D, Jorgensen C, Guicheux J, Noël D. Cartilage engineering: a crucial combination of cells, biomaterials and biofactors. *Trends Biotechnol*. 2009;27(5):307–14.
 84. Waldman SD, Spiteri CG, Grynblas MD, Pilliar RM, Hong J, Kandel RA. Effect of biomechanical conditioning on cartilaginous tissue formation in vitro. *J bone Jt Surg*. 2003;85:101–5.
 85. Nestic D, Whiteside R, Brittberg M, Wendt D, Martin I, Mainil-Varlet P. Cartilage tissue engineering for degenerative joint disease. *Adv Drug Deliv Rev*. 2006;58(2):300–22.
 86. Wendt D, Marsano A, Jakob M, Heberer M, Martin I. Oscillating perfusion of cell

- suspensions through three-dimensional scaffolds enhances cell seeding efficiency and uniformity. *Biotechnol Bioeng.* 2003;84(2):205–14.
87. Pei M, He F, Boyce BM, Kish VL. Repair of full-thickness femoral condyle cartilage defects using allogeneic synovial cell-engineered tissue constructs. *Osteoarthr Cartil.* 2009;17(6):714–22.
 88. Evans CH, Robbins PD, Kang R, Barranger JA, Gay S, Wasko MC, et al. Clinical trial to assess the safety, feasibility, and efficacy of transferring a potentially anti-arthritic cytokine gene to human joints with rheumatoid arthritis. *Hum Gene Ther.* 1996;7:1261–80.
 89. Kallifatidis G, Beckermann BM, Groth A, Schubert M, Apel A, Khamidjanov A, et al. Improved lentiviral transduction of human mesenchymal stem cells for therapeutic intervention in pancreatic cancer. *Cancer Gene Ther.* 2008;15:231–40.
 90. Lin P, Correa D, Lin Y, Caplan AI. Polybrene inhibits human mesenchymal stem cell proliferation during lentiviral transduction. *PLoS One.* 2011;6(8):e23891.
 91. Lin P, Lin Y, Lennon DP, Correa D, Schluchter M, Caplan AI. Efficient lentiviral transduction of human mesenchymal stem cells that preserves proliferation and differentiation capabilities. *Stem Cells Transl Med.* 2012;1:886–97.
 92. Akimov SS, Krylov D, Fleischman LF, Belkin AM. Tissue transglutaminase is an integrin-binding adhesion coreceptor for fibronectin. *J Cell Biol.* 2000;148(4):825–38.
 93. Teixeira LSM, Feijen J, van Blitterswijk CA, Dijkstra PJ, Karperien M. Enzyme-catalyzed crosslinkable hydrogels: emerging strategies for tissue engineering. *Biomaterials.* 2012;33(5):1281–90.
 94. Di Sabatino A, Vanoli A, Giuffrida P, Luinetti O, Solcia E, Corazza GR. The function of tissue transglutaminase in celiac disease. *Autoimmun Rev.* 2012;11(10):746–53.
 95. Gentile V, Saydak M, Chioccas EA, Akandes O, Birckbichlerq PJ, Lees KN, et al. Isolation and characterization of cDNA clones to mouse macrophage and human endothelial cell tissue transglutaminases. *J Biol Chem.* 1991;266(5):478–83.

96. Kapil Mehta. Mammalian transglutaminases: A Family Portrait. *Prog Exp Tumor Res.* 2005;272(38):1–18.
97. Fesus L, Piacentini M. Transglutaminase 2: an enigmatic enzyme with diverse functions. *Trends Biochem Sci.* 2002;27(10):534–9.
98. Venere A Di, Rossi A, Matteis F De, Rosato N, Mei G. Opposite effects of Ca²⁺ and GTP binding on tissue transglutaminase tertiary structure. *J Biol Chem.* 2000;275(6):3915–21.
99. Nurminskaya M, Belkin A. Cellular functions of tissue transglutaminase. *Int Rev Cell Mol Biol.* 2012;1–79.
100. Deasey S, Nurminsky D, Shanmugasundaram S, Lima F, Nurminskaya M. Transglutaminase 2 as a novel activator of LRP6/beta-catenin signaling. *Cell Signal.* 2013;25(12):2646–51.
101. Agnihotri N, Mehta K. Transglutaminase-2: evolution from pedestrian protein to a promising therapeutic target. *Amino Acids.* 2017;49(3):425–39.
102. Griffin M, Casadio R, Bergamini C. Transglutaminases: nature's biological glues. *Biochem J.* 2002;368:377–96.
103. Song H, Chang W, Lim S, Seo H-S, Shim CY, Park S, et al. Tissue transglutaminase is essential for integrin-mediated survival of bone marrow-derived mesenchymal stem cells. *Stem Cells.* 2007;25(6):1431–8.
104. Akimov SS, Belkin a M. Cell-surface transglutaminase promotes fibronectin assembly via interaction with the gelatin-binding domain of fibronectin: a role in TGFbeta-dependent matrix deposition. *J Cell Sci.* 2001;114:2989–3000.
105. Hang J, Belkin AM. The role of tissue transglutaminase in cell-matrix interactions. *Front. Biosci.* 2006; 11:1057-76.
106. Akimov SS, Belkin AM. Cell surface tissue transglutaminase is involved in adhesion and migration of monocytic cells on fibronectin. *Blood.* 2016;98(5):1567–77.
107. Chalovich JM, Eisenberg E. Extracellular TG2: emerging functions and regulation. *Biophys Chem.* 2005;257(5):2432–7.

108. Telci D, Wang Z, Li X, Verderio EAM, Humphries MJ, Baccarini M, et al. Fibronectin-tissue transglutaminase matrix rescues RGD-impaired cell adhesion through syndecan-4 and beta1 integrin co-signaling. *J Biol Chem.* 2008;283(30):20937–47.
109. Nunes I, Gleizes PE, Metz CN, Rifkin DB. Latent transforming growth factor-beta binding protein domains involved in activation and transglutaminase-dependent cross-linking of latent transforming growth factor-beta. *J Cell Biol.* 1997;136(5):1151–63.
110. Niger C, Beazley KE, Nurminskaya M. Induction of chondrogenic differentiation in mesenchymal stem cells by TGF-beta cross-linked to collagen-PLLA [poly(L-lactic acid)] scaffold by transglutaminase 2. *Biotechnol Lett.* 2013;35(12):2193–9.
111. Ritter SJ, Davies PJ. Identification of a transforming growth factor-beta1/bone morphogenetic protein 4 (TGF-beta1/BMP4) response element within the mouse tissue transglutaminase gene promoter. *J Biol Chem.* 1998;273(21):12798–806.
112. Kojima S, Nara K, Rifkin DB. Requirement for transglutaminase in the activation of latent transforming growth factor-beta in bovine endothelial cells. *J Cell Biol.* 1993;121(2):439–48.
113. Telci D, Collighan RJ, Basaga H, Griffin M. Increased TG2 expression can result in induction of transforming growth factor beta1, causing increased synthesis and deposition of matrix proteins, which can be regulated by nitric oxide. *J Biol Chem.* 2009;284(43):29547–58.
114. Tatsukawa H, Furutani Y, Hitomi K, Kojima S. Transglutaminase 2 has opposing roles in the regulation of cellular functions as well as cell growth and death. *Cell Death Dis.* 2016;7(6):e2244.
115. Lai T-S, Greenberg C. TGM2 and implications for human disease: role of alternative splicing. *Front Biosci.* 2013;18(2):504.
116. Blaney Davidson EN, van der Kraan PM, van den Berg WB. TGF-beta and osteoarthritis. *Osteoarthr Cartil.* 2007;15:597–604.
117. Kawakami Y, Rodriguez-León J, Belmonte JCI. The role of TGF-betas and Sox9

- during limb chondrogenesis. *Curr Opin Cell Biol.* 2006;18(6):723–9.
118. Summey BT, Graff RD, Lai T-S, Greenberg CS, Lee GM. Tissue transglutaminase localization and activity regulation in the extracellular matrix of articular cartilage. *J Orthop Res.* 2002;20(1):76–82.
 119. Nurminsky D, Shanmugasundaram S, Deasey S, Michaud C, Allen S, Hendig D, et al. Transglutaminase 2 regulates early chondrogenesis and glycosaminoglycan synthesis. *Mech Dev.* 2011;128(3–4):234–45.
 120. Jürgensen K, Aeschlimann D, Cavin V, Genge M, Hunziker E. A new biological glue for cartilage-cartilage interfaces: tissue transglutaminase. *J Bone Jt Surg.* 1997;(79–A):185–193.
 121. McHale M, Setton L, Chilkoti A. Synthesis and in vitro evaluation of enzymatically cross-linked elastin-like polypeptide gels for cartilaginous tissue repair. *Tissue Eng.* 2005;11(11–12):1768–79.
 122. Shanmugasundaram S, Logan-Mauney S, Burgos K, Nurminskaya M. Tissue transglutaminase regulates chondrogenesis in mesenchymal stem cells on collagen type XI matrices. *Amino Acids.* 2012;42(2–3):1045–53.
 123. Fraij BM, Birckbichler PJ, Patterson Jr. MK, Lee KN, Gonzales RA. A retinoic acid-inducible mRNA from human erythroleukemia cells encodes a novel tissue transglutaminase homologue. *J Biol Chem.* 1992;267(31):22616–23.
 124. Fraij BM, Gonzales RA. A third human tissue transglutaminase homologue as a result of alternative gene transcripts. *Biochim Biophys Acta.* 1996;1306(1):63–74.
 125. Lai T-S, Liu Y, Li W, Greenberg CS. Identification of two GTP-independent alternatively spliced forms of tissue transglutaminase in human leukocytes, vascular smooth muscle, and endothelial cells. *FASEB J.* 2007;21(14):4131–43.
 126. Phatak VM, Croft SM, Rameshaiah Setty SG, Scarpellini A, Hughes DC, Rees R, et al. Expression of transglutaminase-2 isoforms in normal human tissues and cancer cell lines: Dysregulation of alternative splicing in cancer. *Amino Acids.* 2013;44(1):33–44.


127. Bianchi N, Beninati S, Bergamini CM. Spotlight on the transglutaminase 2 gene: a focus on genomic and transcriptional aspects. *Biochem J* (2018) 2018; 475:1643–67.
128. Tee AEL, Marshall GM, Liu PY, Xu N, Haber M, Norris MD, et al. Opposing effects of two tissue transglutaminase protein isoforms in neuroblastoma cell differentiation. *J Biol Chem*. 2010;285(6):3561–7.
129. Antonyak MA, Jansen JM, Miller AM, Ly TK, Endo M, Cerione RA. Two isoforms of tissue transglutaminase mediate opposing cellular fates. *Proc Natl Acad Sci*. 2006;103(49):18609–14.
130. Meshkini A, Yazdanparast R, Nouri K. Intracellular GTP level determines cell's fate toward differentiation and apoptosis. *Toxicol Appl Pharmacol*. 2011;253(3):188–96.
131. Fellows CR, Matta C, Zakany R, Khan IM, Mobasheri A. Adipose, bone marrow and synovial joint-derived mesenchymal stem cells for cartilage repair. *Front Genet*. 2016;7:1–20.
132. Calikoglu Koyuncu AC, Gurel Pekozer G, Ramazanoglu M, Torun Kose G, Hasirci V. Cartilage tissue engineering on macroporous scaffolds using human tooth germ stem cells. *J Tissue Eng Regen Med*. 2017;11(3), 765-777.
133. Stoyanova N, Paneva D, Mincheva R, Toncheva A, Manolova N, Dubois P, et al. Poly(l-lactide) and poly(butylene succinate) immiscible blends: From electrospinning to biologically active materials. *Mater Sci Eng C*. 2014;41:119–26.
134. Verderio E, Nicholas B, Gross S, Griffin M. Regulated expression of tissue transglutaminase in Swiss 3T3 fibroblasts: effects on the processing of fibronectin, cell attachment, and cell death. *Exp Cell Res*. 1998;239(1):119–38.
135. Huang H, Zhang X, Hu X, Dai L, Zhu J, Man Z, et al. Directing chondrogenic differentiation of mesenchymal stem cells with a solid-supported chitosan thermogel for cartilage tissue engineering. *Biomed Mater*. 2014;9(3):35008.
136. Kumar A, Xu J, Sung B, Kumar S, Yu D, Aggarwal BB, et al. Evidence that GTP-binding domain but not catalytic domain of transglutaminase 2 is essential for epithelial-to-mesenchymal transition in mammary epithelial cells. *Breast Cancer Res*.

2012;14(1):R4.

137. Fisher ML, Adhikary G, Xu W, Kerr C, Keillor JW, Eckert RL. Type II transglutaminase stimulates epidermal cancer stem cell epithelial-mesenchymal transition. *Oncotarget*. 2015;6(24):20525–39.
138. Shao M, Cao L, Shen C, Satpathy M, Chelladurai B, Bigsby RM, et al. Epithelial-to-mesenchymal transition and ovarian tumor progression induced by tissue transglutaminase. *Cancer Res*. 2009;69(24):9192–201.
139. Lin C, Tsai P, Kandaswami CC, Chang G, Cheng C, Huang C, et al. Role of tissue transglutaminase 2 in the acquisition of a mesenchymal-like phenotype in highly invasive A431 tumor cells. *Mol Cancer*. 2011;10(87):1–13.
140. Ayinde O, Wang Z, Griffin M, Ayinde O, Wang Z, Griffin M, et al. Tissue transglutaminase induces Epithelial-Mesenchymal-Transition and the acquisition of stem cell like characteristics in colorectal cancer cells. *Oncotarget*. 2017;8(12):20025–41.
141. DuBridge RB, Tang P, Hsia HC, Leong PM, Miller JH, Calos MP. Analysis of mutation in human cells by using an Epstein-Barr virus shuttle system. *Mol Cell Biol*. 1987;7(1):379–87.
142. Pear WS, Nolan GP, Scott ML, Baltimore D. Production of high-titer helper-free retroviruses by transient transfection (retroviral packaging cells/gene therapy). *Cell Biol*. 1993;90:8392–6.
143. Karaoz E, Aksoy A, Ayhan S, Sarıboyacı AE, Kaymaz F, Kasap M. Characterization of mesenchymal stem cells from rat bone marrow: ultrastructural properties, differentiation potential and immunophenotypic markers. *Histochem Cell Biol*. 2009;132(5):533–46.
144. Zhang X-Y, La Russa VF, Bao L, Kolls J, Schwarzenberger P, Reiser J. Lentiviral vectors for sustained transgene expression in human bone marrow-derived stromal cells. *Mol Ther*. 2002;5:555–65.
145. Zhang X-Y, La Russa VF, Reiser J. Transduction of bone-marrow-derived mesenchymal stem cells by using lentivirus vectors pseudotyped with modified

- RD114 envelope glycoproteins. *J Virol.* 2004;78(3):1219–29.
146. McMahon JM, Conroy S, Lyons M, Greiser U, O'shea C, Strappe P, et al. Gene transfer into rat mesenchymal stem cells: a comparative study of viral and nonviral vectors. *Stem Cells Dev.* 2006;15(1):87–96.
147. Strehl R, Schumacher K, de Vries U, Minuth WW. Proliferating cells versus differentiated cells in tissue engineering. *Tissue Eng.* 2002;8(1):37–42.
148. Gigli M, Fabbri M, Lotti N, Gamberini R, Rimini B, Munari A. Poly(butylene succinate)-based polyesters for biomedical applications: A review. *Eur Polym J.* 2016;75:431–60.
149. Di Lorenzo ML, Androsch R, Righetti MC. Low-temperature crystallization of poly(butylene succinate). *Eur Polym J.* 2017;94:384–91.
150. Hariraksapitak P, Suwantong O, Pavasant P, Supaphol P. Effectual drug-releasing porous scaffolds from 1,6-diisocyanatohexane-extended poly(1,4-butylene succinate) for bone tissue regeneration. *Polymer (Guildf).* 2008;49(11):2678–85.
151. Haleem AM, Chu CR. Advances in tissue engineering techniques for articular cartilage repair. *Oper Tech Orthop.* 2010;20(2):76–89.
152. Ratner BD, Hoffman AS, Schoen FJ, Lemons JE. *Biomaterials science: an introduction to materials in medicine.* Elsevier Academic Press, London, 2004.
153. Li H, Chang J, Cao A, Wang J. In vitro evaluation of biodegradable poly(butylene succinate) as a novel biomaterial. *Macromol Biosci.* 2005;5(5):433–40.
154. Kanneci Altinişik İA, Kök FN, Yücel D, Torun Köse G. In vitro evaluation of PLLA/PBS sponges as a promising biodegradable scaffold for neural tissue engineering. *Turkish J Biol.* 2017;41(5):734–45.
155. Akiyama H, Chaboissier M-C, Martin JF, Schedl A, de Crombrughe B. The transcription factor Sox9 has essential roles in successive steps of the chondrocyte differentiation pathway and is required for expression of Sox5 and Sox6. *Genes Dev.* 2002;16(21):2813–28.
156. Tew SR, Clegg PD. Analysis of post transcriptional regulation of SOX9 mRNA

- during in vitro chondrogenesis. *Tissue Eng Part A*. 2011;17(13–14):1801–7.
157. Lefebvre V, Li P, De Crombrughe B. A new long form of Sox5 (L-Sox5), Sox6 and Sox9 are coexpressed in chondrogenesis and cooperatively activate the type II collagen gene. *EMBO J*. 1998;17(19):5718–33.
 158. Sekiya I, Tsuji K, Koopman P, Watanabe H, Yamada Y, Shinomiya K, et al. SOX9 enhances aggrecan gene promoter/enhancer activity and is up-regulated by retinoic acid in a cartilage-derived cell. *J Biol Chem*. 2000;275(15):10738–44.
 159. Kleinman HK, Ph D, Murray JC, Ph D, Mcgoodwin EB, Martin GR, et al. Connective tissue structure : cell binding to collagen. *J Invest Dermatol*. 1978;71(1):9–11.
 160. Karlsson C, Brantsing C, Svensson T, Brisby H, Asp J, Tallheden T, et al. Differentiation of human mesenchymal stem cells and articular chondrocytes: Analysis of chondrogenic potential and expression pattern of differentiation-related transcription factors. *J Orthop Res*. 2007;25(2):152–63.
 161. Webster TJ, Ahn ES. Nanostructured biomaterials for tissue engineering bone. *Adv Biochem Eng Biotechnol*. 2007;103:275–308.
 162. Tanaka K, Yokosaki Y, Higashikawa F, Saito Y, Eboshida A, Ochi M. The integrin $\alpha 5 \beta 1$ regulates chondrocyte hypertrophic differentiation induced by GTP-bound transglutaminase 2. *Matrix Biol*. 2007;26(6):409–18.
 163. Mwale F, Stachura D, Roughley P, Antoniou J. Limitations of using aggrecan and type X collagen as markers of chondrogenesis in mesenchymal stem cell differentiation. *J Orthop Res*. 2006;24(8):1791–8.
 164. Miwa HE, Gerken TA, Huynh TD, Flory DM, Hering TM. Mammalian expression of full-length bovine aggrecan and link protein: formation of recombinant proteoglycan aggregates and analysis of proteolytic cleavage by ADAMTS-4 and MMP-13. *Biochim Biophys Acta*. 2006;1760(3):472–86.
 165. Habib NA, Levicar N, Gordon MY, Jiao L, Fisk N. *Stem cell repair and regeneration*. Imperial College Press, London, 2008.
 166. Caplan AI. Mesenchymal stem cells. *J Orthop Res*. 1991;9(5):641–50.

167. Cao L, Youn I, Guilak F, Setton LA. Compressive properties of mouse articular cartilage determined in a novel micro-indentation test method and biphasic finite element model. *J Biomech Eng.* 2006;128(5):766–71.
 168. Wallace IJ, Worthington S, Felson DT, Jurmain RD, Wren KT, Maijanen H, et al. Knee osteoarthritis has doubled in prevalence since the mid-20th century. *PNAS.* 2017;114(35), 9332-9336.
 169. Harris JD, Siston RA, Brophy RH, Lattermann C, Carey JL, Flanigan DC. Failures, re-operations, and complications after autologous chondrocyte implantation - a systematic review. *Osteoarthr Cartil.* 2011;19(7):779–91.
- 

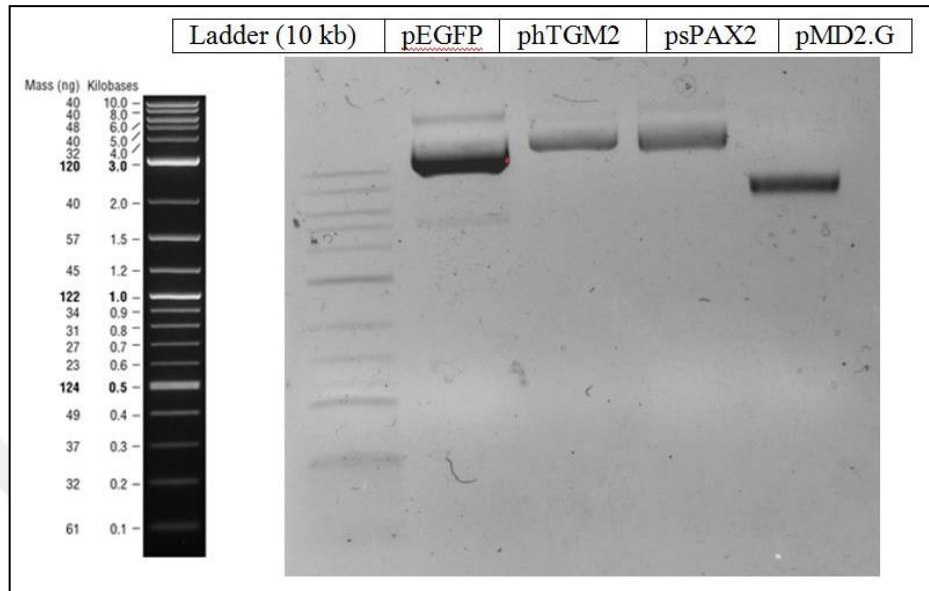
APPENDIX A: AGAROSE GEL ELECTROPHORESIS OF PLASMIDS

Figure A.1. Agarose gel electrophoresis of plasmids. pEGFP= 9088 bp, phTGM2_v2=10015 bp, psPAX2=10,668 bp, pMD2.G= 5824 bp.

APPENDIX B: CALIBRATION CURVES FOR THE GROWTH OF RBMSC AND CHONDROCYTES

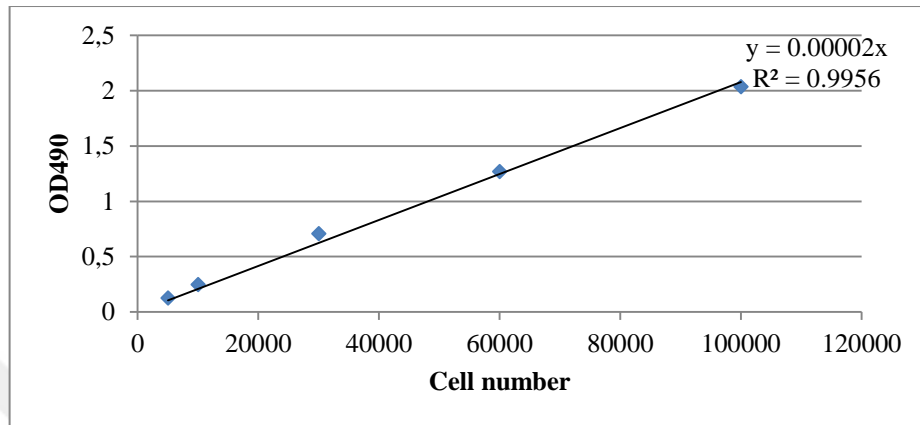


Figure B.1. Calibration curve of rBMSCs (P5) at the end of 3 hours. Slope=0.00002.

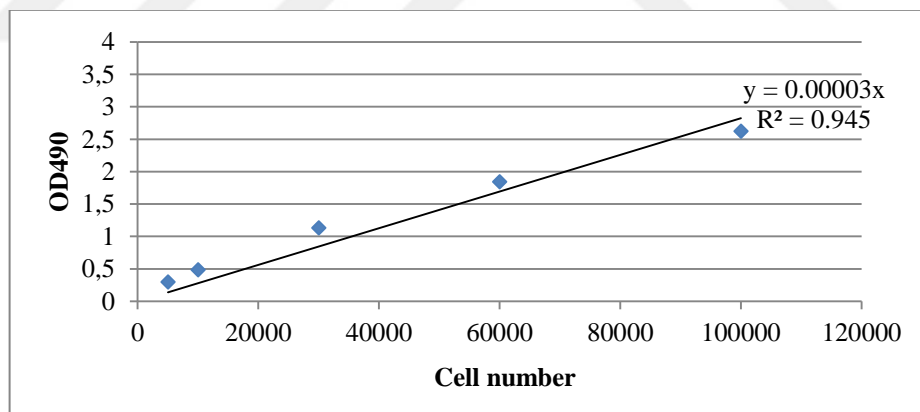


Figure B.2. Calibration curve of rat knee chondrocytes (P5) at the end of 3 hours.
Slope=0.00003.

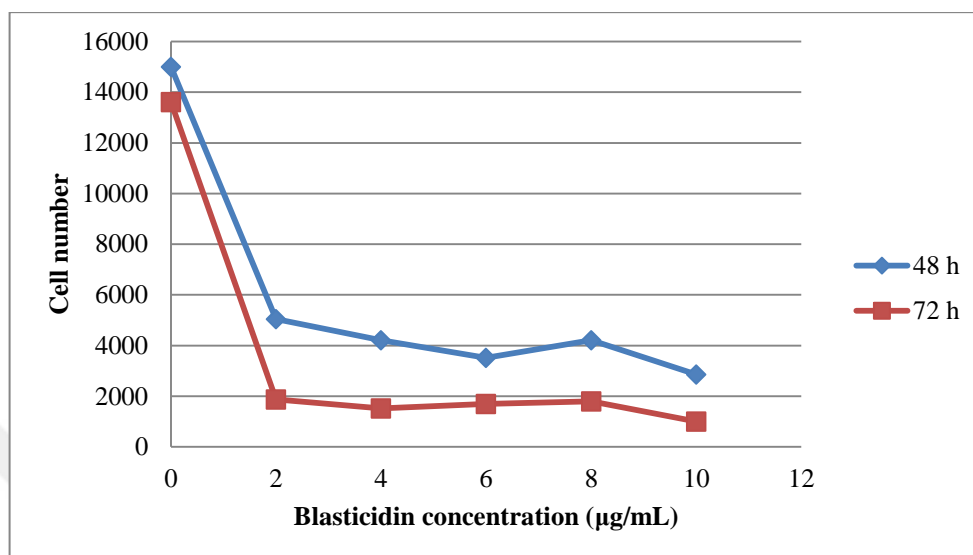
APPENDIX C: BLASTICIDIN KILL CURVE

Figure C.1. Viability of rBMSCs after 48 and 72 hours of incubation in the presence of Blasticidin

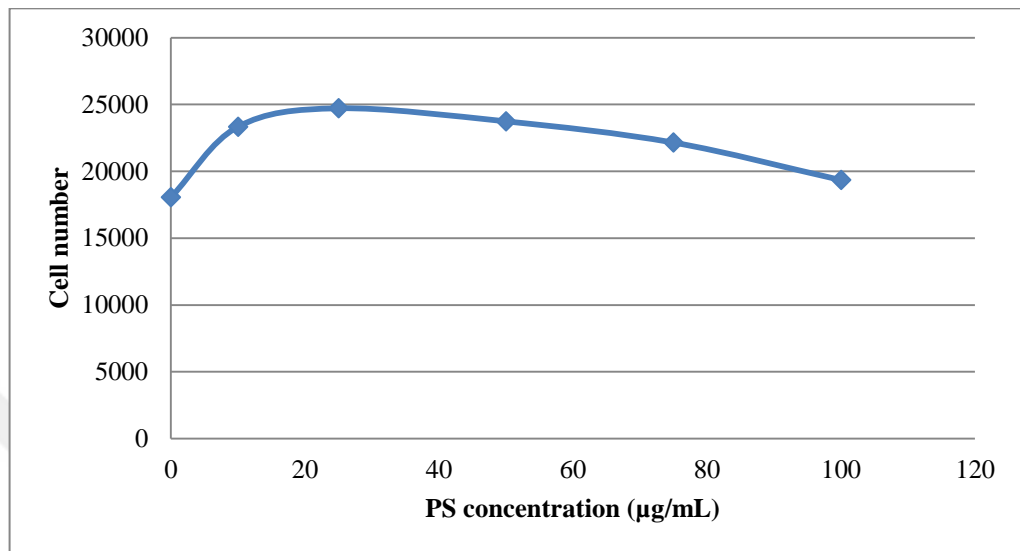
APPENDIX D: PROTAMINE SULFATE KILL CURVE

Figure D.1. Kill curve of PS for rBMSCs

APPENDIX E: CALIBRATION CURVE FOR BSA IN BCA PROTEIN ANALYSIS

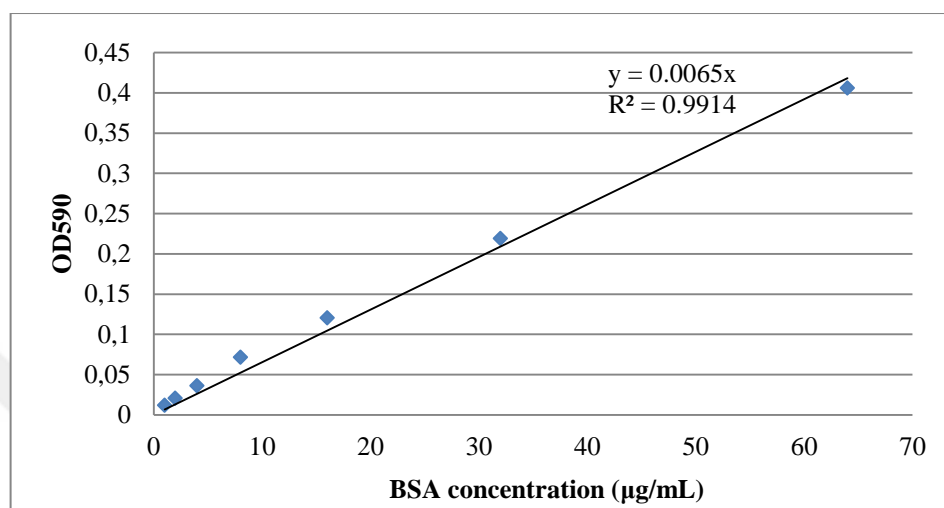


Figure E.1. Calibration curve of BSA at 590 nm. Slope=0.0065.

APPENDIX F: IMMUNOSTAINING OF NEGATIVE CONTROL GROUPS

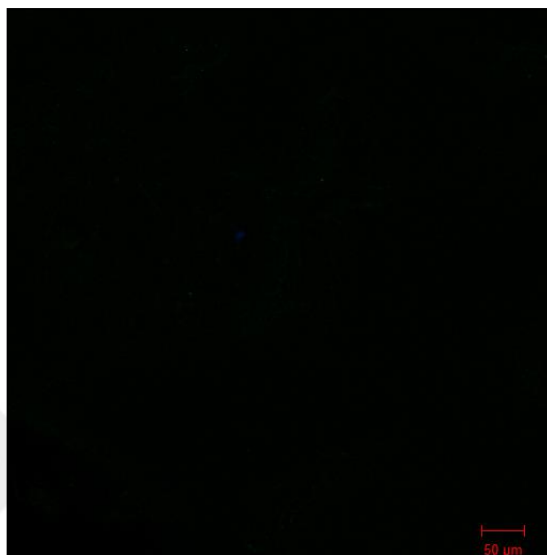


Figure F.1. Confocal microscope image of an empty scaffold that was incubated in Alexa Fluor® 488 conjugated anti-mouse secondary antibody and DAPI. Objective: 10X, scale bar: 50 μm.

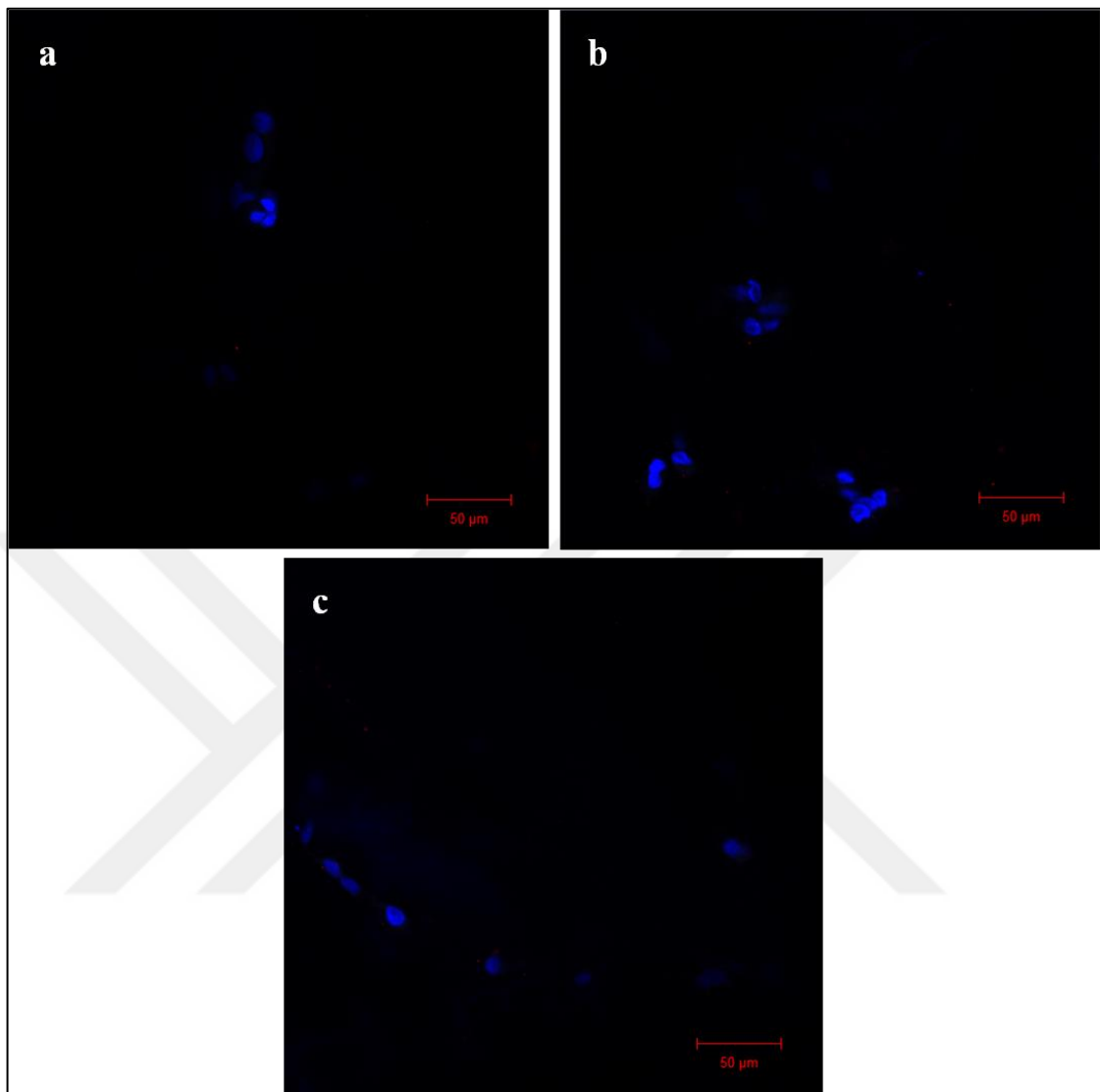


Figure F.2. Confocal microscope image of cells (a: 2ML, b: MSC, c: CH) on scaffolds which were incubated in Alexa Fluor® 488 (green) conjugated anti-mouse secondary antibody, Alexa Fluor® 647 (red) conjugated anti-rabbit secondary antibody, Alexa Fluor® 568 (orange) conjugated anti-goat secondary antibody, and DAPI (blue).

Objective: 20X, scale bar: 50 μm.